

REHABILITATION OF DAMAGED COASTS USING BEACH
NOURISHMENT AND A CASE STUDY IN IZMIT BAY

by

Alper Mert

B.S., Civil Engineering, Karadeniz Technical University, 2006

Submitted to the Institute for Graduate Studies in
Science and Engineering in partial fulfillment of
the requirements for the degree of
Master of Science

Graduate Program in Civil Engineering
Boğaziçi University

2012

ACKNOWLEDGEMENTS

I would like to thank my thesis supervisor Assoc. Prof. Emre Otay for introducing me to the field of coastal engineering and his valuable guidance throughout this study.

I would like to express my appreciations to Assoc. Prof. Osman Breki and Assoc. Prof. Murat İ. Kmrc for their helpful comments and discussions.

I am thankful to the General Coordinator of Kocaeli Metropolitan Municipality Adnan Bilgi and the Director of the Directorate of Park and Gardens Cenan Turan for their positive encouragement about the study.

I would like to thank my friends Hasan, Aykut, Sinan, Yksel, Bahacan, Yiit and Sinem for their aid and hard work on the field and in the laboratory.

I would like to express my appreciations to the Turkish State Meteorological Service (TSMS) to supply the long-term wind data of Izmit.

Lastly, I would like to thank my family for their endless understanding and support.

This project was funded by Kocaeli Municipality Environmental Protection and Control Department.

The physical model was constructed in the Hydraulic Laboratory of Karadeniz Technical University and the material used as natural bottom was dredged by Istanbul Anatolian Side Marine Sand and Gravel Miners Association.

ABSTRACT

REHABILITATION OF DAMAGED COASTS USING BEACH NOURISHMENT AND A CASE STUDY IN IZMIT BAY

Part of Izmit Bay had been filled with excavation waste after the 1999 Earthquake causing beaches around the Bay to lose their natural form and usability. The main purpose of this study is to investigate the existing conditions of a typical fill area and find a feasible solution to reinstate a natural coast. After theoretical and experimental investigations, beach nourishment is proposed as a solution to rehabilitate the coasts of İzmit Bay by transforming them into recreational beaches. The geology, sediment properties, morphological structure and wave regime of the selected pilot site, Derince, is determined by field measurements, laboratory experiments and computer analysis. Along the coastal profile, sediment diameter differs from place to place, and especially in deeper zones, the rate of fine material (silt and clay) increases significantly. Bathymetric measurements indicate that the coastal profile is not in equilibrium. A physical model is established to examine the interaction between the native mixed soil and the granular nourishment sand. Laboratory experiments showed that there is no mixing between the native fine material and nourishment sand. Even after extreme storms, no silt and clay have been found on the nourished nearshore profile. Therefore, it is concluded that the predefined coasts can be rehabilitated using beach nourishment. Using the site specific parameters, alternative beach nourishment designs are developed including calculation of the required sand volumes and the project cost.

ÖZET

TAHRİP EDİLMİŞ KIYILARIN KUMSAL BESLEMESİ İLE REHABİLİTASYONU: İZMİT KÖRFEZİNDE ÖRNEK ÇALIŞMA

İzmit Körfezindeki bazı kıyıların 1999'daki depremden sonra bina yıkıntı atıklarıyla doldurulması, bu kıyıların doğal yapısını ve kullanılabilirliğini kaybetmesine sebep olmuştur. Bu çalışmanın ana amacı, tipik bir dolgu alanının özelliklerini belirleyerek doğal bir kıyı oluşturmak için uygulanabilir bir çözüm bulmaktır. Teorik ve deneysel çalışmalar sonucunda İzmit Körfezi kıyılarının kumsal beslemesi ile rekreasyon amaçlı rehabilitasyonun mümkün olduğu tespit edilmiştir. Seçilen pilot bölgenin (Derince) jeolojisi, sediment özellikleri, morfolojik yapısı ve dalga rejimi; saha ölçümleri, laboratuvar deneyleri ve bilgisayar analizleri ile belirlenmiştir. Sediment çapı kıyı profili boyunca değiştirmekte ve özellikle derin kesimlerde ince malzeme oranı oldukça artmaktadır. Batimetri ölçümleri mevcut kıyının denge profili teorisine uymadığını göstermektedir. Kum ve kil/silt gibi daha ince malzemenin bir karışımı olan doğal zemin ile besleme kumunun etkileşimini saptamak amacıyla bir fiziksel model kurulmuştur. Laboratuvar deneyleri, kum ile ince malzemenin karışmadığını göstermiştir. Sert fırtınalardan sonra bile yakın kıyı profilinde silt ve kil gibi ince malzemelere rastlanılmamıştır. Böylece, yukarıda tanımlanan kıyıların kumsal beslemesi ile rehabilitasyonunun mümkün olduğu sonucuna varılmıştır. Proje alanına özgü parametreler kullanılarak, gerekli kum hacimleri ve maliyetleri içerecek şekilde alternatif kumsal besleme dizaynları geliştirilmiştir.

TABLE OF CONTENTS

ACKNOWLEDGEMENTS.....	iii
ABSTRACT.....	iv
ÖZET	v
LIST OF FIGURES	viii
LIST OF TABLES.....	xiii
LIST OF SYMBOLS	xiv
LIST OF ACRONYMS/ABBREVIATIONS.....	xvi
1. INTRODUCTION	1
1.1. Field Observations	4
2. LITERATURE SURVEY	5
2.1. Theoretical and Experimental Studies about the Recreation of Damaged Coasts by Beach Nourishment.....	5
2.2. Survey of Site Related Experimental Studies	8
2.2.1. Geology of the Eastern Marmara Sea.....	8
2.2.2. Historic Maps of Kocaeli and Izmit Bay	9
2.2.3. Soil Characteristics of Derince Coast.....	10
3. FIELD MEASUREMENTS AND ANALYSES	13
3.1. Identification of the Fill Material	13
3.2. Wind and Wave Analyses	14
3.3. Nearshore Topographic and Hydrographic Surveys.....	22
3.3.1. Bathymetry and Shoreline Measurements	22
3.3.2. Survey of Coastal Profiles	24
3.4. Sediment Characteristics of the Nearshore	27
4. LABORATORY MODEL	32
4.1. Supply of the Necessary Material	32
4.2. Properties of the Wave Flume.....	33
4.3. Determination of the Model Scale	34
4.3.1. Noda’s Modeling Criteria.....	34
4.3.2. Ito and Tsuchiya’s Modeling Criteria.....	35
4.3.3. Hallermeier’s Modeling Criteria	35

4.3.4. Comparison of Model Criteria and Selection of Model Scale.....	37
4.4. Establishment of the Laboratory Model.....	38
4.4.1. Determination of the Wave Conditions	38
4.4.2. Calibration of the Wave Maker	40
4.4.3. Placement of the Model Material	41
4.5. Results	42
5. ENGINEERING DESIGN	45
5.1. Equilibrium Beach Profiles	45
5.2. Alternative Nourishment Designs	46
5.3. Cost Calculation	48
6. CONCLUSION	50
APPENDIX A: WIND AND WAVE ANALYSES	52
APPENDIX B: BEACH PROFILE DRAWINGS.....	57
B.1. Design Profiles for Grain Diameter 0.32 mm	57
B.2. Design Profiles for Grain Diameter 0.45 mm	70
B.3. Plan View of 20 m Beach Width for Grain Diameter 0.45 mm.....	83
REFERENCES	85

LIST OF FIGURES

Figure 1.1. Location of the pilot site (Google Earth, 2011).	1
Figure 1.2. Borders of the project site (Google Earth, 2011).	2
Figure 1.3. Coastal damage and wastes on beachface.	2
Figure 1.4. Old photo of the project area (Press and publication directorate of Derince Municipality).	3
Figure 1.5. Natural diversity in the project area.	4
Figure 2.1. Sketch of the cross-shore evolution of a nourished beach.	5
Figure 2.2. Geology map of the East Marmara (Tubitak, 2006).	8
Figure 2.3. Photogrammetric map of the project site (Ana-Kent, 2006).	9
Figure 2.4. The aerial photo of the project area (Ana-Kent, 2005).	9
Figure 2.5. Oceanography map of the project site (SHOD, 1997, map no: 2911).	10
Figure 3.1. Position of soil borings and test pits.	13
Figure 3.2. Test pit opened 10 m landward from the shoreline: at 5 m depth still fill material was observed.	14
Figure 3.3. Locations of Local and Izmit meteorology stations.	15
Figure 3.4. Joint probability of wind speed and direction for local weather station data.	16
Figure 3.5. Joint probability of wind speed and direction for Izmit weather station data.	17

Figure 3.6. Comparison of local and Izmit stations according to the joint distribution of wave height and direction (radial axis: wave height [m], angles: direction where the waves come from [°], contours: probability of occurrence [%]).	19
Figure 3.7. Comparison of local and Izmit stations according to the joint distribution of wave period and direction (radial axis: wave period [s], angles: direction where the waves come from [°], contours: probability of occurrence [%]).	20
Figure 3.8. Comparison of local and Izmit stations according to the joint distribution of significant wave height and peak wave period (contours: number of occurrences, color bar: probability of occurrence [%]).	21
Figure 3.9. Boat survey equipment.	22
Figure 3.10. Hydrographic survey trajectories (MCH-TECH Marine Research, 2011).	23
Figure 3.11. Shorelines at four different times.	24
Figure 3.12. Coastal profiles in plan view.	25
Figure 3.13. Coastal profiles in side view.	26
Figure 3.14. Locations of the sediment samples.	27
Figure 3.15. Seabed sediment sampling techniques.	28
Figure 3.16. Variation of sediment median diameter (D_{50}) in sections.	28
Figure 3.17. The sediment map of the project site.	30
Figure 3.18. Change in sediment size with respect to depth.	30
Figure 3.19. Change in organic content ratio with respect to depth.	31
Figure 4.1. Extraction of model native material.	32

Figure 4.2. Sieve analysis of model native sediment.	33
Figure 4.3. Schematic representation of the flume.	34
Figure 4.4. Selection of storms from the data.	38
Figure 4.5. Grouping for the first storm.	39
Figure 4.6. Model dimensions (horizontal and vertical scales: $N_x = N_z = 7$, diameter scale: $N_d = 2.51$, time scale: $N_T = 2.65$, model native sediment: $D_{native} = 0.13$, model fill sediment: $D_{fill} = 0.18$).	41
Figure 4.7. Placement of the model materials into the wave channel.	42
Figure 4.8. Profile evolution of the model.	42
Figure 4.9. The model profile after water discharge.	43
Figure 4.10. Comparison of the theoretical and model profiles before and after wave penetration.	44
Figure 5.1. Typical nourished coastal profile scheme.	45
Figure 5.2. Comparison of alternative nourishment quantities.	49
Figure A.1. Wind speed histograms for both stations.	53
Figure A.2. Wind/wave direction histograms for both stations.	53
Figure A.3. Significant wave height histograms for both stations.	54
Figure A.4. Peak wave period histograms for both stations.	54
Figure A.5. Joint distribution of wind speed and wind direction for both stations in Cartesian coordinates.	55
Figure A.6. Joint distribution of significant wave height and wave direction for both stations in Cartesian coordinates.	55

Figure A.7. Joint distribution of peak wave period and wave direction for both stations in Cartesian coordinates.	56
Figure B.1. Design profiles of Section 1,2 and 3 for 5 m new dry beach width ($D_{fill}=0.32$ mm).	58
Figure B.2. Design profiles of Section 4,5 and 6 for 5 m new dry beach width ($D_{fill}=0.32$ mm).	59
Figure B.3. Design profiles of Section 1,2 and 3 for 10 m new dry beach width ($D_{fill}=0.32$ mm).	60
Figure B.4. Design profiles of Section 4,5 and 6 for 10 m new dry beach width ($D_{fill}=0.32$ mm).	61
Figure B.5. Design profiles of Section 1,2 and 3 for 15 m new dry beach width ($D_{fill}=0.32$ mm).	62
Figure B.6. Design profiles of Section 4,5 and 6 for 15 m new dry beach width ($D_{fill}=0.32$ mm).	63
Figure B.7. Design profiles of Section 1,2 and 3 for 20 m new dry beach width ($D_{fill}=0.32$ mm).	64
Figure B.8. Design profiles of Section 4,5 and 6 for 20 m new dry beach width ($D_{fill}=0.32$ mm).	65
Figure B.9. Design profiles of Section 1,2 and 3 for 25 m new dry beach width ($D_{fill}=0.32$ mm).	66
Figure B.10. Design profiles of Section 4,5 and 6 for 25 m new dry beach width ($D_{fill}=0.32$ mm).	67
Figure B.11. Design profiles of Section 1,2 and 3 for 30 m new dry beach width ($D_{fill}=0.32$ mm).	68
Figure B.12. Design profiles of Section 4,5 and 6 for 30 m new dry beach width ($D_{fill}=0.32$ mm).	69

Figure B.13. Design profiles of Section 1,2 and 3 for 5 m new dry beach width ($D_{\text{fill}}=0.45$ mm).	71
Figure B.14. Design profiles of Section 4,5 and 6 for 5 m new dry beach width ($D_{\text{fill}}=0.45$ mm).	72
Figure B.15. Design profiles of Section 1,2 and 3 for 10 m new dry beach width ($D_{\text{fill}}=0.45$ mm).	73
Figure B.16. Design profiles of Section 4,5 and 6 for 10 m new dry beach width ($D_{\text{fill}}=0.45$ mm).	74
Figure B.17. Design profiles of Section 1,2 and 3 for 15 m new dry beach width ($D_{\text{fill}}=0.45$ mm).	75
Figure B.18. Design profiles of Section 4,5 and 6 for 15 m new dry beach width ($D_{\text{fill}}=0.45$ mm).	76
Figure B.19. Design profiles of Section 1,2 and 3 for 20 m new dry beach width ($D_{\text{fill}}=0.45$ mm).	77
Figure B.20. Design profiles of Section 4,5 and 6 for 20 m new dry beach width ($D_{\text{fill}}=0.45$ mm).	78
Figure B.21. Design profiles of Section 1,2 and 3 for 25 m new dry beach width ($D_{\text{fill}}=0.45$ mm).	79
Figure B.22. Design profiles of Section 4,5 and 6 for 25 m new dry beach width ($D_{\text{fill}}=0.45$ mm).	80
Figure B.23. Design profiles of Section 1,2 and 3 for 30 m new dry beach width ($D_{\text{fill}}=0.45$ mm).	81
Figure B.24. Design profiles of Section 4,5 and 6 for 30 m new dry beach width ($D_{\text{fill}}=0.45$ mm).	82
Figure B.25. Design plan view for 20 m new dry beach width ($D_{\text{fill}}=0.45$ mm).	84

LIST OF TABLES

Table 2.1.	Summary of the geological-geotechnical research report (Kes-ka, 2008).	11
Table 2.2.	Sieve analysis of soil samples for borings close to the site (Kes-ka, 2008).	12
Table 3.1.	Wind and wave parameters.	19
Table 3.2.	Sieve analysis results of the existing beach and seabed sediments.	29
Table 4.1.	Comparison of model criteria.	37
Table 4.2.	Significant wave height, peak wave period and run time values for each storm event.	40
Table 4.3.	Median diameters of bottom samples (numbers in mm).	43
Table 5.1.	Extreme wave parameters and closure depths for both station records.	46
Table 5.2.	Volume calculations for seven alternative beach widths.	47
Table 5.3.	Quantities for alternative nourishment options.	48

LIST OF SYMBOLS

A	Profile scale parameter
d_p	Prototype sediment median diameter
D	Sediment diameter
D_{fill}	Nourishment sediment median diameter
D_{native}	Native sediment median diameter
D_{50}	Median diameter
F	Fetch length
g	Gravity
h	Water depth
h_c	Closure depth
h_{max}	Maximum water depth
H_e	Extreme wave height
H_s	Significant wave height
$H_{s(max)}$	Maximum significant wave height
N_d	Sediment diameter scale
N_L	Length scale
N_T	Time scale
N_x	Horizontal length scale
N_z	Vertical length scale
t_m	Model run time
T_e	Extreme wave period
T_m	Model wave period
T_{max}	Maximum wave period
T_p	Peak wave period
U	Wind speed at 10 meter above the sea level

U_*	Critical velocity for incipient motion of the sediment
$U_{*(m)}$	Critical velocity of model
$U_{*(p)}$	Critical velocity of prototype
\bar{U}	Wind speed at 10 meter
$V_{w(max)}$	Maximum wind speed
$V_{w(avg)}$	Average wind speed
V_x	Horizontal velocity
V_z	Vertical velocity
x	Fetch length
\bar{x}	Dimensionless fetch
y	Distance from shoreline
γ	Peak-shape parameter
ρ_p'	Prototype sediment immersed relative density
ψ	Similarity of prototype and model
Ω	Model distortion

LIST OF ACRONYMS/ABBREVIATIONS

CL	Sandy Clays, Silty Clays
E	East
ESE	East-South-East
JONSWAP	Joint North Sea Wave Project
KTU	Karadeniz Technical University
MTA	General Directorate of Mineral Research and Exploration
N	North
SE	South-East
SHOD	Office of Navigation and Hydrography and Oceanography
SK	Soil Boring
SL	Clayey Sands, Sand-Clay Mixture
SPM	Shore Protection Manual
SSE	South-South-East
TSMS	Turkish State Meteorological Service

1. INTRODUCTION

The coasts of the Gulf of Izmit which is one of the most important economy centers of Turkey lost its natural structure and suitability for human use in parallel with industrial development.

Kocaeli Metropolitan Municipality has launched a large-scale project in order to transform the coasts of Izmit Bay which filled with a wide variety of wastes and contain high proportion of silt/clay naturally. The main aim of the project is to rehabilitate such coasts by using beach nourishment and to develop recreational parks for public use. The coast of Derince was chosen as a pilot site (Figure 1.1).



Figure 1.1. Location of the pilot site (Google Earth, 2011).

The project area is in the northern part of the Gulf of Izmit and covers approximately one kilometer-long coast that is the east of the intersection point of the borders of Derince and Körfez counties. The boundaries of the project site are the fisherman shelter in the east and the Kaşgal Creek in the west (Figure 1.2).

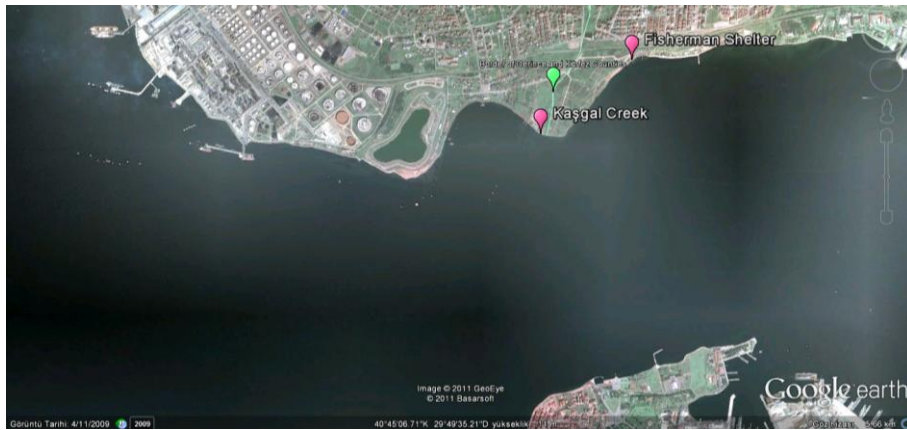


Figure 1.2. Borders of the project site (Google Earth, 2011).

This coast was filled with excavation waste after the Kocaeli earthquake in 1999, and over time turned into a storage area for all kinds of wastes (Figure 1.3).



Figure 1.3. Coastal damage and wastes on beachface.

Old photos of the project area revealed by archival research show the change in the region clearly. Figure 1.4 indicates the situation of the project site before the earthquake in 1999. As seen in the photo, the coastline was not damaged with fill material yet.



Figure 1.4. Old photo of the project area (Press and publication directorate of Derince Municipality).

Aerial photographs taken in recent years and other documents obtained from archives show the damage in the region clearly. Such documents will be examined in detail in later parts.

In this study, it is investigated that whether rehabilitation is technically and economically possible for this coast and others in similar situation by using environmentally sound engineering techniques.

As it can be seen in the following chapters, according to the results of theoretical/mathematical and physical models constructed to achieve an engineering solution, it is determined whether the recreation of damaged coasts is possible by using beach nourishment.

1.1. Field Observations

In the preliminary investigation of the site, the fill material was observed up to 3-4 meters high along the coastline. Vegetation on the fill material prevents making observational prediction about the content. Although coastline was heavily covered with domestic and industrial waste, the diversity of coastal and marine life is remarkable. During the examination, many bird and fish species were observed in the field (Figure 1.5).

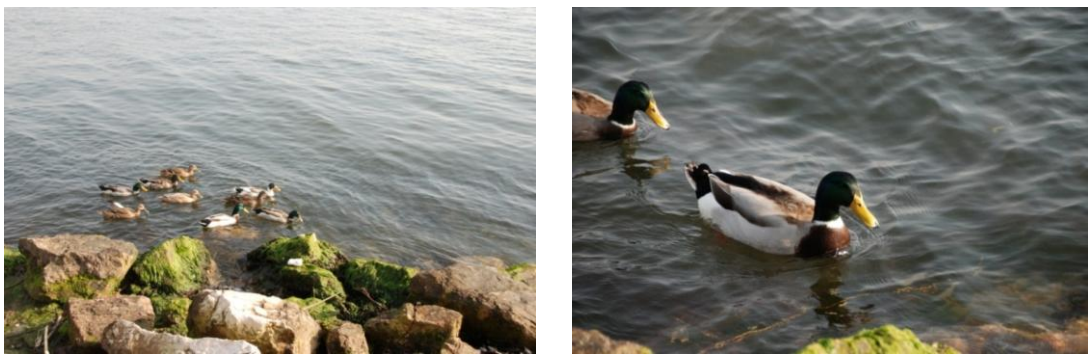


Figure 1.5. Natural diversity in the project area.

2. LITERATURE SURVEY

2.1. Theoretical and Experimental Studies about the Recreation of Damaged Coasts by Beach Nourishment

Theoretical studies about recreation of damaged coasts are few in the literature since these works are commonly site specific. In addition, experimental studies are even scarcer. However, beach nourishment theory and applications have been examined by various researchers for a long time. A quite brief summary of theoretical and experimental studies about beach nourishment is given below.

Beach nourishment projects have been realized since the beginning of 1920's. The first rational approaches about beach nourishment practices were suggested by Krumbein (1957) and Krumbein and James (1965). They estimated needed borrow material volume per unit volume of beach and sorting through natural forces. The method of calculation was reformulated by Dean (1974). The equilibrium beach profile theory (Bruun, 1954; Dean, 1977; Moore, 1982) was built to understand the evolution of the original and nourished beach profiles (Figure 2.1).

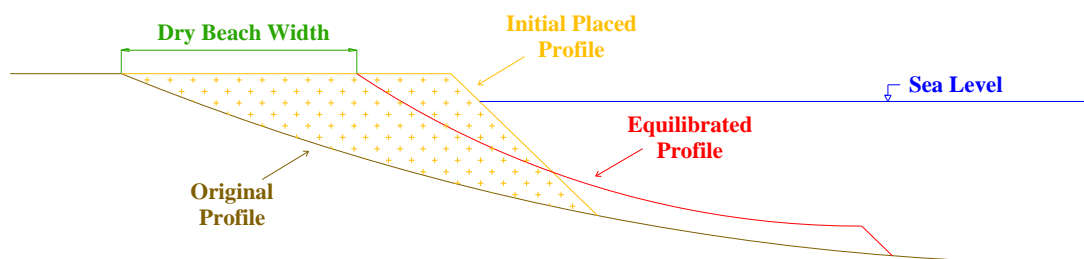


Figure 2.1. Sketch of the cross-shore evolution of a nourished beach.

Bruun(1954) examined profiles from Denmark and Monterey Bay, CA and found out the following expression.

$$h(y) = Ay^{2/3} \quad (2.1)$$

where h is the water depth at a distance y from the shoreline and A is profile scale parameter.

Dean (1977) showed that the Bruun's equation is consistent with uniform wave energy dissipation per unit volume. The A parameter was associated to sediment size, D , by Moore (1982) according to many laboratory and field profiles. Moore (1982) showed that the scale parameter increases in increasing sediment size. As a result, fine sediments have milder slope than coarse sediments. Therefore, it is expected that for the equal volume of nourishment, the dry beach width would be less for the finer material. Dean (1991) defined nourished beach profiles as 'intersecting', 'nonintersecting', and 'submerged' according to the comparison of A values of the native and fill sediments.

Determination of borrow areas is another crucial issue for beach nourishment projects. One of the design stages of a beach nourishment project is to determine one or more borrow areas with the required quality and quantity sand. Dean (2002) states that more than 95% of the sediment used in beach nourishment projects is obtained from offshore sources which should be immediately seaward of the nourished beach and have similar features with the natural sediment in size and color.

Theoretical and experimental studies of beach nourishment given above are valid for naturally sandy coasts. In other words, it was assumed that the beach to be nourished contains no cohesive sediment. However, the coasts of İzmit Bay are composed of a wide variety of materials ranging from sand to mud. Therefore, the understanding of the mixing and transport processes of fine and coarse sediments under wave action should be examined. Related studies in the literature are summarized below.

Aubry *et al.* (2009) conducted a one year field experiment to understand the surface sediment change and temporal variations, in a beach east of Calais on the North Sea coast of France, that exhibit large variability in sediment composition ranging from sand to mud and exposed to semi-diurnal tides with a mean spring tide range of about 6.4 m. They found out that under low energy conditions mud was stable on the lower part of the beach,

however, an onshore migration of fine sediments occurred during winter characterized by high energy events. They tried to explain this mud deposition phenomenon by the specific morphology, the availability of muddy sediment from the shoreface and a decrease in wave energy during summer.

Jepsen *et al.* (2010) made a laboratory experiment using a modified shear stress straight flume including downstream bed load traps to analyze the transport modes of sands and finer sediments in natural and artificial mixed sediments via separation of bed load and suspended load transport. They claimed that mixed sediment erosion rate and transport mode are highly sediment specific and they will be affected not only by grain size distribution but also by bulk density, mineralogy, pore water chemistry, organic content, and presence of gas bubbles. They also suggested that if mixed sediments with large sand friction placed in nearshore, erosion should result in rapid separation of fine material from sand, therefore, sand will remain in the littoral system. Fine sediments, moving as individual suspended particles, cannot settle in the nearshore due to high wave energy, thus, they will move offshore and deposit in areas where fine material resides naturally.

Profile change of coarse and fine material composite beach (CFMC beach) was discussed both in the field and in the laboratory by Yamashita *et al.* (2004). From the field observation data on the Kochi Coast, Shikoku Island, Japan, facing the Pacific Ocean, they found that coarse material is transported offshore after mixing processes under severe storm conditions. After the storm, when waves and currents become smaller, the suspended mixed material settles starting from the coarser sediments and this layer is covered by fine sand later. Kochi coast is a typical river mouth coast, where the difference of diameters of coarse (2-100 mm) and fine (0.1-0.5 mm) material is significantly large. In the laboratory experiment, they tried to investigate the movement on the nourishment-gravel composed of cobble due to very large waves. They found that the nourishment-gravel moves rapidly into the surf zone within 30 minutes after wave operation; and after 1 hour wave operation the moved nourishment-gravel is gradually buried under the seabed by the sedimentation of moved beach sand.

2.2. Survey of Site Related Experimental Studies

Investigation of past studies is crucial to understand the project site totally. Therefore, some crucial data are compiled from the Municipality of Derince and Kocaeli.

2.2.1. Geology of the Eastern Marmara Sea

The geology map (Figure 2.2) was prepared in 2006 by Tubitak Marmara Research Center (TÜBİTAK-MAM) through using 1/25.000, 1/100.000 and 1/500.000 scaled analog and digital geological data of General Directorate of Mineral Research and Exploration (MTA). The map shows that the project area is an alluvial-quaternary zone that consists of alluvial deposits of sand, gravel, silt, and clay.

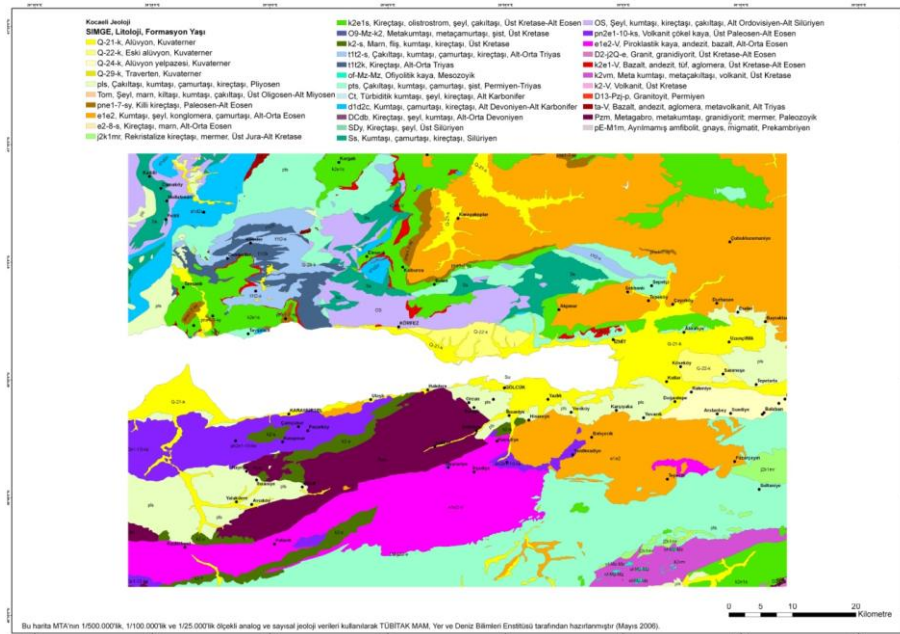


Figure 2.2. Geology map of the East Marmara (Tubitak, 2006).

2.2.2. Historic Maps of Kocaeli and Izmit Bay

The photogrammetric map of Kocaeli was made in 2006 by a private company contracted by the Municipality of Kocaeli. The scale of the original map shown in Figure 2.3 is 1/5000.

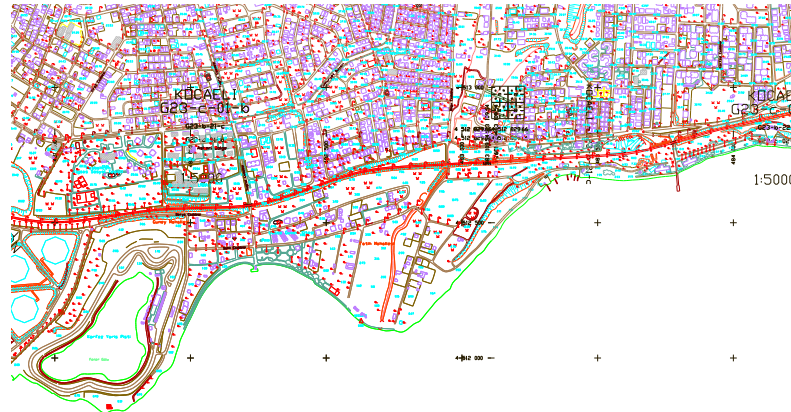


Figure 2.3. Photogrammetric map of the project site (Ana-Kent, 2006).

The aerial photos of Kocaeli were taken in 2005 by the same company making the photogrammetric map. Figure 2.4 shows the aerial photo of the project area.



Figure 2.4. The aerial photo of the project area (Ana-Kent, 2005).

Izmit Bay (SH-291, 1992) and Port of Izmit (SH-2911, 1997) oceanography maps established by Office of Navigation Hydrography and Oceanography (SHOD) are used as a reference for subsequent detailed bathymetry measurements (Figure 2.5).

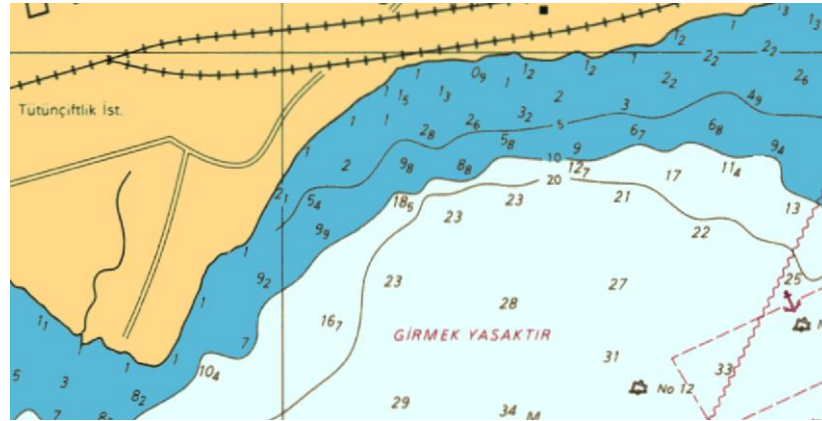


Figure 2.5. Oceanography map of the project site (SHOD, 1997, map no: 2911).

2.2.3. Soil Characteristics of Derince Coast

The Municipality of Kocaeli employed a private company in 2008 in order to determine whether the coastal region of Derince is earthquake-resistant or not. The geological-geotechnical research report of the study gives information about the properties of native soil and fill material (Table 2.1).

Table 2.1. Summary of the geological-geotechnical research report (Kes-ka, 2008).

	Native Soil	Fill Material
Formation	Alluvial/Quaternary	Örencik(Tör)
Classification	CL	SC-CL
Electrical Resistivity Tomography (ERT)	Silt/Clay	Silt/Clay
Liquefaction	high potential	liquefied
Percent Fine (%)	55-71	31-58
Percent Coarse (%)	0-1	3-19

Örencik(Tör): Soft landband gravel, sand and silt stone.

CL: Inorganic clays of low to medium plasticity, sandy clays, silty clays.

SC: Clayey sands, sand-clay mixture.

According to the report, there exist Pliocene Örencik formation, Quaternary alluviums and artificial fill material in the study field. 12 soil boring tests (total length of 12 borings was 172.5 m) were performed and at SK-9 boring 10 m thick fill material was detected. In addition, it is mentioned in the report that in some places 3-5 m thick artificial fill was identified on the native soil. At the conclusion of the report it was determined that due to the high potential of liquefaction, the region is not suitable for construction. The sieve analysis results of disturbed and undisturbed soil samples for all borings are given in the report. Table 2.2 shows the sieve analysis results of borings that are the closest ones to the project site. The locations of such borings are shown in Figure 3.1.

Table 2.2. Sieve analysis of soil samples for borings close to the site (Kes-ka, 2008).

Boring Code	Depth (m)	Sieve No. 4 (D=4.76 mm) Retained %	Sieve No. 200 (D=0.074 mm) Passing %
SK-4	3	0	56
	6	0	50
SK-5	3	6	42
	4.5	2	59
	6	3	56
SK-9	1.5	19	31
	4.5	14	34
	7.5	3	58
SK-10	3	0	55
	4.5	1	68
	6	1	76
	7.5	0	71
SK-11	1.5	0	91
	3	0	99
	6	4	68

As it can be seen from the above findings, the native soil of the project site is mainly formed of fine material.

3. FIELD MEASUREMENTS AND ANALYSES

3.1. Identification of the Fill Material

For a better understanding of the fill material, two test pits were opened with the help of an excavator on the existing beach in December, 2010 (Figure 3.1). The native soil was shown in the pit opened on the water line at a depth 1.5-2 m, however, in the other pit opened 10 m landward from the water line fill material composed of construction, industrial and household waste was seen at 5 m depth (Figure 3.2). It is estimated that 1.5-2 m thick natural-looking granular sediment on the shoreline formed after filling as a result of the movement of waves and currents.

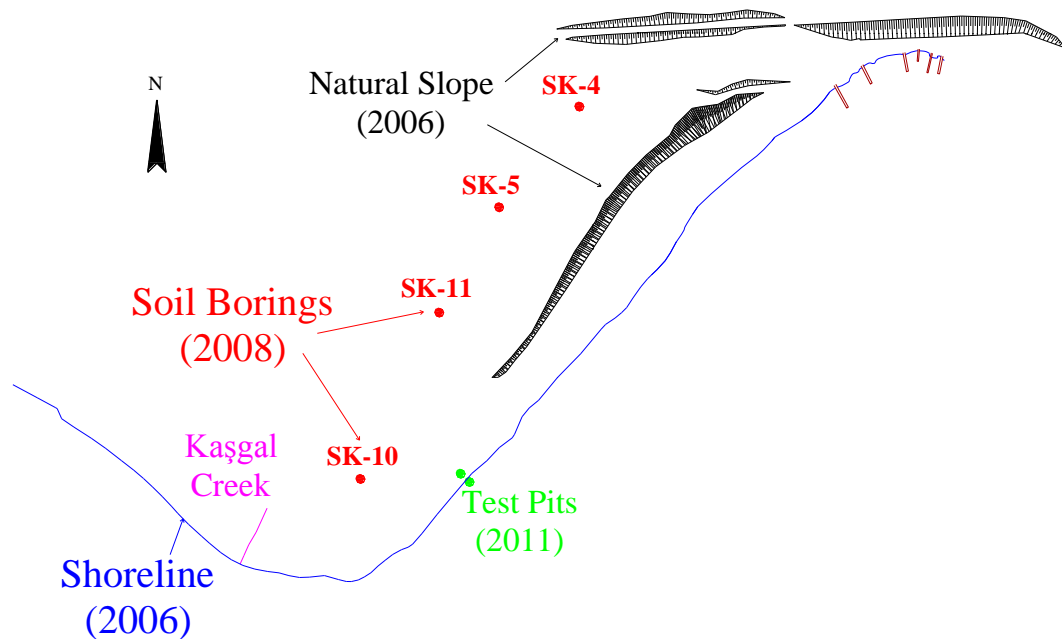


Figure 3.1. Position of soil borings and test pits.

To summarize, according to the information given previously, natural geological structure of the project site includes high percentage of fine sediment and thickness of fill material on the native soil reaches 10 m in some places.



Figure 3.2. Test pit opened 10 m landward from the shoreline: at 5 m depth still fill material was observed.

3.2. Wind and Wave Analyses

Determination of wave characteristics is essential in order to ensure the utilization of coastal regions, to examine the impact of shore protection and beach nourishment. Generally, two main approaches are used for determining the local wave regime. The first is to make long-term wave measurements, and the other is to extract wave statistics from wind records with the help of numerical modeling. There are no wave measurements for the project site, Derince. Therefore, it was decided to benefit from wind data which had been already recorded by the station located at the site with the purpose of finding out the region's wind energy potential. Wind records are crucial for such cases because winds are the primary phenomenon generating waves.

There are several approaches to calculate the expected wave spectra for a wind speed and fetch length. For a given wind speed, the waves depend on fetch length and storm duration. The longer the fetch or duration, the bigger the waves generated.

Records of the weather station located at the project site are the most important data source in determining the wave regime. In similar projects, because no pre-established

weather station exists in the region, the nearest meteorology station measurements were taken as the valid data source. In this project, in addition to the analysis of local station records, the closest meteorology station, Izmit, measurements are analyzed (Figure 3.3).

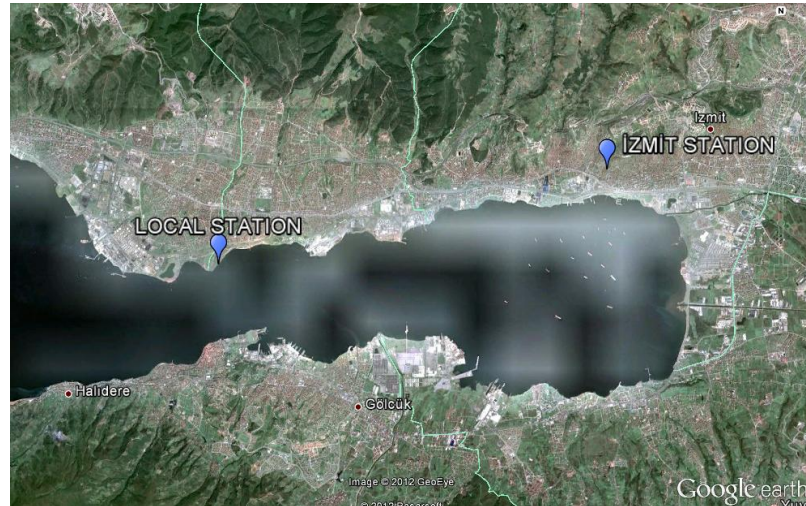


Figure 3.3. Locations of Local and Izmit meteorology stations.

Meteorological records of the local weather station for the dates from October 13, 2007 to August 6, 2009 were obtained. The station measures wind speed, wind direction, temperature, pressure and humidity with the sensors placed at 10, 30, 50 and 51 m heights. The wind speed and wind direction were continuously measured with a precision of 0.1 m/s and 1° , respectively, and 10 minute averages, maximum and minimum values, and standard deviations of both were recorded. The joint probability distribution of wind speed and direction for local wind statistics is given in Figure 3.4. Wind speed measured at 10 m above the sea level and wind directions at 30 m were used in wave modeling.

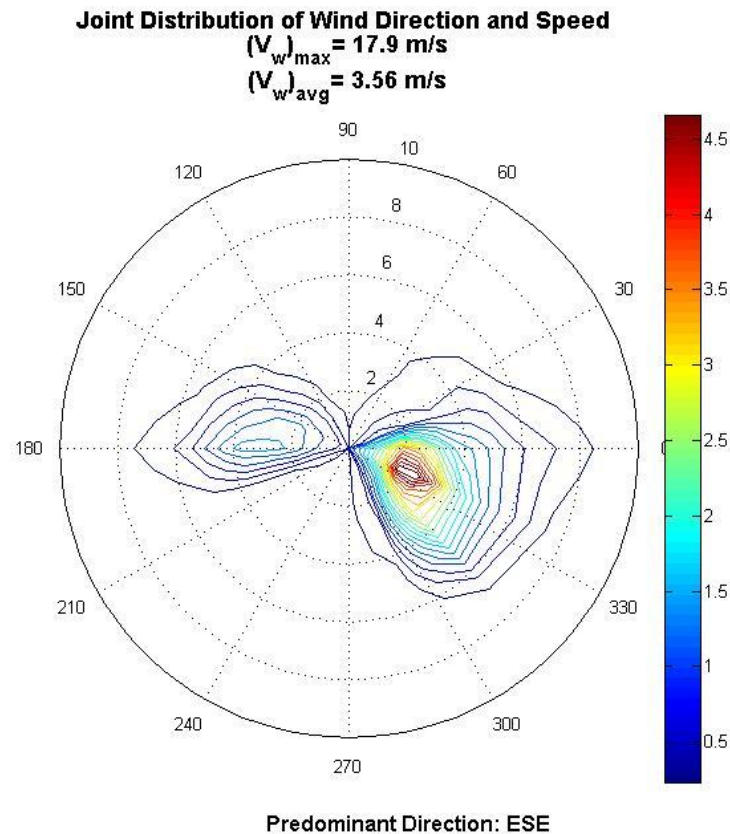


Figure 3.4. Joint probability of wind speed and direction for local weather station data (radial axis: wind speed [m/s], angles: direction where the winds come from [$^{\circ}$], contours: probability of occurrence [%]).

The record of local station covers approximately two years is, therefore, not of sufficient length for long-term wave statistics. Therefore, 29-year data from Izmit meteorology station 10 km to the east was obtained from the Turkish State Meteorological Service (TSMS).

Izmit weather station is located at $40^{\circ} 46'$ N latitude and $29^{\circ} 56'$ E longitude. The station is at 76 meters height above the sea level and of automatic t2 type. Wind measurements between 1981 and 2010 have been obtained. These measurements, covering the past twenty-nine years, are sufficient for long-term wave statistics. Figure 3.5 shows the joint probability distribution of wind speed and direction for Izmit wind statistics.

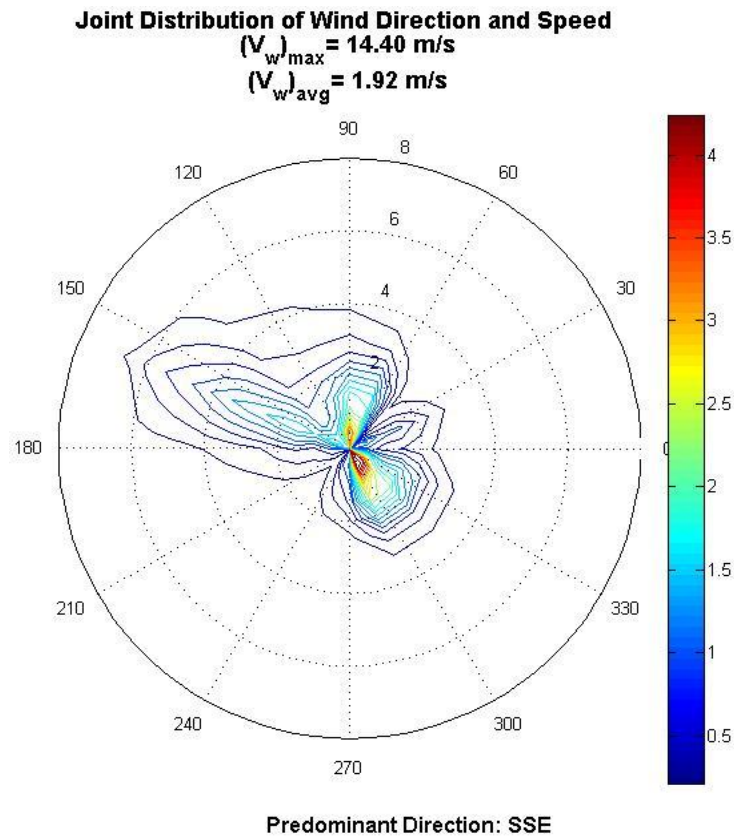


Figure 3.5. Joint probability of wind speed and direction for Izmit weather station data (radial axis: wind speed [m/s], angles: direction where the winds come from [$^{\circ}$], contours: probability of occurrence [%]).

Wave spectra were calculated according to one of the wave prediction models, the JONSWAP spectrum which is based on experimental data (SPM, 1984). The JONSWAP spectrum has the form,

$$S(\omega) = \alpha \frac{g^2}{\omega^5} \times e^{-1.25 \left(\frac{\omega_m}{\omega} \right)^4} \times \gamma e^{\left(\frac{-(\omega - \omega_m)^2}{2(\sigma \omega_m)^2} \right)} \quad (3.1)$$

where γ is the peak shape parameter and taken as 3.30, α is equal to $0.076 \bar{x}^{0.22}$ where \bar{x} is the dimensionless fetch, σ is 0.07 for $\omega \leq \omega_m$ and 0.09 for $\omega > \omega_m$ and ω_m equals to $(2\pi)3.5(g/\bar{U})\bar{x}^{-0.33}$ where \bar{U} is the wind speed at 10 meter above the sea level.

As seen in the formula, the JONSWAP spectral formulation depends on wind speed and fetch length.

The significant wave height (H_s) and peak wave period (T_m) are formulated as follows by using the JONSWAP spectrum.

$$H_s = (5.112 \times 10^{-4}) \times U \times F^{1/2} \quad (3.2)$$

$$T_m = (6.238 \times 10^{-2}) \times (U \times F)^{1/3} \quad (3.3)$$

where F is fetch length and U is the wind speed at 10 meter above the sea level.

Fetch lengths for each geographic direction were taken as the linear distance from the coordinates 40°44'44.00" N latitude and 29°47'57.38" E longitude to the farthest Marmara Sea coast in that direction.

Joint probabilities (significant wave height-wave direction and peak wave period-wave direction and significant wave height-peak wave period) of both stations are shown in Figure 3.6, Figure 3.7 and Figure 3.8, respectively.

The summary of all wind and wave parameters is given in Table 3.1 for both station records. Other studies about meteorology that contain detailed information are given in Appendix A. To be on the safe side, local station results are preferred as design parameters.

Table 3.1. Wind and wave parameters.

	Local Station	Izmit Station
Measurement Period	2 years	29 years
Predominant Wind Direction	ESE	SSE
Max. Wind Speed	17.9 m/s	14.4 m/s
Predominant Wave Direction	ESE	SE
Max. Significant Wave Height	1.22 m	1.01 m
Max. Peak Wave Period	4.47 s	4.2 s

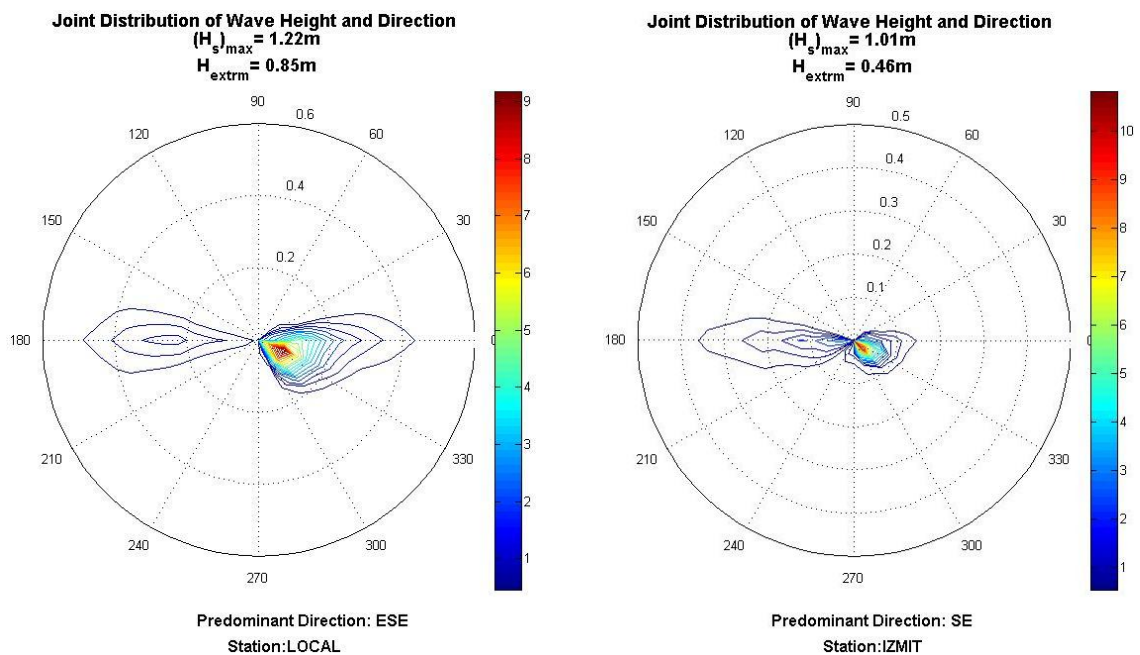


Figure 3.6. Comparison of local and Izmit stations according to the joint distribution of wave height and direction (radial axis: wave height [m], angles: direction where the waves come from [°], contours: probability of occurrence [%]).

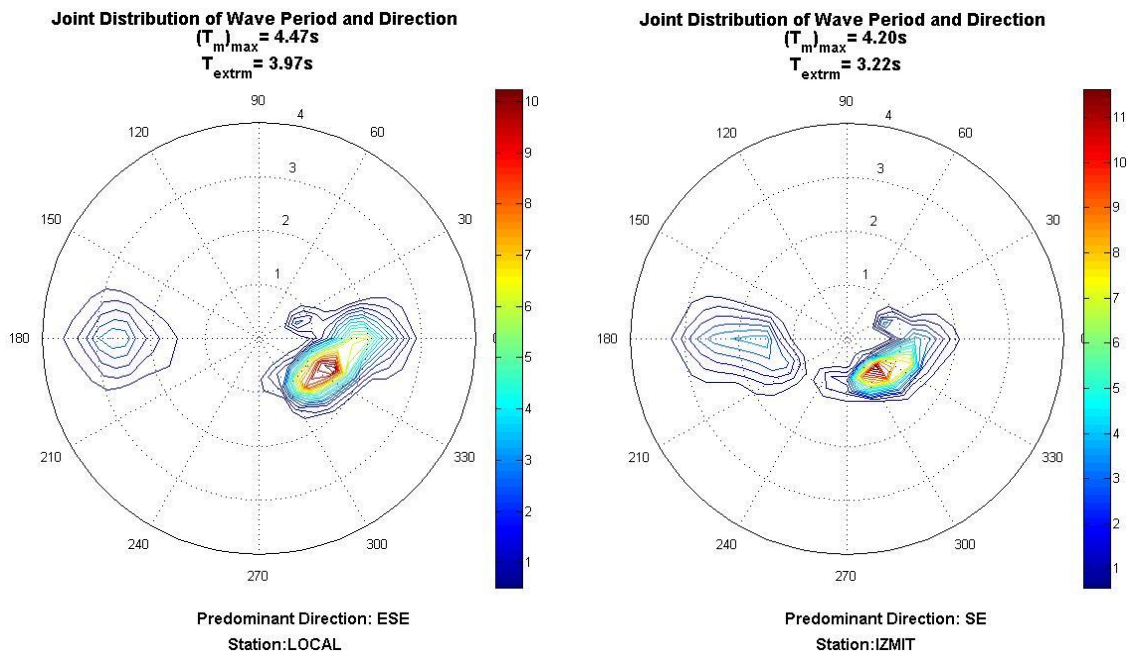


Figure 3.7. Comparison of local and Izmit stations according to the joint distribution of wave period and direction (radial axis: wave period [s], angles: direction where the waves come from [°], contours: probability of occurrence [%]).

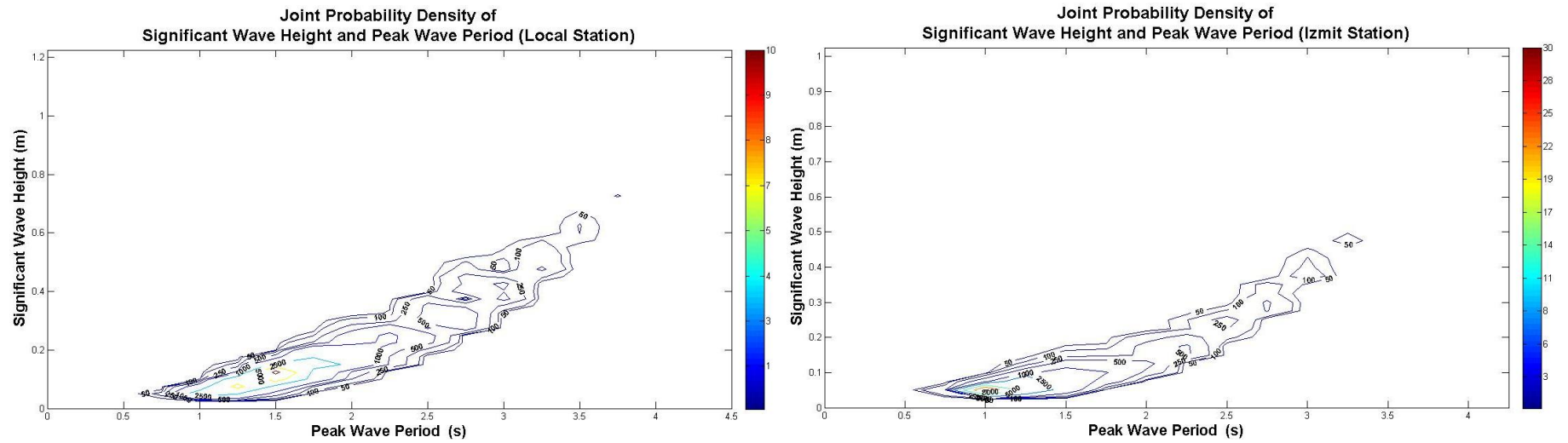


Figure 3.8. Comparison of local and Izmit stations according to the joint distribution of significant wave height and peak wave period (contours: number of occurrences, color bar: probability of occurrence [%]).

3.3. Nearshore Topographic and Hydrographic Surveys

In addition to compilation of existing information, some of the necessary data were obtained by measuring in the field. These are the measurement of bathymetry, shoreline and offshore profiles and collection of dry and wet sediment samples. Obtained data were analyzed in the laboratory and numerically.

3.3.1. Bathymetry and Shoreline Measurements

Nearshore bathymetry measurements were carried out by three separate groups. These are (i) a private hydrographic survey company (March 11, 2011), (ii) The Municipality of Kocaeli who measured the coastal topography and shoreline (June 20, 2011) and (iii) Boğaziçi University researchers who measured the coastal profiles (June 20, 2011).

Hydrographic measurements were carried out in March 2011 by MCH-TECH Marine Research Company through making use of a boat equipped with RTK-GPS and sonar (Figure 3.9). Data were collected on 12 lines perpendicular to the shore at approximately 200 m intervals, and on 2 lines parallel to the shore (Figure 3.10).



Figure 3.9. Boat survey equipment.

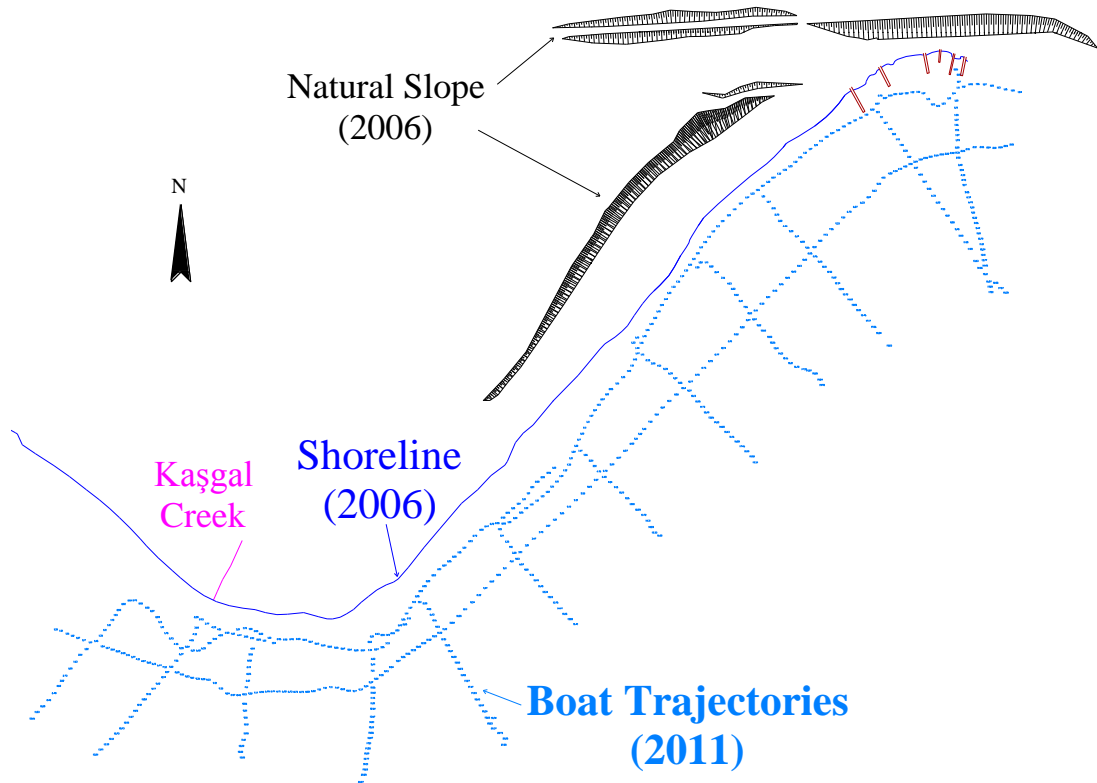


Figure 3.10. Hydrographic survey trajectories (MCH-TECH Marine Research, 2011).

Measurements showing the shoreline are available for four different times. These are (i) the shoreline for the period prior to filling (the Setback Line, the exact date is unknown but is estimated as before 1999), (ii) the shoreline drawn by the Municipality through using the aerial photograph of 2006, (iii) the shoreline measured under the current project by the Department of Infrastructural Operations of the Municipality on January 21, 2011 and (iv) the shoreline measured by the Department of Housing and Urban Development of the Municipality on June 14, 2011. These four different shorelines are shown in Figure 3.11.

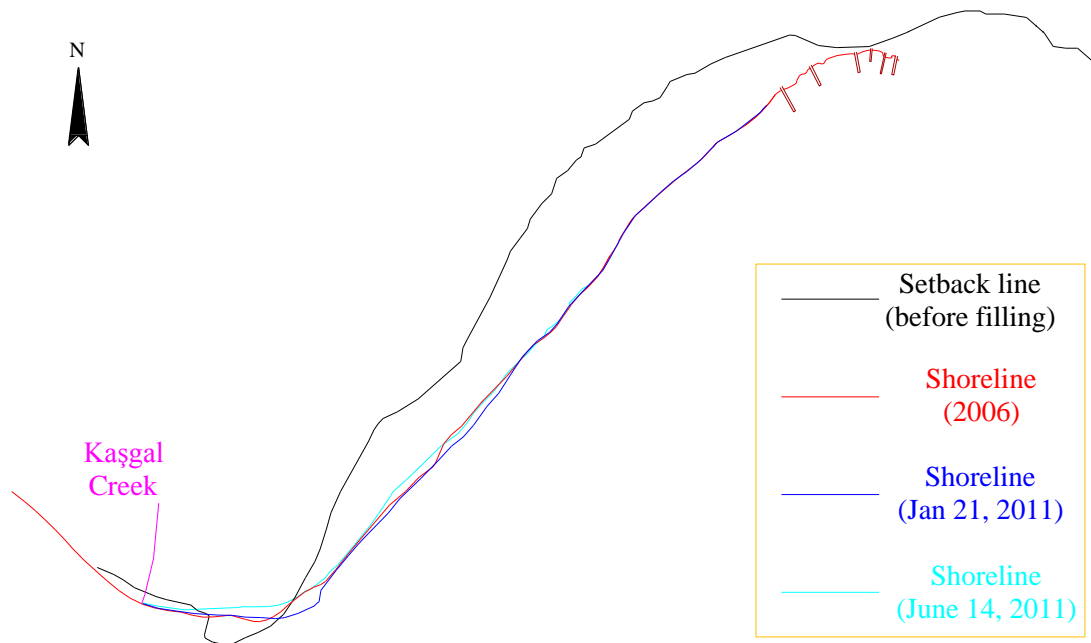


Figure 3.11. Shorelines at four different times.

Landward coastal topography was measured by the Department of Housing and Urban Development of the Municipality on June 14, 2011. Finally, the gaps between topographic and hydrographic measurements were filled with the help of a swimmer and using the leveling method.

3.3.2. Survey of Coastal Profiles

Using the bathymetry and topography data sets, coastal profiles are formed on six pre-determined sections along the coast (Figure 3.12). These profiles will be used in the equilibrium profile calculation and beach nourishment design.

The measured profiles do not exactly follow the equilibrium beach profile form (Figure 3.13) prescribed by Dean (1977). The reasons can be the lack of equilibrium due to the coastal fill and presence of silt and clay in the native bottom.

Alternative solutions produced for the creation of equilibrium through adding new sand are examined in later parts.

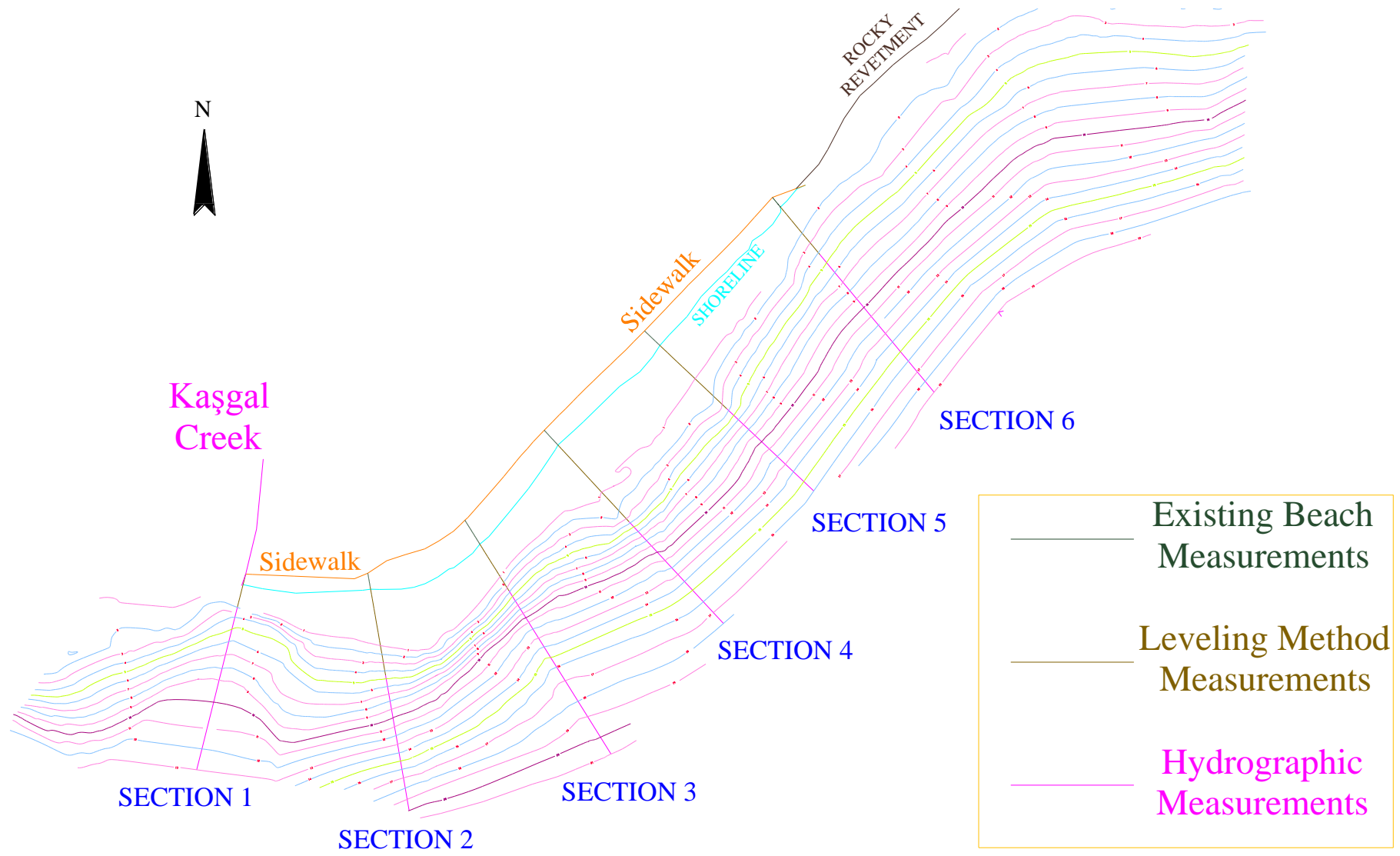


Figure 3.12. Coastal profiles in plan view.

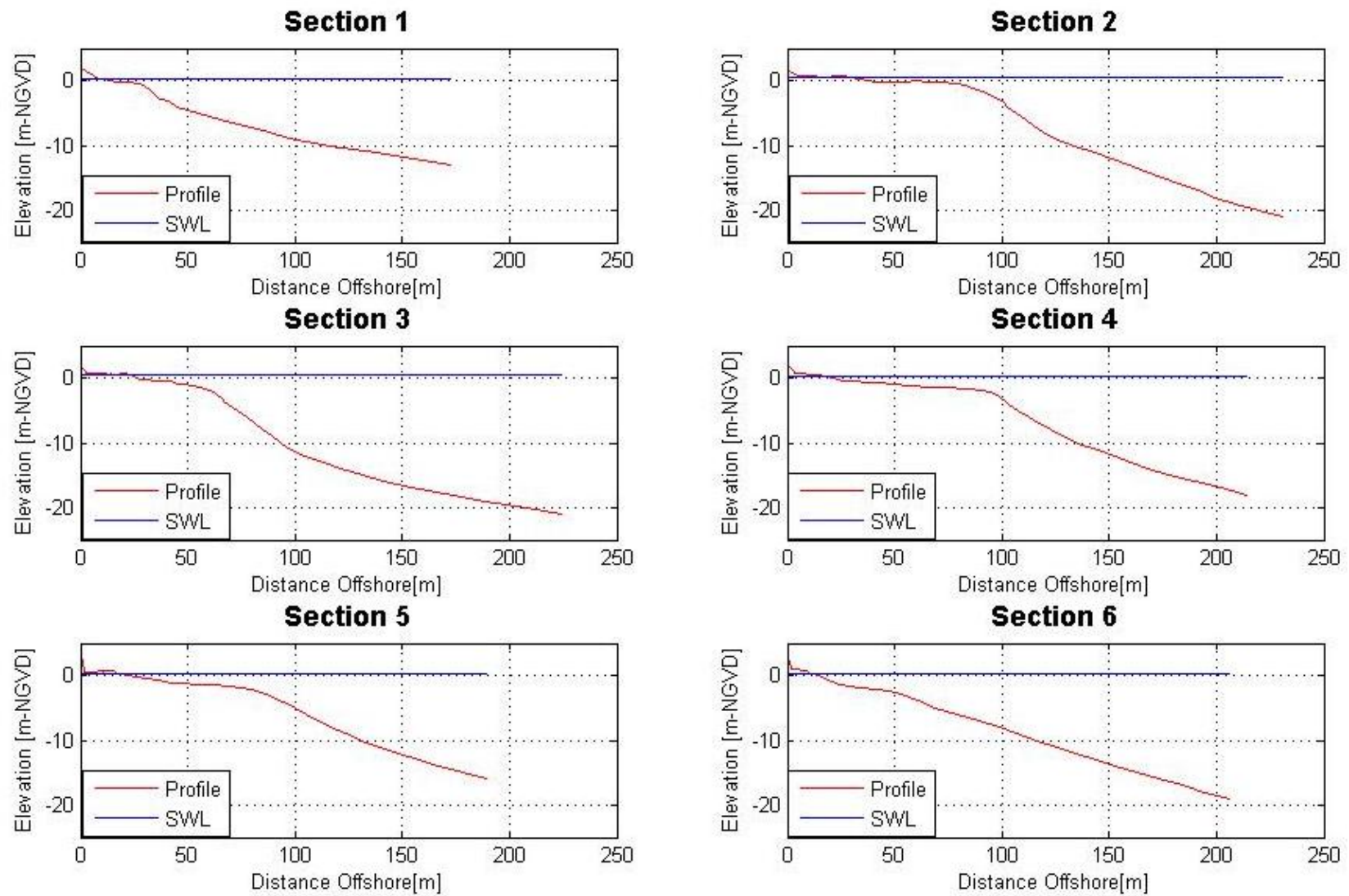


Figure 3.13. Coastal profiles in side view.

3.4. Sediment Characteristics of the Nearshore

Determination of the material lying on the sea floor is quite important for the future of rehabilitation studies. In this regard, surface sediment samples are collected from the existing beach and seabed on four sections at various depths (Figure 3.14). To collect seabed sediment samples, divers and a Van Veen-type seabed sediment collector were used (Figure 3.15).

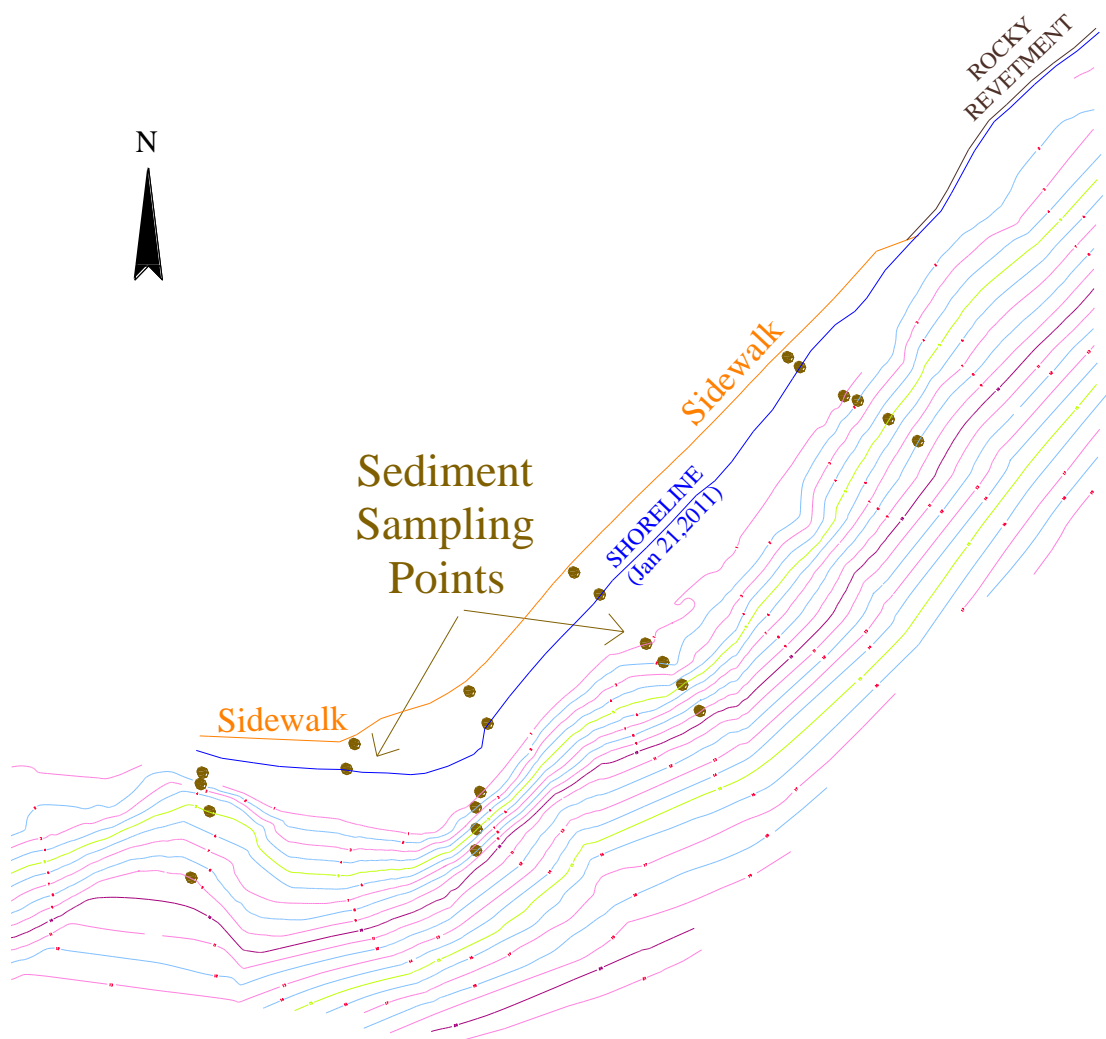


Figure 3.14. Locations of the sediment samples.

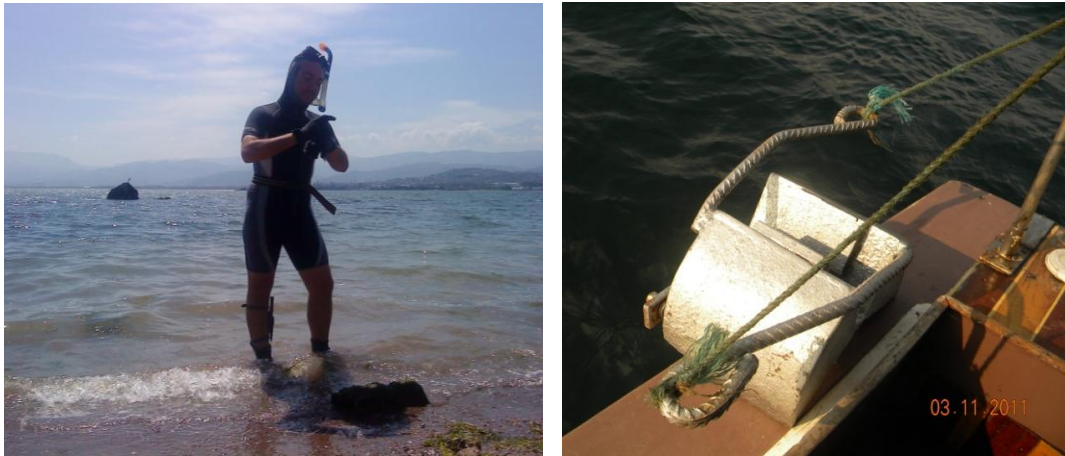


Figure 3.15. Seabed sediment sampling techniques.

The content and sieve analysis results of each sample taken from different depths of four sections are summarized in Table 3.2. Median diameter variation of each section is shown in Figure 3.16.

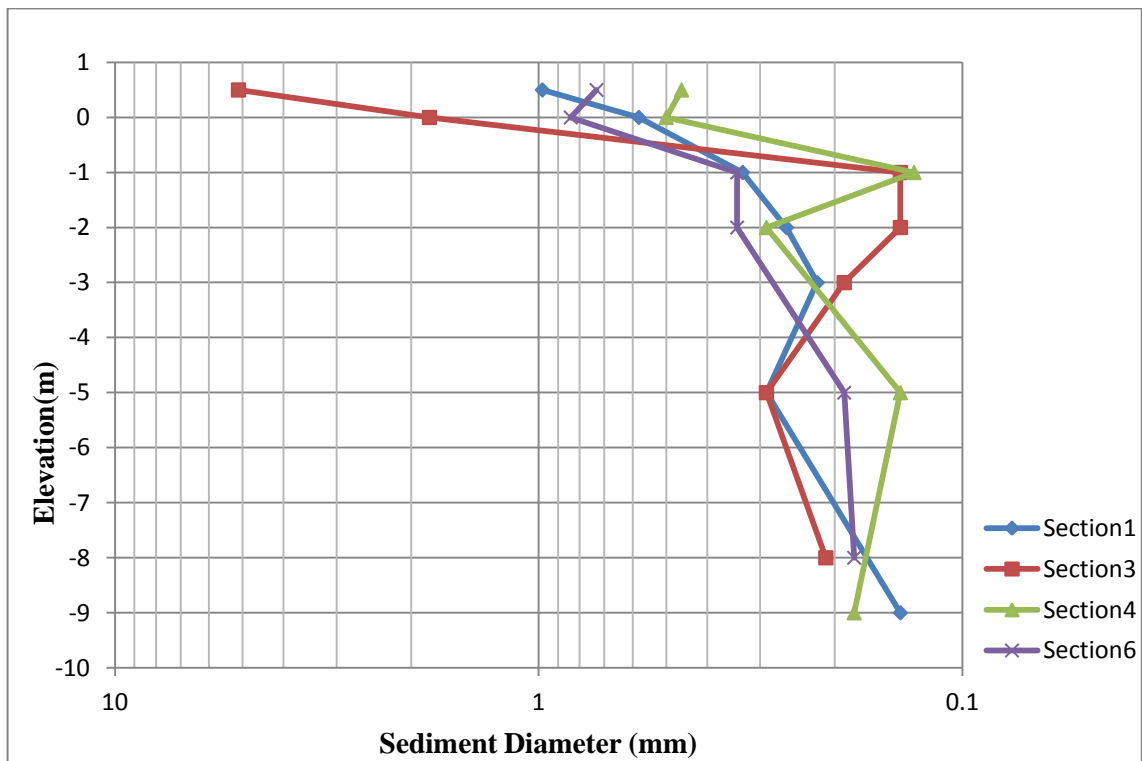


Figure 3.16. Variation of sediment median diameter (D_{50}) in sections.

Table 3.2. Sieve analysis results of the existing beach and seabed sediments.

Section No.	Elevation (m)	Sample Weight (g)	Organic Content (%)	Median Diameter (D_{50} , mm)	Fine Sediment (%)	Unified Soils Classification
1	0.5	956.3	0	0.98	0	Medium Sand
	0	907.1	0	0.58	0	Medium Sand
	-1	1326	1	0.33	0	Fine Sand
	-2	1239	1	0.26	1	Fine Sand
	-5	819.3	6	0.29	4	Fine Sand
	-9	405.4	49	0.14	30	Fine Sand
3	0.5	772	0	5.11	0	Fine Gravel
	0	930.4	0	1.81	0	Medium Sand
	-1	884.2	1	0.14	8	Fine Sand
	-2	736.3	2	0.14	9	Fine Sand
	-5	1611	3	0.29	3	Fine Sand
	-8	687	36	0.21	11	Fine Sand
4	0.5	487	0	0.46	0	Medium Sand
	0	774.3	0	0.5	0	Medium Sand
	-1	765.2	51	0.13	14	Fine Sand
	-2	1217	17	0.29	2	Fine Sand
	-5	725.7	74	0.14	23	Fine Sand
	-9	746	50	0.18	13	Fine Sand
6	0.5	644.2	0	0.73	0	Medium Sand
	0	658.5	0	0.84	3	Medium Sand
	-1	1008	12	0.34	5	Fine Sand
	-2	631.8	25	0.34	2	Fine Sand
	-5	872.5	81	0.19	20	Fine Sand
	-8	545.2	69	0.18	23	Fine Sand

Organic content column in Table 3.2 gives the amount of mussels and algae attached to No.4 sieve ($D > 4.76$ mm) as a percentage of total sample weight. For the remaining inorganic (granular) parts, the median diameter (D_{50}) and the percentage of fine material (sediment passing No. 200 sieve) were determined through sieve analysis. Finally, by considering median diameter, sediment types were classified according to the Unified Soils Classification. The sediment map of the project site (Figure 3.17) is drawn using Table 3.2.

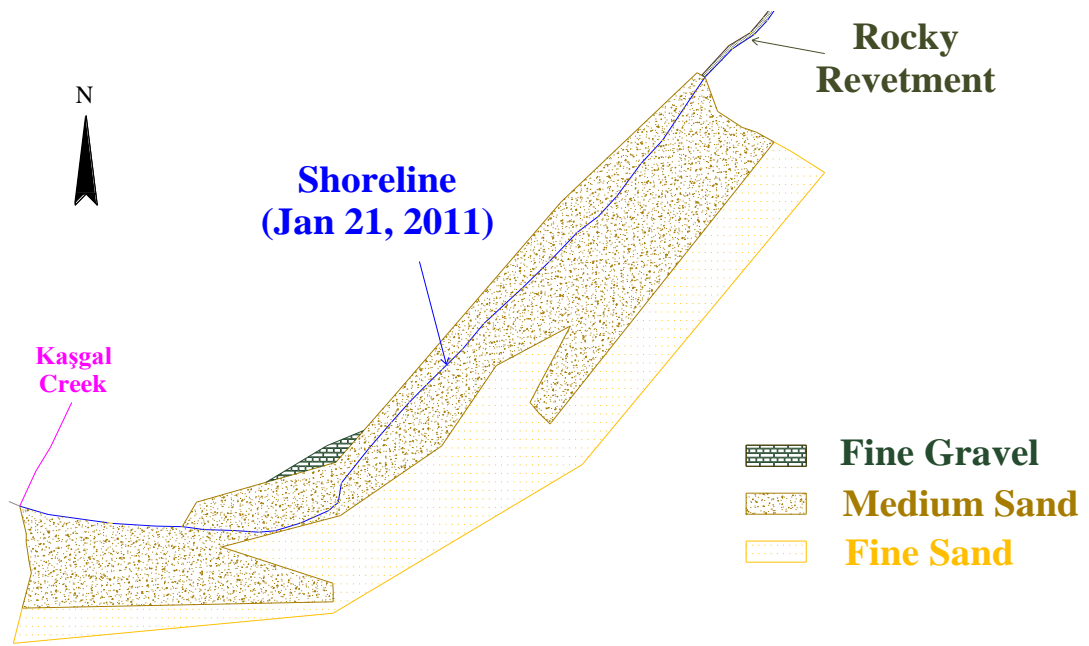


Figure 3.17. The sediment map of the project site.

It is apparent that the granular structure of the existing beach contains a small amount of fine material (silt and clay). However, the fine content increases in deeper zones. The change of grain size with depth is shown in Figure 3.18 regardless of section differences. Cohesive/non-cohesive interface of profiles are shown in Appendix B.1.

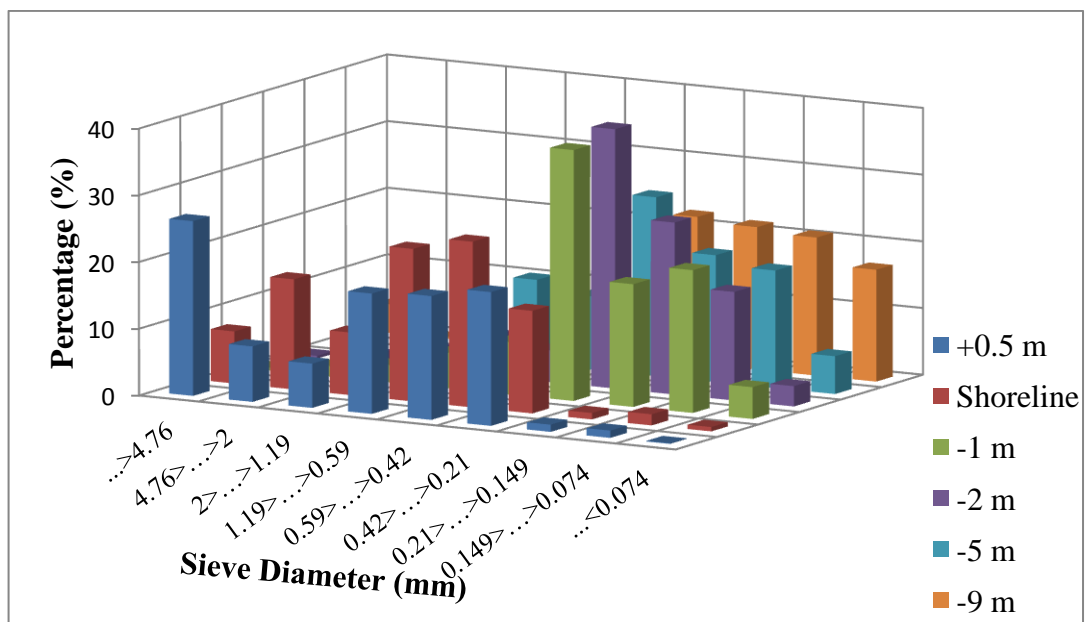


Figure 3.18. Change in sediment size with respect to depth.

In addition, increase in organic content rates particularly at -2 m and deeper regions are noteworthy (Figure 3.19). It is important that before nourishment work, marine fauna and flora should be examined in more detail and no sand would be placed over such organisms.

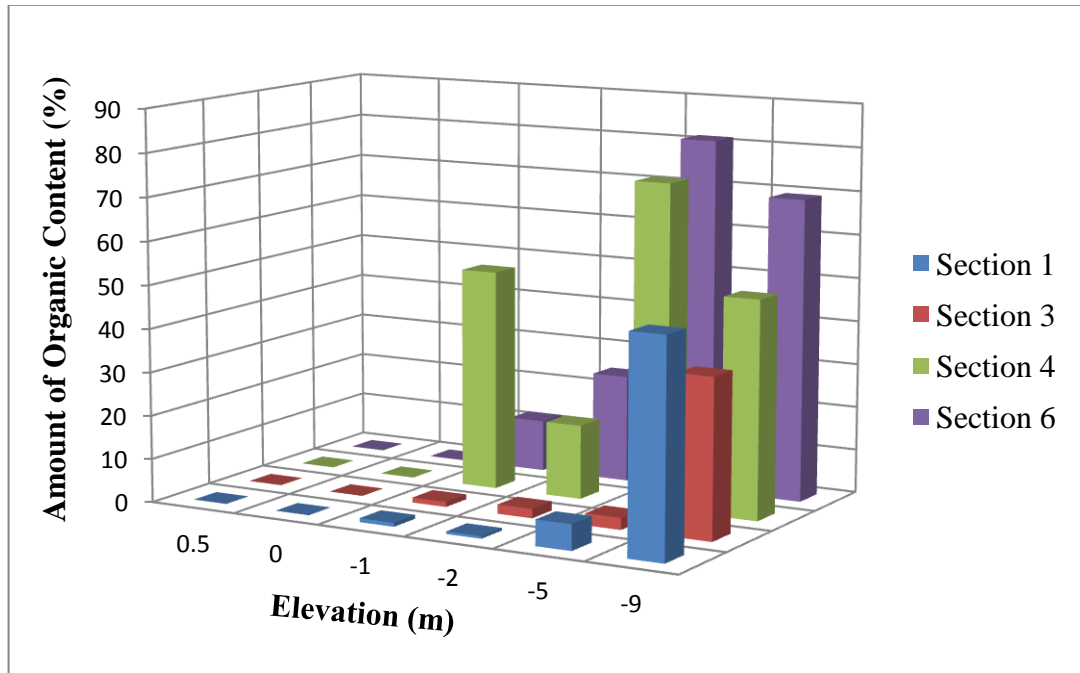


Figure 3.19. Change in organic content ratio with respect to depth.

4. LABORATORY MODEL

In order to examine the possible interaction between the mixed natural soil and nourishment sand, it was decided to establish a physical model. The experiment was conducted in the Hydraulic Laboratory of Karadeniz Technical University (KTU).

4.1. Supply of the Necessary Material

To be used as native material in the model, natural sediment was extracted from the sea bottom at three different points in the project area (Figure 4.1). Approximately 10 m^3 sediment was taken from the seabed. The median grain diameter of the material is found to be 0.13 mm (Figure 4.2). Nourishment sand which has 0.18 mm diameter (well-sorted) for the model was provided by KTU.



Figure 4.1. Extraction of model native material.

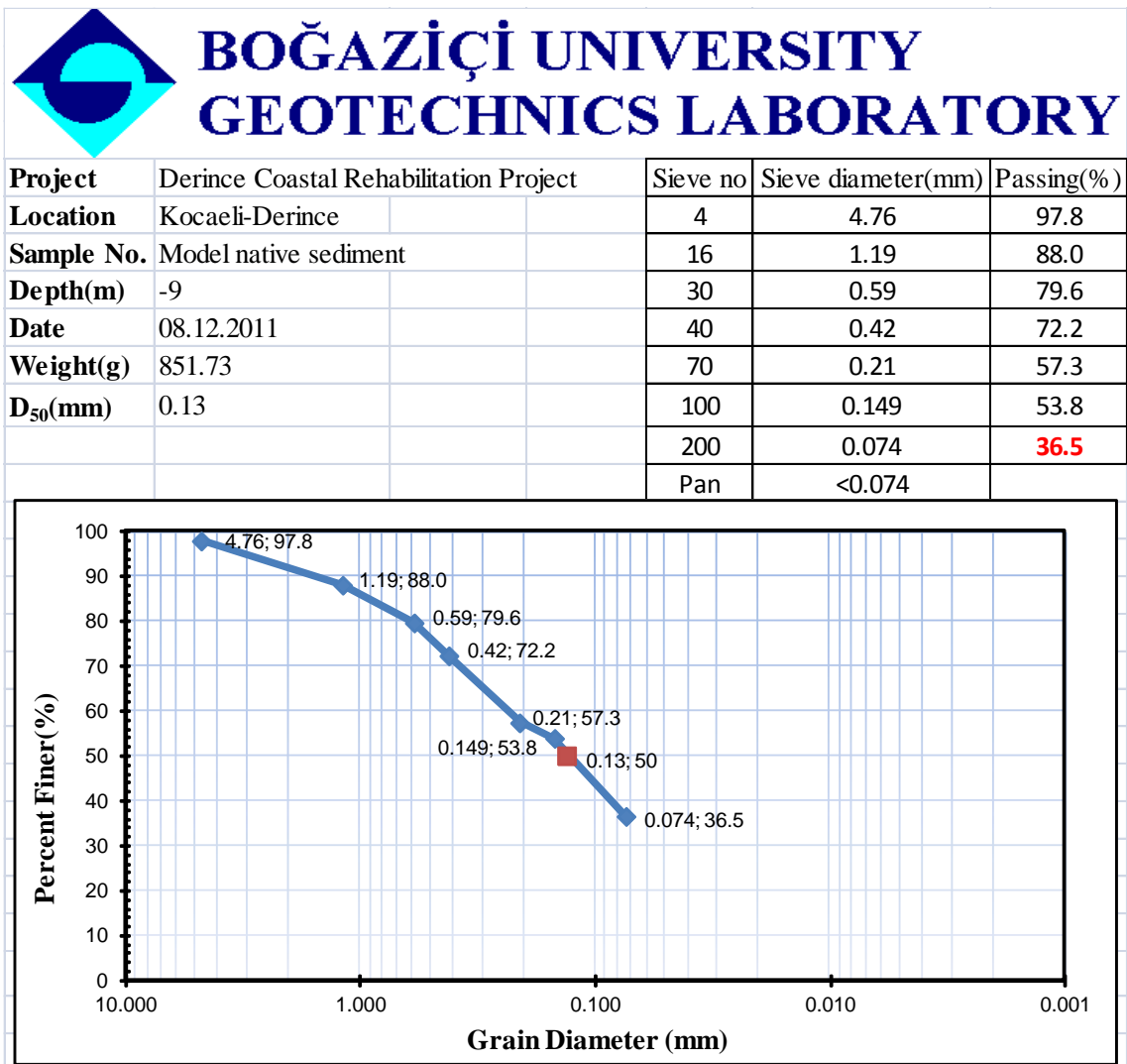


Figure 4.2. Sieve analysis of model native sediment.

4.2. Properties of the Wave Flume

The KTU flume is made of concrete with dimensions of 32.5 m length, 1.4 m width and 1.2 m depth. The wave maker which produces the desired wave spectrum is controlled by a hydraulic and computer combined system designed by the KTU staff and it can generate regular and irregular waves. The software creates a surface elevation according to the JONSWAP spectrum by using the total energy of the desired wave. The maximum water depth that can be used in the channel is 0.8 m. Figure 4.3 shows the flume properties schematically.

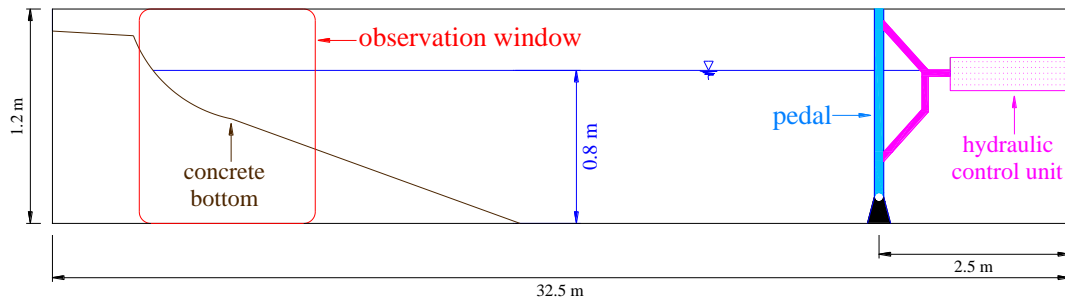


Figure 4.3. Schematic representation of the flume.

4.3. Determination of the Model Scale

Scale of the physical model was determined by comparing three different laboratory model criteria.

4.3.1. Noda's Modeling Criteria

Noda (1971, 1972) developed an empirical relationship based on his laboratory tests. He found that profile similitude could not be formed (for tested sediment sizes) unless the model horizontal scale was different from the vertical scale (i.e., a distorted model). Noda introduced the following relationships between the horizontal scale (N_x), the vertical scale (N_z), and the sediment diameter scale (N_d). It should be noted that these relationships are valid if the model sediment has the same density as the prototype.

$$N_d = (N_z)^{0.55} \quad (4.1)$$

$$N_x = (N_z)^{1.32} \quad (4.2)$$

The model, therefore, has a distortion ($\Omega = N_x / N_z$) of

$$\Omega = (N_z)^{0.32} \quad (4.3)$$

It is important to note that Noda's distortion is only for the beach profile, not for the waves because the hydrodynamics were scaled according to geometrically undistorted Froude scaling which is based on the vertical scale.

4.3.2. Ito and Tsuchiya's Modeling Criteria

Ito and Tsuchiya (1984) conducted experiments in two wave flumes to develop scale criteria to model equilibrium beach profiles. The equilibrium profiles that developed in the larger flume were taken as prototype, and tests in the smaller flume were scaled according to the larger flume conditions based on the Froude criterion. They compared the profile evolution between prototype and model and introduced an empirical relationship between the length scale (N_L) and the sediment diameter scale (N_d) which is given as

$$N_d = (1.7)^0 (N_L)^{0.83} \quad \text{for } N_L \leq 2.2 \quad (4.4)$$

and

$$N_d = (1.7)^1 (N_L)^{0.2} \quad \text{for } N_L > 2.2 \quad (4.5)$$

4.3.3. Hallermeier's Modeling Criteria

Hallermeier's (1985) modeling law was based on maintaining similarity of a ψ parameter which gives the ratio of normalized horizontal velocity to the vertical velocity between prototype and model while scaling the hydrodynamics according to Froude scaling criterion.

$$\psi = \frac{(V_x / U_*)}{V_z} \quad (4.6)$$

where V_x is the horizontal velocity, V_z is the vertical velocity and U_* is the critical velocity for incipient motion of the sediment.

The model distortion was given as

$$N_{U_*} = \frac{N_x}{N_z} = \Omega \quad (4.7)$$

Hallermeier used two formulas to represent the critical velocity for sediment motion. For prototype the critical velocity was given as

$$(U_*)_p = \sqrt{8 \times \rho_p' \times g \times d_p} \quad (4.8)$$

where ρ_p' is the prototype sediment immersed relative density, d_p is the prototype sediment median diameter, and g is gravity.

In the model the critical velocity can be represented as

$$(U_*)_m = 0.14(\rho_m' g)^{3/4} d_m^{1/4} T_m^{1/2} \quad (4.9)$$

where the subscript m refers to model values, and T_m is the model wave period.

Forming the scale ratio of U_* gives

$$N_{U_*} = 20.2(N_{\rho'} N_d)^{1/2} \left(\frac{d_m}{\rho_m' \times g \times T_m^2} \right)^{1/4} \quad (4.10)$$

which is expressed according to scale ratios and model parameters.

Hallermeier's modeling law requires recalculation of the length scale for different wave periods due to his assumption that the first movement of sediment is controlled by different relationships in different regimes.

4.3.4. Comparison of Model Criteria and Selection of Model Scale

Laboratory limitations especially on the vertical dimension and the sediment diameter have made the selection of the model scales difficult. In other words, the dependency between the vertical and the diameter scale greatly restricts the choice of the model scale (Equation 4.1, 4.3 and 4.4). The model fill sediment diameter should be large enough to behave as non-cohesive and small enough to represent medium size nourishment sand (after applying the scale factor) in the prototype. The maximum wave height that can be generated in the laboratory was the most effective parameter in the determination of the length scale. These constraints limited the range of the model scale options. Table 4.1 gives the computed values for three modeling criteria.

Table 4.1. Comparison of model criteria.

		Units	Noda	Ito and Tsuchiya	Hallermeier
Prototype	$H_s(\max)$	m	1.22	1.22	1.22
	h_c	m	1.62	1.62	1.62
	h_{\max}	m	5.60	5.60	5.60
	D_{native}	mm	0.30	0.30	0.30
	D_{fill}	mm	0.45	0.45	0.45
	T_{\max}	s	4.47	4.47	4.47
	T_m	s	1.90	1.90	1.90
Model	$H_s(\max)$	m	0.18	0.18	0.18
	h_c	m	0.23	0.23	0.23
	h_{\max}	m	0.80	0.80	0.80
	D_{native}	mm	0.10	0.12	0.11
	D_{fill}	mm	0.15	0.18	0.25
	T_{\max}	s	0.91	1.69	1.69
	T_m	s	0.39	0.72	0.72
Scale	vertical (N_Z)		7.00	7.00	7.00
	horizontal (N_X)		13.05	7.00	14.00
	distortion (Ω)		1.86	1.00	2.00
	diameter (N_d)		2.92	2.51	1.78
	time (N_T)		4.93	2.65	2.65

Among all three alternative models (Noda, Ito and Tsuchiya, and Hallermeier) Ito's modeling criteria provides the best match between the limited alternatives for fill sediment available in the laboratory and the measured prototype sediment diameter. Noda's modeling criteria were not used because its sediment diameter scale formulation gives very small model diameters for the native and fill sediments. Hallermeier's scaling criteria necessitates determining the length scale for each wave period; therefore, it would not be used for the present experiment. As a result, according to the results given in Table 4.1, the usage of Ito and Tsuchiya's (1984) modeling criteria is the most suitable one for this study.

4.4. Establishment of the Laboratory Model

4.4.1. Determination of the Wave Conditions

Hydrodynamic conditions are designated according to the waves generated from two-year wind data through selecting the largest and the most long-lasting four storms. Storms chosen from all the waves and their corresponding periods are shown in Figure 4.4.

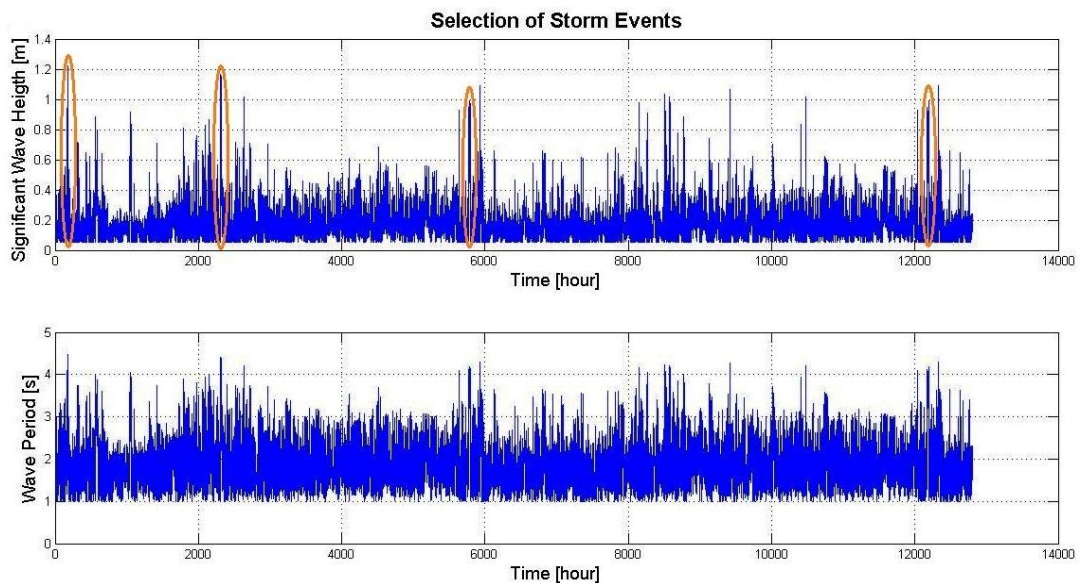


Figure 4.4. Selection of storms from the data.

Since it is not possible to generate the exact wave height variation of a selected storm with the existing wave maker (i.e. Figure 4.5), each storm event is represented by three to four consecutive wave groups consisting of a uniform wave height (average of the group) and the average wave period for the selected storm duration. Figure 4.5 shows the grouping for the first storm.

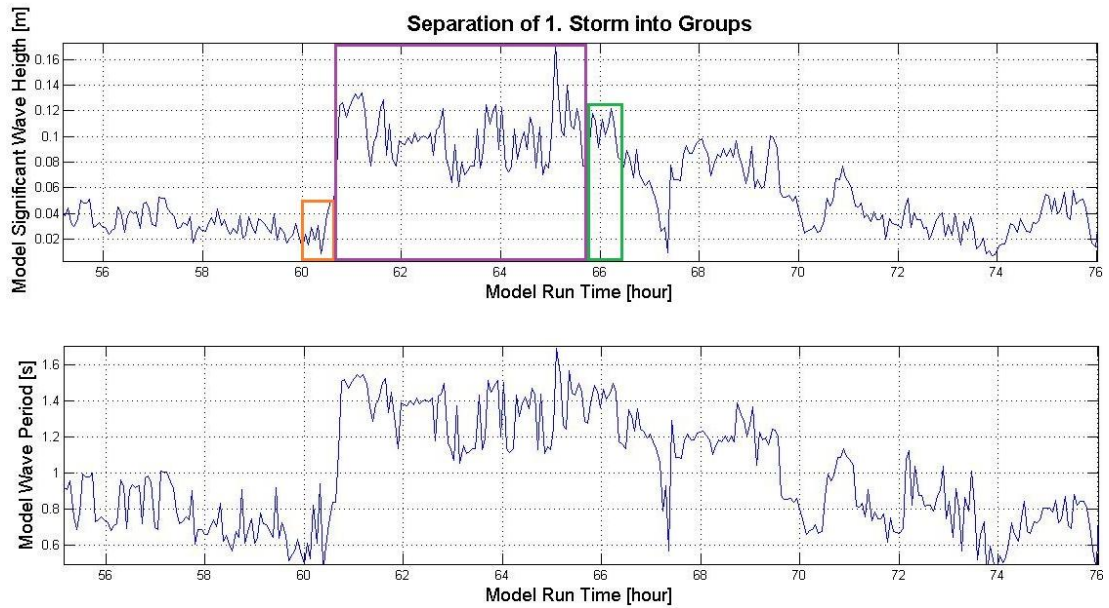


Figure 4.5. Grouping for the first storm.

After grouping, the wave maker was calibrated according to wave parameters. For each selected storm event, grouping and calibration values are given in Table 4.2

Table 4.2. Significant wave height, peak wave period and run time values for each storm event.

	After Grouping			Generated in the Lab.		
	H _s [mm]	T _m [s]	t _m [min]	H _s [mm]	T _m [s]	t _m [min]
Storm 1	34	0.8	15	27.2	0.80	25
	120	1.4	298	107.3	1.39	268
	94	1.4	72	109.9	1.25	48
Storm 2	135	1.5	57	134.6	1.52	240
	60	1.3	61	71.8	1.29	110
	140	1.6	320	171.7	1.60	225
	60	1.4	102	78.1	1.39	150
Storm 3	111	1.4	87	129.9	1.40	90
	70	1.4	181	80.4	1.40	120
	120	1.5	174	158.8	1.44	145
Storm 4	120	1.4	234	139.0	1.39	200
	80	1.3	196	95.1	1.29	145
	30	0.7	162	26.6	0.7	180
Total time	1959			1946		

4.4.2. Calibration of the Wave Maker

In physical models, in order to generate desired wave conditions in the laboratory, calibration of the wave maker is required. Wave parameters prescribed from selected storms were imported to the wave maker's software and created waves were measured in deep water to make a comparison between generated and desired values.

After intensive studies to attain predetermined wave conditions, the final approximations to the real values are given in Table 4.2. The difference between generated and pre-determined storm conditions' wave parameters was calculated using the root mean square method.

$$\varepsilon_{rms} = \sqrt{\frac{1}{n} \sum_{i=1}^n [H_{p_i} - H_{m_i}]^2} \quad (4.11)$$

where H_{p_i} is the wave height in the prototype and H_{m_i} is the wave height generated in the model.

The differences for the wave height and the wave period were determined as 1.8 cm and 0.05 s respectively.

4.4.3. Placement of the Model Material

According to the computations given in Table 4.1 the horizontal scale (N_x), the vertical scale (N_z), the sediment diameter scale (N_d), and time scale (N_T) are determined. The model dimension lines were drawn on wave channel walls according to Ito and Tsuchiya's modeling criteria by assuming that the shoreline advance after nourishment is to be 15 meters in prototype (Figure 4.6). The calculation of offshore limit of sediment motion (closure depth) will be examined in detail in the following part.

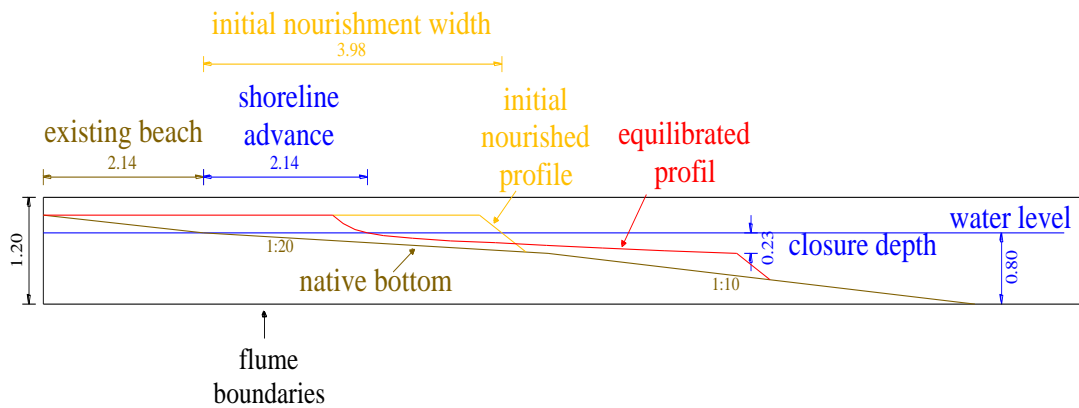


Figure 4.6. Model dimensions (horizontal and vertical scales: $N_x = N_z = 7$, diameter scale:

$N_d = 2.51$, time scale: $N_T = 2.65$, model native sediment: $D_{native} = 0.13$, model fill

sediment: $D_{fill} = 0.18$).

Natural bottom and nourishment sand of the model are placed in the flume (Figure 4.7). Due to the muddy structure of the native material, it was impossible to form a smooth natural bottom which did not affect the test results because after all storms, no change was observed on the above mentioned uneven bottom in the deeper part of the flume. Even a

footprint that was left accidentally on the sea bed was seen to be preserved after the experiment.



Figure 4.7. Placement of the model materials into the wave channel.

4.5. Results

Following the placement of model material into the flume, waves were generated according to the calibrated values. Profile measurement and sediment sampling were done after every storm event. Model profile evolution is given in Figure 4.8.

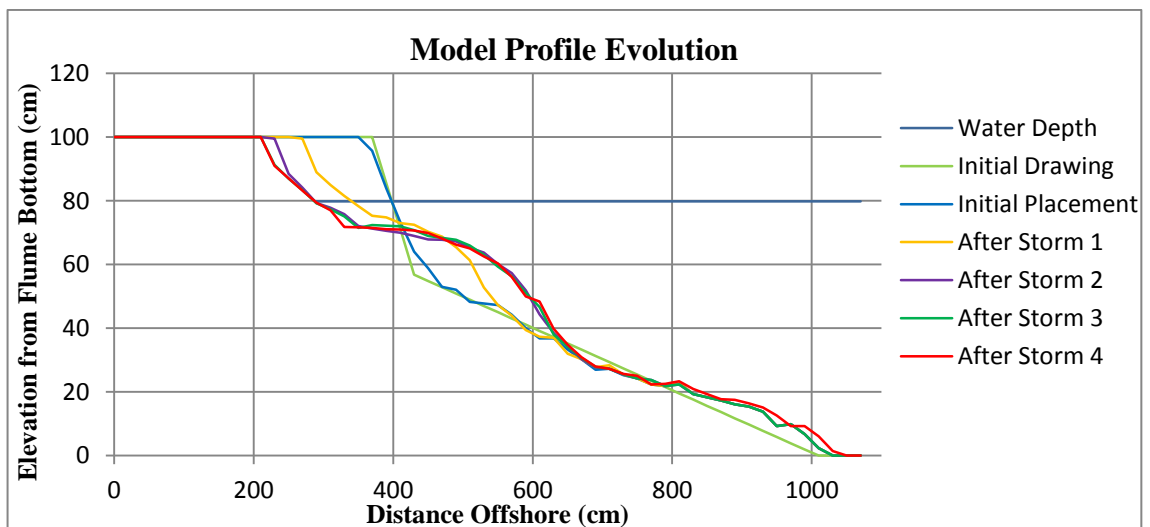


Figure 4.8. Profile evolution of the model.

Sieve analyses were done after every storm to examine the mixing interaction between silt/clay dominated native material and nourishment sand. Table 4.3 shows that fine material in the native soil was not mixed in the fill sand.

Table 4.3. Median diameters of bottom samples (numbers in mm).

Distance Offshore [cm]	350	400	450	500	550	600	650
After Storm 1			0.18	0.18	0.17		
After Storm 2	0.18		0.19	0.18		0.18	0.15
After Storm 3		0.18				0.18	
After Storm 4						0.19	

Figure 4.10 shows the difference between theoretical equilibrium beach profile and the model profile. As it can be seen from the figure, profile adjustment and shoreline recession have not reached the full equilibrium form as it was shown in the original laboratory experiment of Hallermeier (1978) and the experiment of Srisuwan *et al.* (2011) who used the same flume. The reasons for the lack of full equilibrium might be the run time constraints in the laboratory and a possible damping of wave energy over the deeper mud bottom (Dean and Dalrymple, 1984). However, this second effect requires further investigations. Figure 4.9 shows the situation after the discharge of the water.



Figure 4.9. The model profile after water discharge.

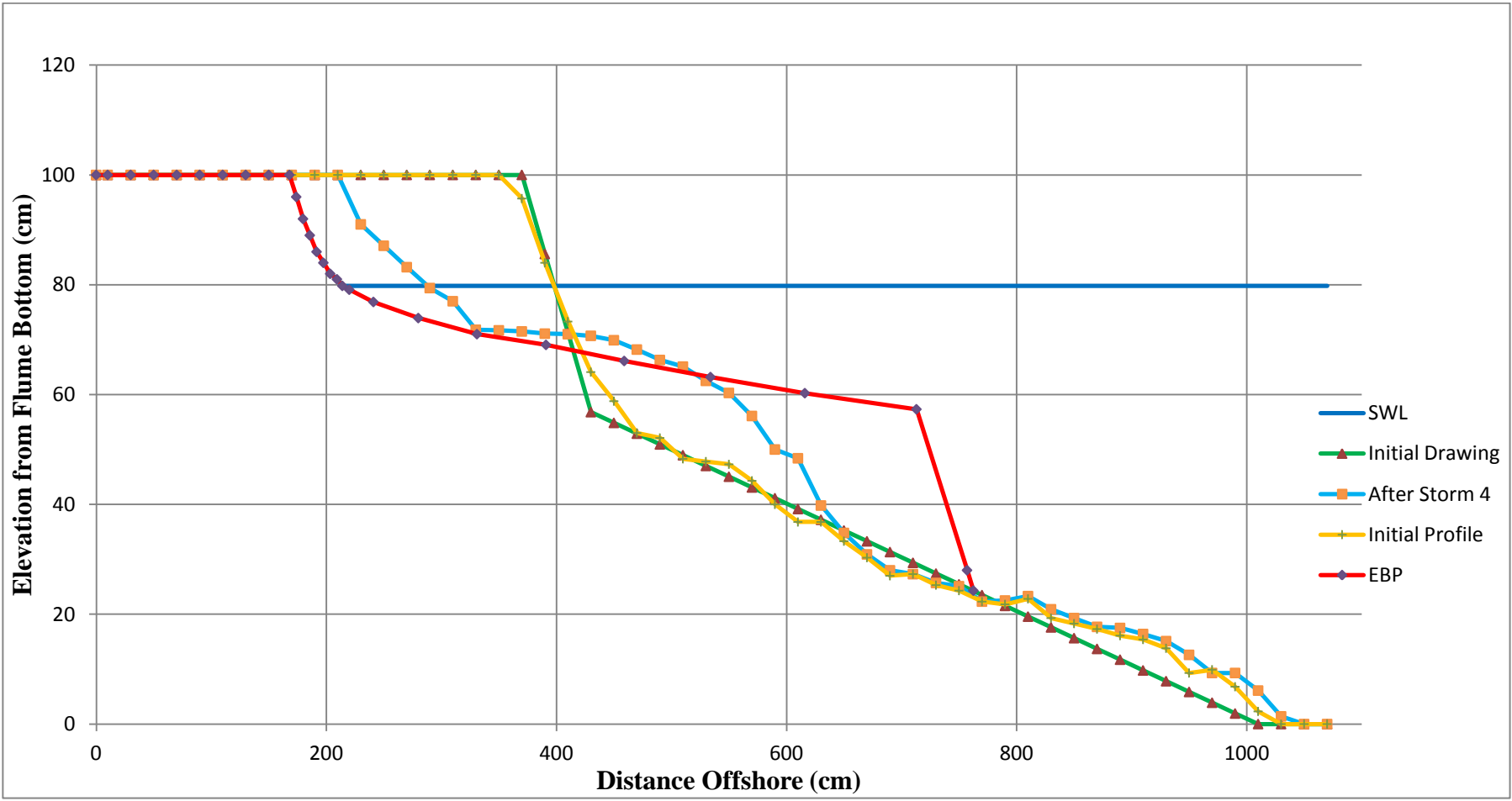


Figure 4.10. Comparison of the theoretical and model profiles before and after wave penetration.

5. ENGINEERING DESIGN

5.1. Equilibrium Beach Profiles

For the improvement of the existing 600 m long sandy beach by sand addition, alternative widths have been considered. The foreseen changes after nourishment on the coastal profile are shown in Figure 5.1 schematically.

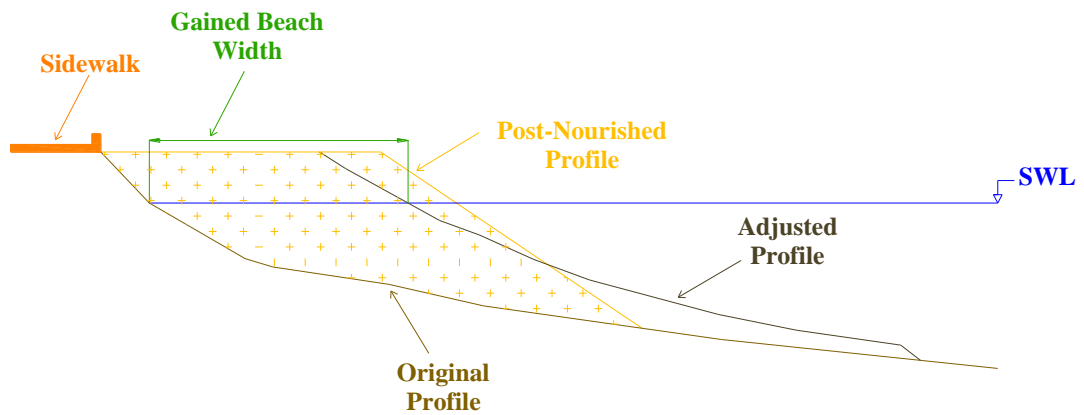


Figure 5.1. Typical nourished coastal profile scheme.

The initial width and slope of the new beach varies according to the volume and median diameter of sand used for nourishment. The equilibrium positions of the new profiles (adjusted profiles) are determined according to previously discussed equilibrium beach profile theory (Bruun, 1954; Dean, 1977; Moore, 1982).

The offshore limit of the sediment motion, closure depth (h_c), is calculated using the following expression (Hallermeier, 1978).

$$h_c = 2.28H_e - 68.5 \left(\frac{H_e^2}{gT_e^2} \right) \quad (5.1)$$

where H_e is the nearshore significant wave height exceeded 12 hours per year and T_e is the corresponding wave period.

Extreme wave height (H_e) and wave period values (T_e) and closure depth calculation results are given in Table 5.1.

Table 5.1. Extreme wave parameters and closure depths for both station records.

	Local Station	Izmit Station
Max. Significant Wave Height	1.22 m	1.01 m
Max. Peak Wave Period	4.47 s	4.2 s
Extreme Wave Height	0.85 m	0.46 m
Extreme Wave Period	3.97 s	3.22 s
Closure Depth	1.62 m	0.9 m

5.2. Alternative Nourishment Designs

For seven alternative beach widths (5-30 m), needed sand volumes are calculated based on two different nourishment sands which have 0.32 mm and 0.45 mm diameter. The purpose of the calculation done by two different grain diameters is to investigate how the usage of fine or coarse nourishment material, affect the project quantities. Required sand volumes for the alternative beach widths are given in Table 5.2 that are determined according to 0.32 mm and 0.45 mm sand diameters. Detailed profile and plan view drawings are given in Appendix B.2 and B.3.

The most important parameter while determining the required sand volume is the thickness of sand that was used for the isolation of the native muddy bottom from wave penetration. In the laboratory model, initial nourishment thickness from sea level was 20 cm which represents 140 cm in the prototype. Results showed that this thickness is adequate for isolation.

Table 5.2. Volume calculations for seven alternative beach widths.

Shoreline Advance [m]	SECTION		1		2		3		4		5		6		AVERAGE	
	Existing Beach Width [m]		2		11		23		16		17		10		13	
	Distance Between Sections [m]		110		107		112		117		146				118.4	
	Sediment Diameter [mm]		0.32	0.45	0.32	0.45	0.32	0.45	0.32	0.45	0.32	0.45	0.32	0.45	0.32	0.45
5	Adjusted Beach Width [m]		7		16		28		21		22		15		18	
	Initial Nourished Width [m]		33	25	19	19	49	34	25	23	28	25	34	27	31	26
	$\Delta V[m^3/m]$		112	65	27	25	90	50	35	31	54	45	85	58	67	46
	$\Delta V_{section}[m^3]$		7666	4971	6260	4043	6989	4560	5194	4461	10132	7534	$\Delta V_{total}[m^3]$		36241	25569
10	Adjusted Beach Width [m]		12		21		33		26		27		20		23	
	Initial Nourished Width [m]		39	32	25	24	61	45	32	29	35	32	42	34	39	33
	$\Delta V[m^3/m]$		154	102	39	37	137	80	52	46	74	65	119	85	96	69
	$\Delta V_{section}[m^3]$		10656	7698	9457	6275	10605	7018	7384	6446	14134	10930	$\Delta V_{total}[m^3]$		52235	38367
15	Adjusted Beach Width [m]		17		26		38		31		32		25		28	
	Initial Nourished Width [m]		45	38	29	29	69	58	38	35	41	38	49	41	45	40
	$\Delta V[m^3/m]$		200	143	51	49	195	119	69	61	96	85	157	115	128	95
	$\Delta V_{section}[m^3]$		13791	10575	13165	9037	14801	10116	9667	8540	18451	14594	$\Delta V_{total}[m^3]$		69875	52863
20	Adjusted Beach Width [m]		22		31		43		36		37		30		33	
	Initial Nourished Width [m]		51	44	37	33	76	67	45	41	47	44	56	48	52	46
	$\Delta V[m^3/m]$		248	186	70	61	232	173	87	78	119	105	197	150	159	125
	$\Delta V_{section}[m^3]$		17465	13599	16158	12513	17870	14041	12051	10726	23075	18611	$\Delta V_{total}[m^3]$		86617	69489
25	Adjusted Beach Width [m]		27		36		48		41		42		35		38	
	Initial Nourished Width [m]		57	49	47	39	82	73	51	48	54	50	63	55	59	52
	$\Delta V[m^3/m]$		298	231	94	75	331	228	105	95	145	127	240	188	202	157
	$\Delta V_{section}[m^3]$		21569	16875	22774	16220	24436	18086	14638	13019	28131	22994	$\Delta V_{total}[m^3]$		111548	87194
30	Adjusted Beach Width [m]		32		41		53		46		47		40		43	
	Initial Nourished Width [m]		62	55	61	48	87	79	57	54	62	56	69	61	66	59
	$\Delta V[m^3/m]$		351	280	129	95	405	294	124	113	176	151	286	228	245	194
	$\Delta V_{section}[m^3]$		26403	20620	28576	20830	29629	22814	17565	15455	33768	27671	$\Delta V_{total}[m^3]$		135941	107389

$\Delta V_{section} [m^3]$: volume between successive sections

$\Delta V_{total} [m^3]$: total required volume for nourishment

The gains obtained by the expansion of the existing beach are calculated for the alternative designs (Table 5.3). Gain rate is the ratio of initial shoreline advance to width of adjusted new beach. As shown in the table, the bigger the project, the higher the gain rate. In addition, the use of coarser sand affects gain rate and initial nourishment width positively.

Table 5.3. Quantities for alternative nourishment options.

Gained Beach Width [m]	Adjusted Beach Width [m]	Gained Beach Area [x1000 m ²]	Initial Nourishment Width [m]		Gain Rate [%]		Total Volume [m ³]	
			0.32	0.45	0.32	0.45	0.32	0.45
Nourishment Sand Diameter [D _{fill} , mm]			0.32	0.45	0.32	0.45	0.32	0.45
5	18	3	31	26	28	41	36241	25569
10	23	6	39	33	39	52	52235	38367
15	28	9	45	40	47	57	69875	52863
20	33	12	52	46	52	61	86617	69489
25	38	15	59	52	55	64	111548	87194
30	43	18	66	59	57	66	135941	107389

5.3. Cost Calculation

Figure 5.2 shows that increase in sand volume, consequently increase the cost of the project, results in approximately linear escalation in the gained beach area. While calculating the cost of the each alternative, 1 m³ sand fill was considered as 10 dollars.

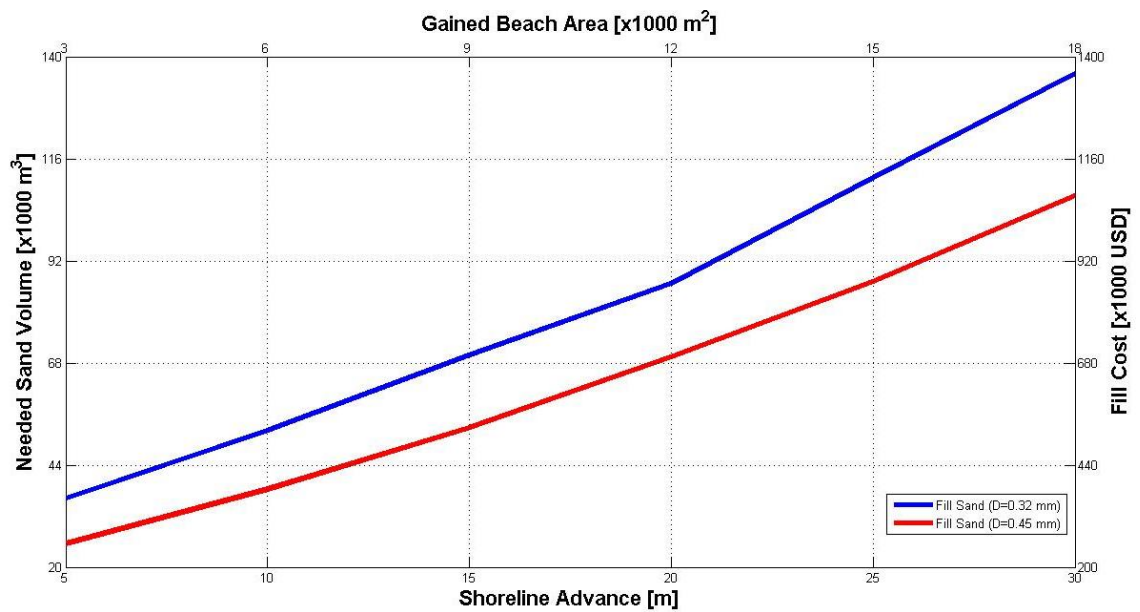


Figure 5.2. Comparison of alternative nourishment quantities.

One of the alternatives in Table 5.3 can be applied according to the project owner's decision. While choosing one of these options the main parameters that should be taken into consideration are the net beach gain for each alternative, required sand volume for such nourishment and the cost of the project.

The beach utilization rate per person is accepted as 10 m^2 in the most intense conditions (da Silva, 2002) 20 m wide sandy beach (12 acres) accommodates approximately 1200 visitors at the same time.

6. CONCLUSION

In this study, the main objective was to determine whether a damaged coast containing large fractions of fine sediment can be rehabilitated by beach nourishment. The study area is a fill coast in İzmit Bay and the fill material consists of mainly ruins of earthquake in 1999.

Wave characteristics of the site were estimated using İzmit and local wind statistics covering 29 years and 2 years, respectively. Local wind data showed more severe storm conditions. To be on the safe side, waves predicted from local wind records were used to calculate the design parameters for the beach nourishment. The offshore limit of sediment motion was investigated based on wave predictions. The same methodology can be used for similar studies in the region if possible supported by direct wave and current measurements.

Available reports and collected sediment samples indicated that the coastal native soil contains a wide variety of sediments ranging from gravel to silt. It was found that sediment diameter decreases seaward from the shoreline. Since the behavior of cohesive and non-cohesive mixed sediments under wave action has not been well-understood, a physical model was developed to simulate the behavior of mixed sediments.

A qualitative physical model was established to discover the interaction of sand/mud mixed native material and nourishment sand. It was revealed that the mixing of muddy native soil with the nourishment sand placed on top is not significant. Although it could not be observed in the laboratory, field observations show that even if the fine and coarse sediments mix, finer sediments cannot settle in the surf zone because of the high wave energy. The top soil samples taken in the field around the water line and shallow depths consist of mainly medium to coarse sand and gravel, showing very small fraction of fines. Grain size analyses of sediments collected after every storm generated in the laboratory indicated that the median diameter of nourishment sand does

not change due to wave action. Therefore, it is concluded that coastal rehabilitation is sustainable using beach nourishment.

Profile measurements in the laboratory were not entirely consistent with the theoretical equilibrium beach profile. The fact that the native soil contains a high proportion of fine material may be the reason for this; however, this phenomenon should be investigated in detail as future work.

For seven different dry beach widths, required sand volumes are calculated based on two specific sediment diameters. In addition, the gain rate defined as the ratio of initial shoreline advance to width of adjusted new beach of each alternative is determined to compare the efficiency of suggested nourishment options.

Due to the fact that the longshore transport of nourishment sand was blocked by the groins constructed at either end of the project site, longshore transport phenomena has not been investigated in this study. However, predominant wave direction gives the idea that the longshore sediment transport will be from east to west and this may cause sand accumulation in the west end of the project site.

Future efforts might be concentrated on construction works. Although the interaction of natural and artificial environments is well defined with the physical model, in order to facilitate further studies, project site should be monitored in the long-term after construction.

APPENDIX A: WIND AND WAVE ANALYSES

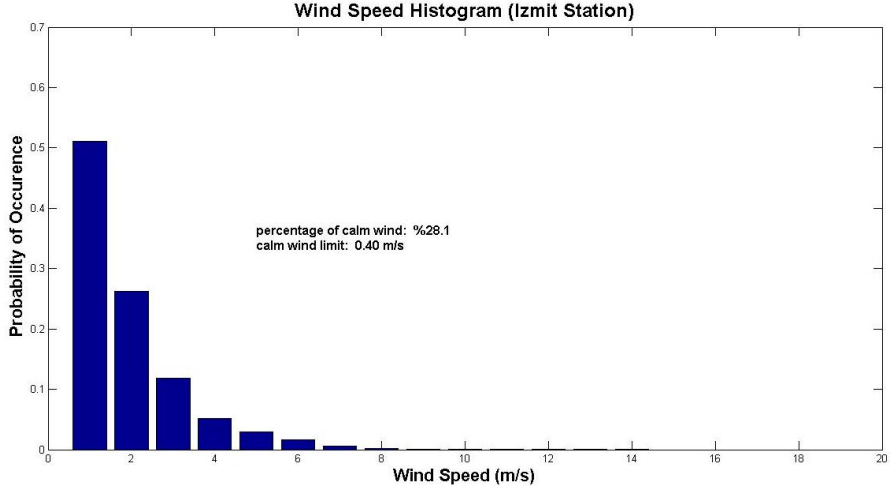
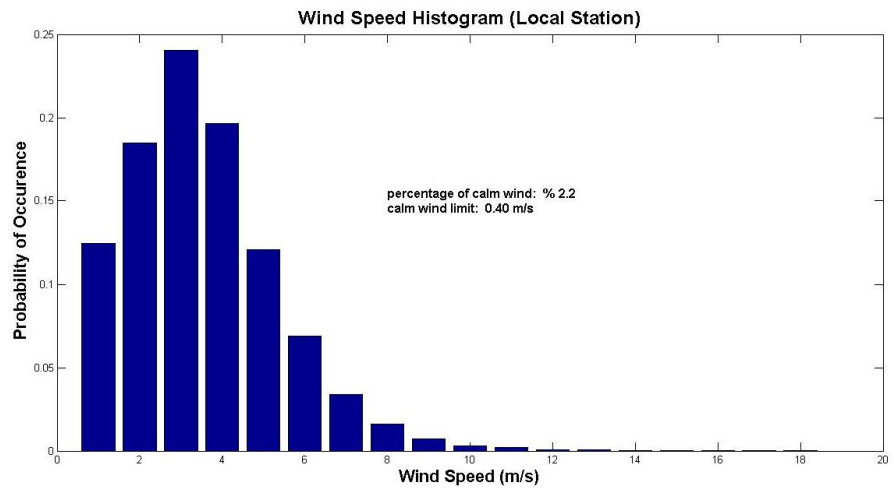


Figure A.1. Wind speed histograms for both stations.

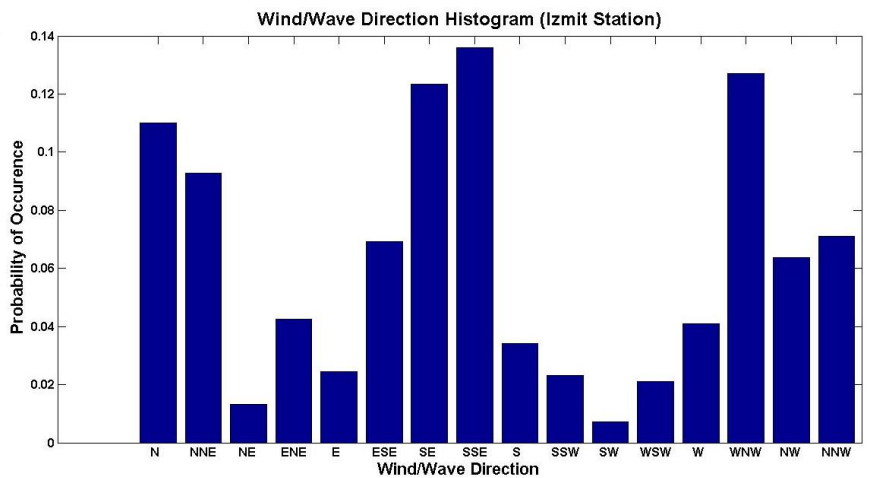
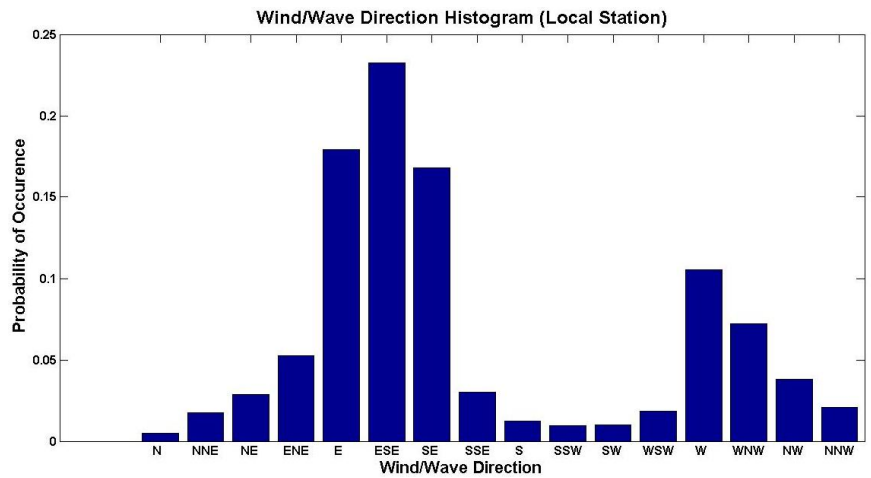


Figure A.2. Wind/wave direction histograms for both stations.

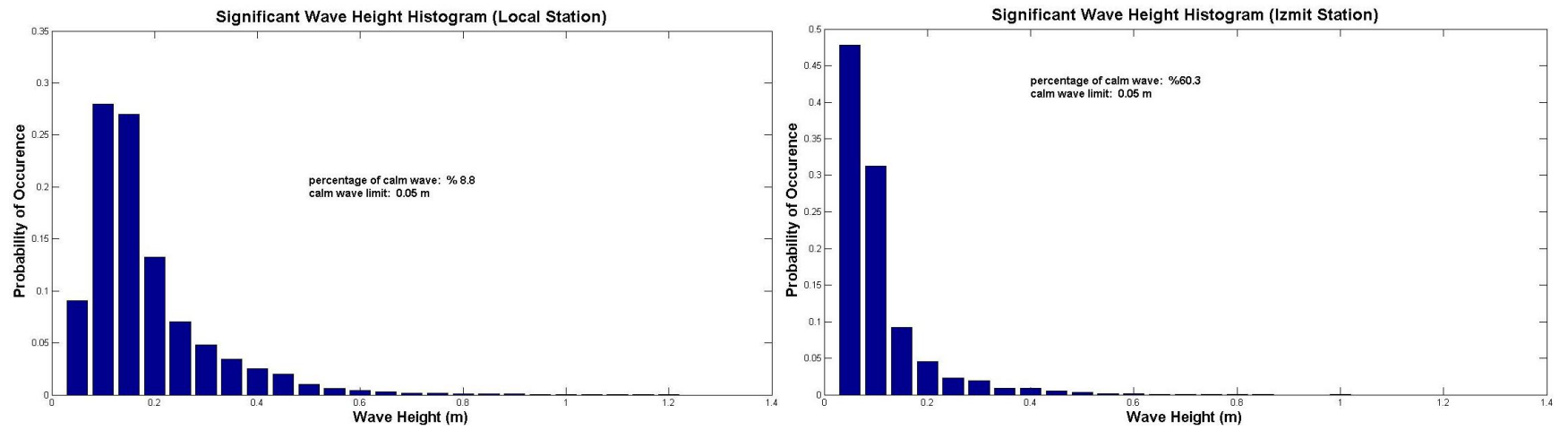


Figure A.3. Significant wave height histograms for both stations.

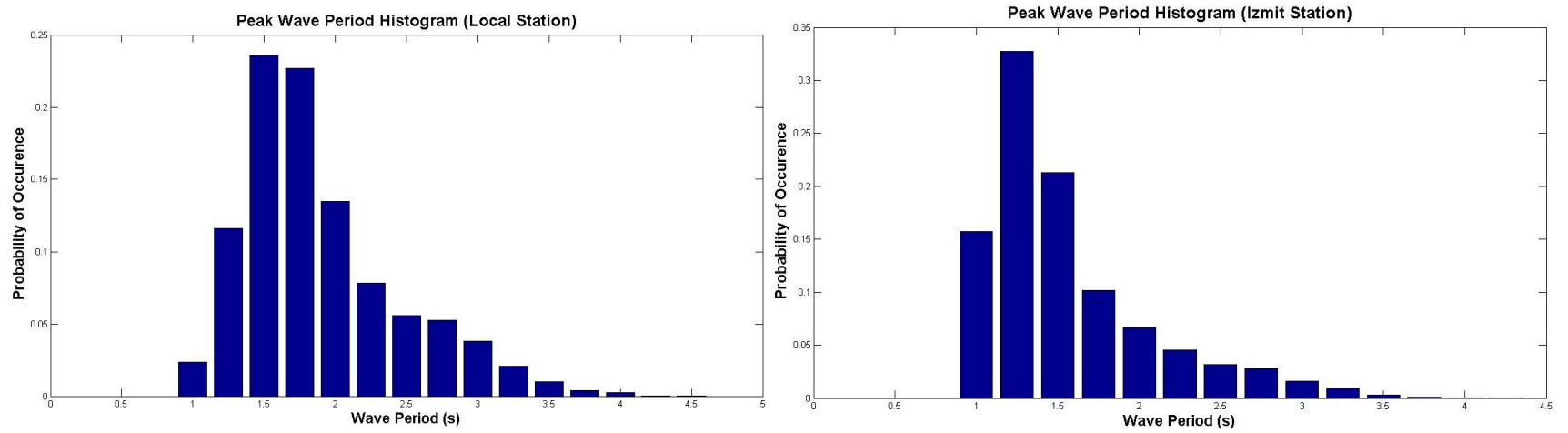


Figure A.4. Peak wave period histograms for both stations.

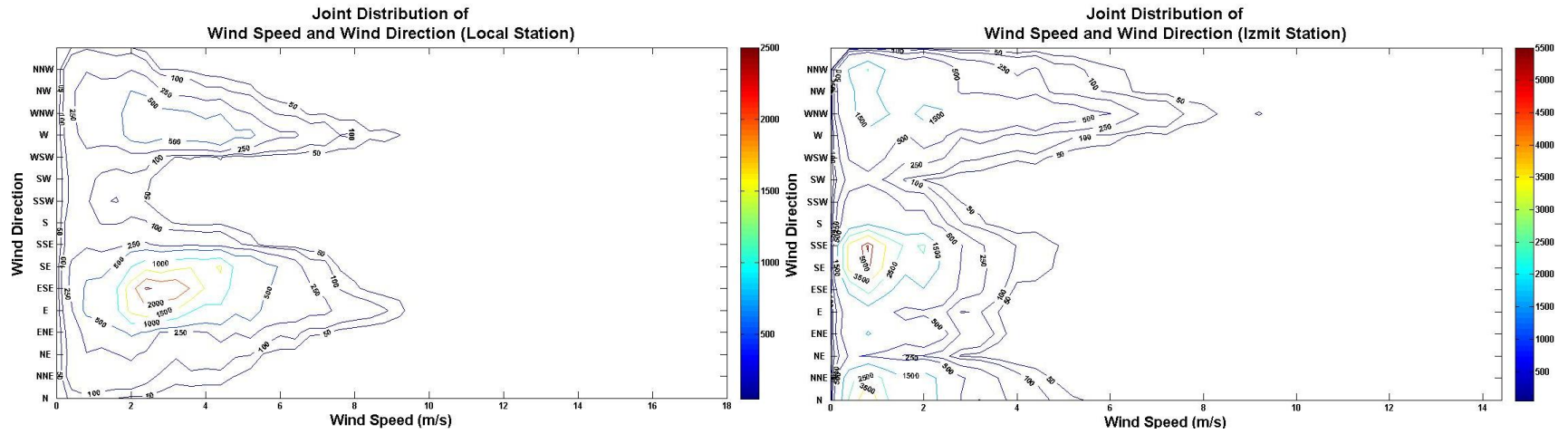


Figure A.5. Joint distribution of wind speed and wind direction for both stations in Cartesian coordinates.

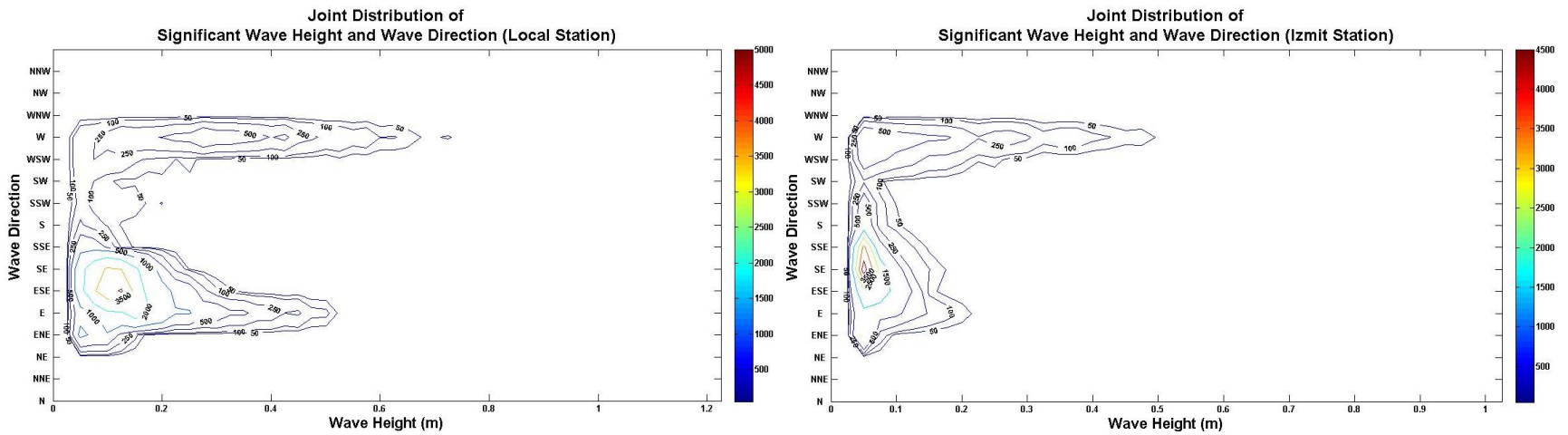


Figure A.6. Joint distribution of significant wave height and wave direction for both stations in Cartesian coordinates.

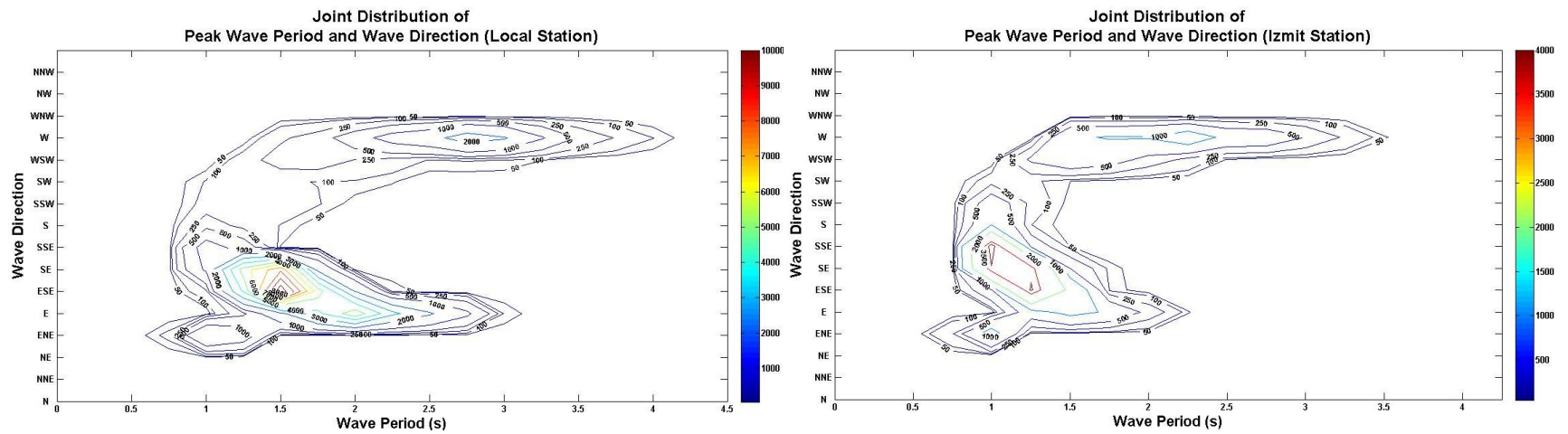


Figure A.7. Joint distribution of peak wave period and wave direction for both stations in Cartesian coordinates.

APPENDIX B: BEACH PROFILE DRAWINGS

B.1. Design Profiles for Grain Diameter 0.32 mm

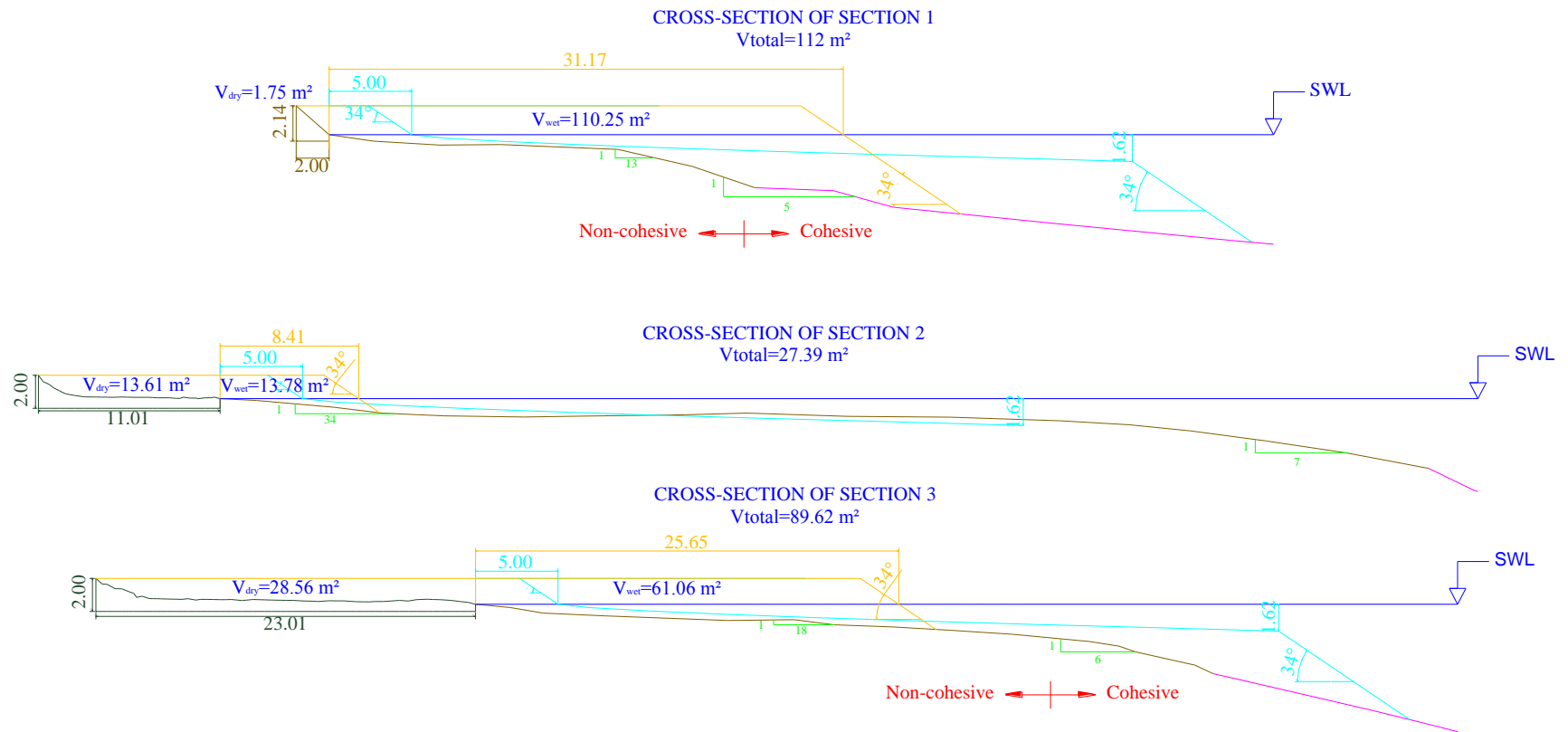


Figure B.1. Design profiles of Section 1,2 and 3 for 5 m new dry beach width ($D_{fill}=0.32 \text{ mm}$).

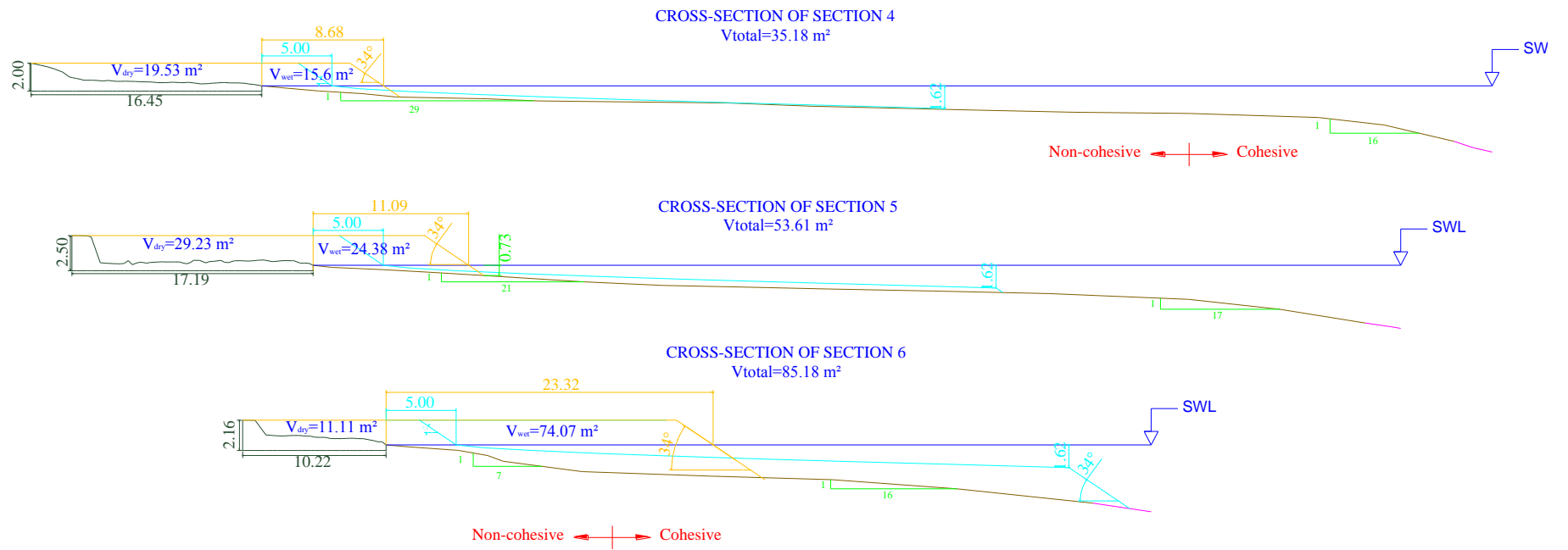


Figure B.2. Design profiles of Section 4,5 and 6 for 5 m new dry beach width ($D_{\text{fill}}=0.32 \text{ mm}$).

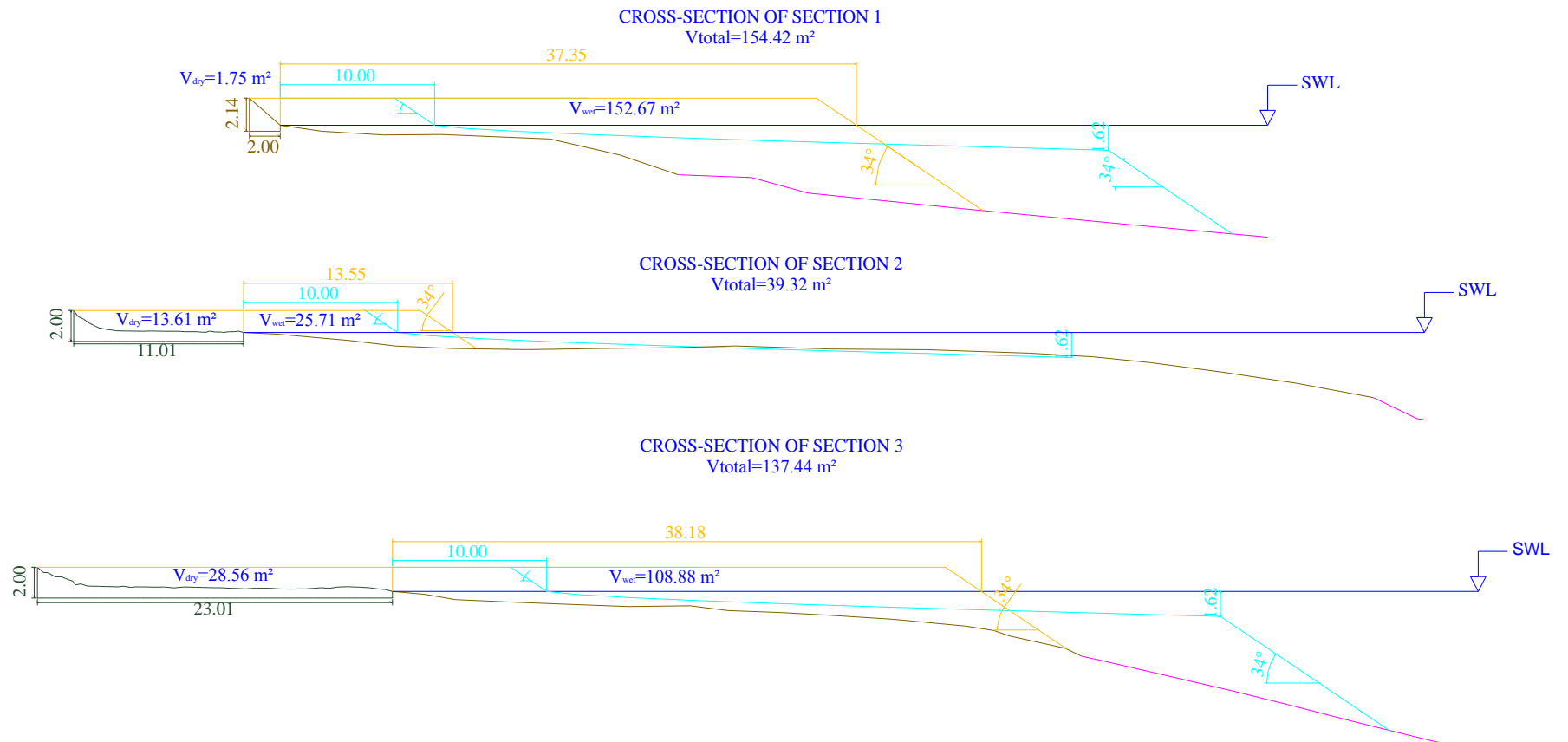


Figure B.3. Design profiles of Section 1,2 and 3 for 10 m new dry beach width ($D_{fill} = 0.32 \text{ mm}$).

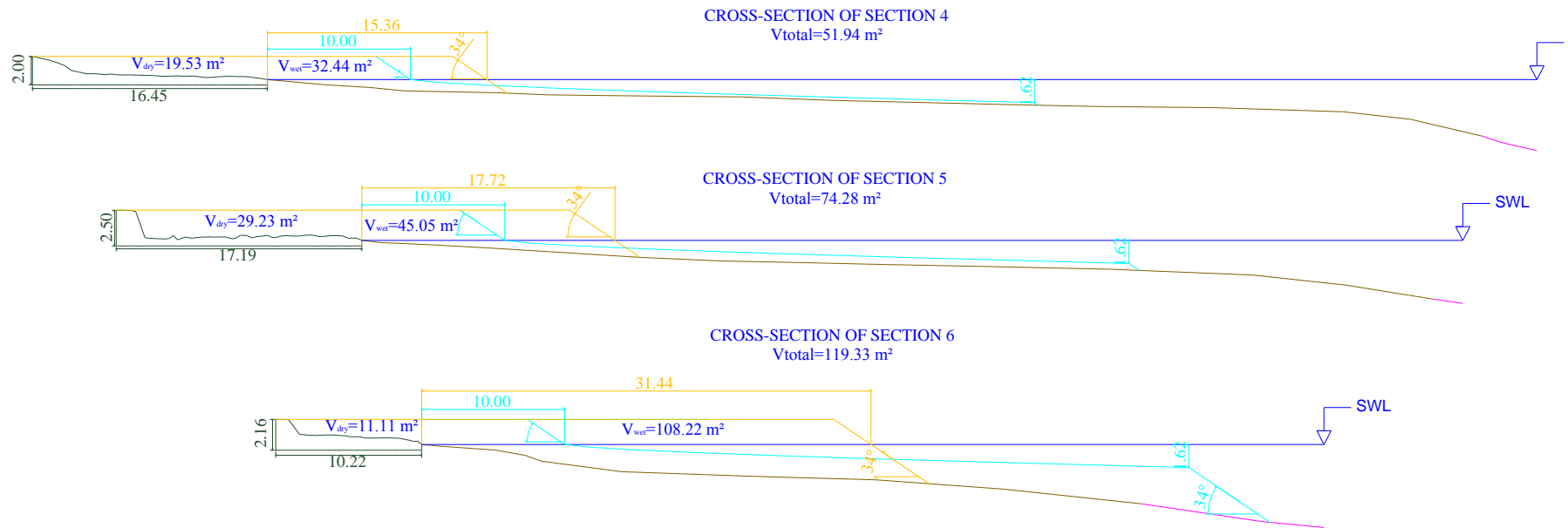


Figure B.4. Design profiles of Section 4,5 and 6 for 10 m new dry beach width ($D_{fill}=0.32 \text{ mm}$).

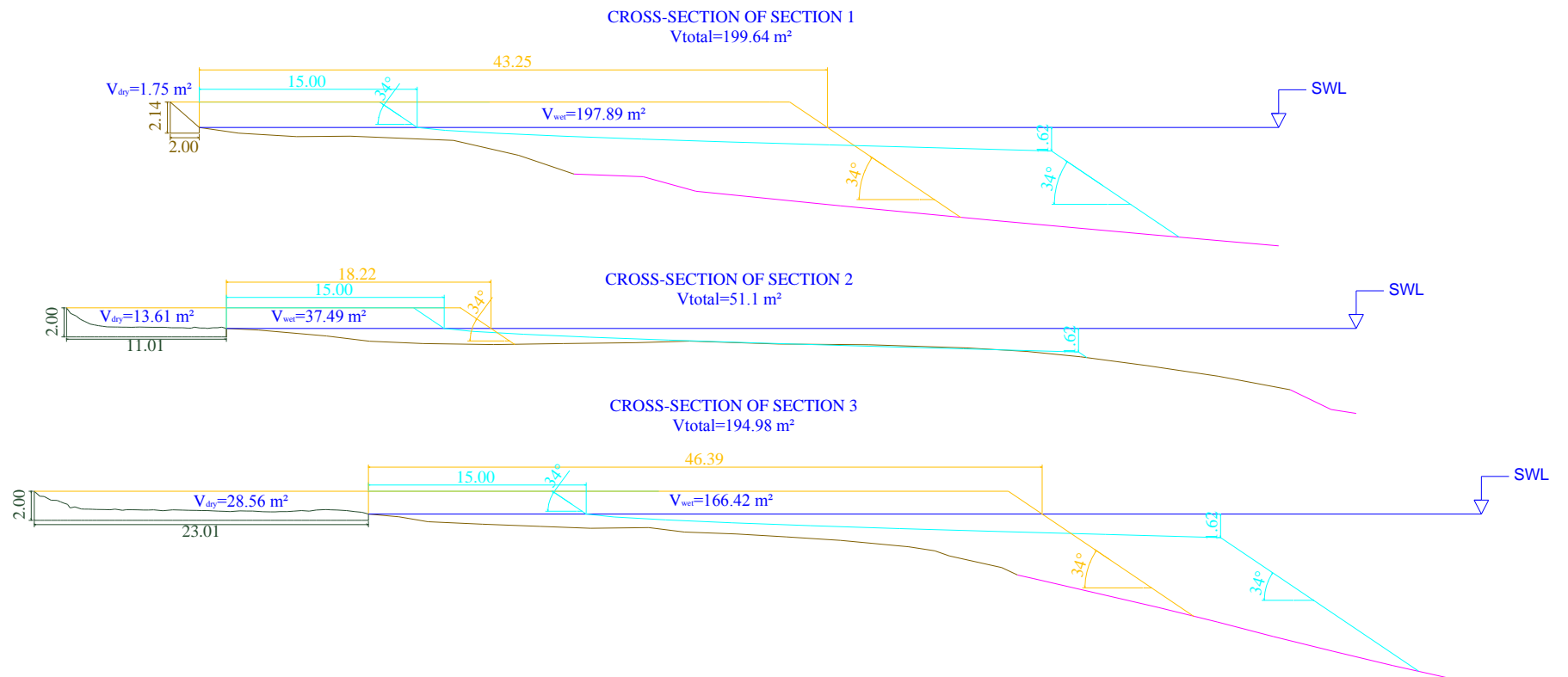


Figure B.5. Design profiles of Section 1,2 and 3 for 15 m new dry beach width ($D_{fill}=0.32 \text{ mm}$).

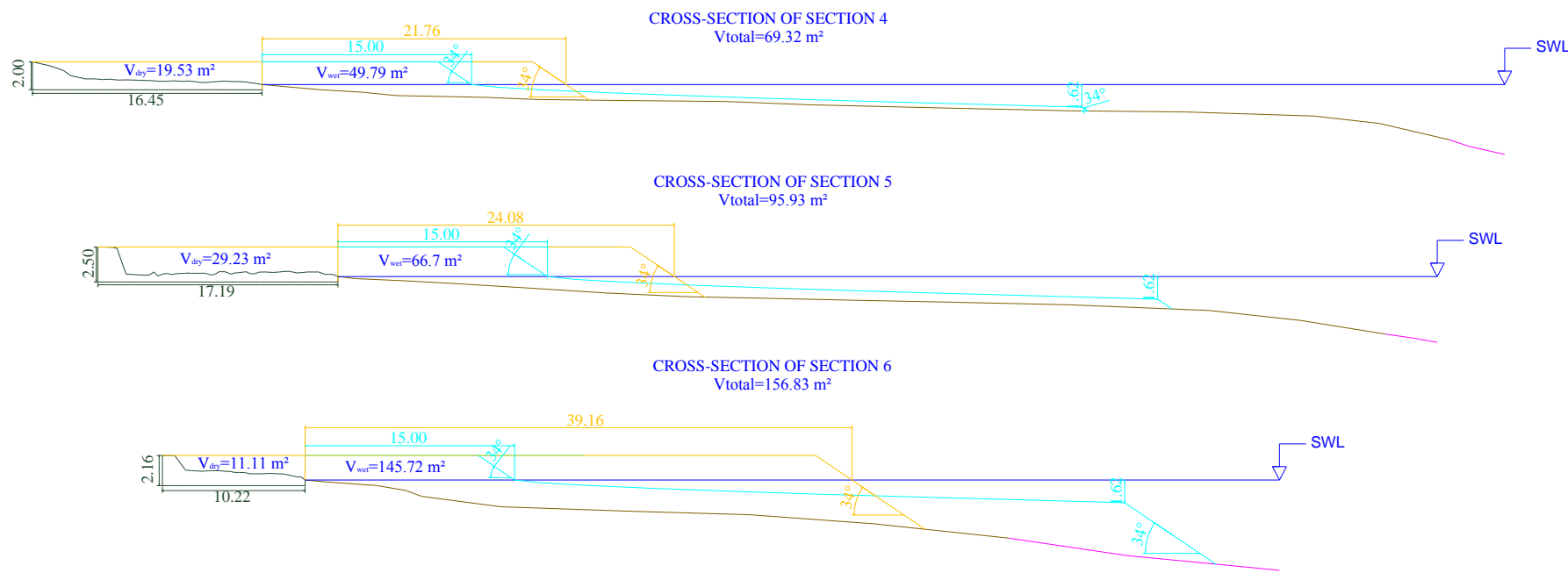


Figure B.6. Design profiles of Section 4,5 and 6 for 15 m new dry beach width ($D_{fill}=0.32$ mm).

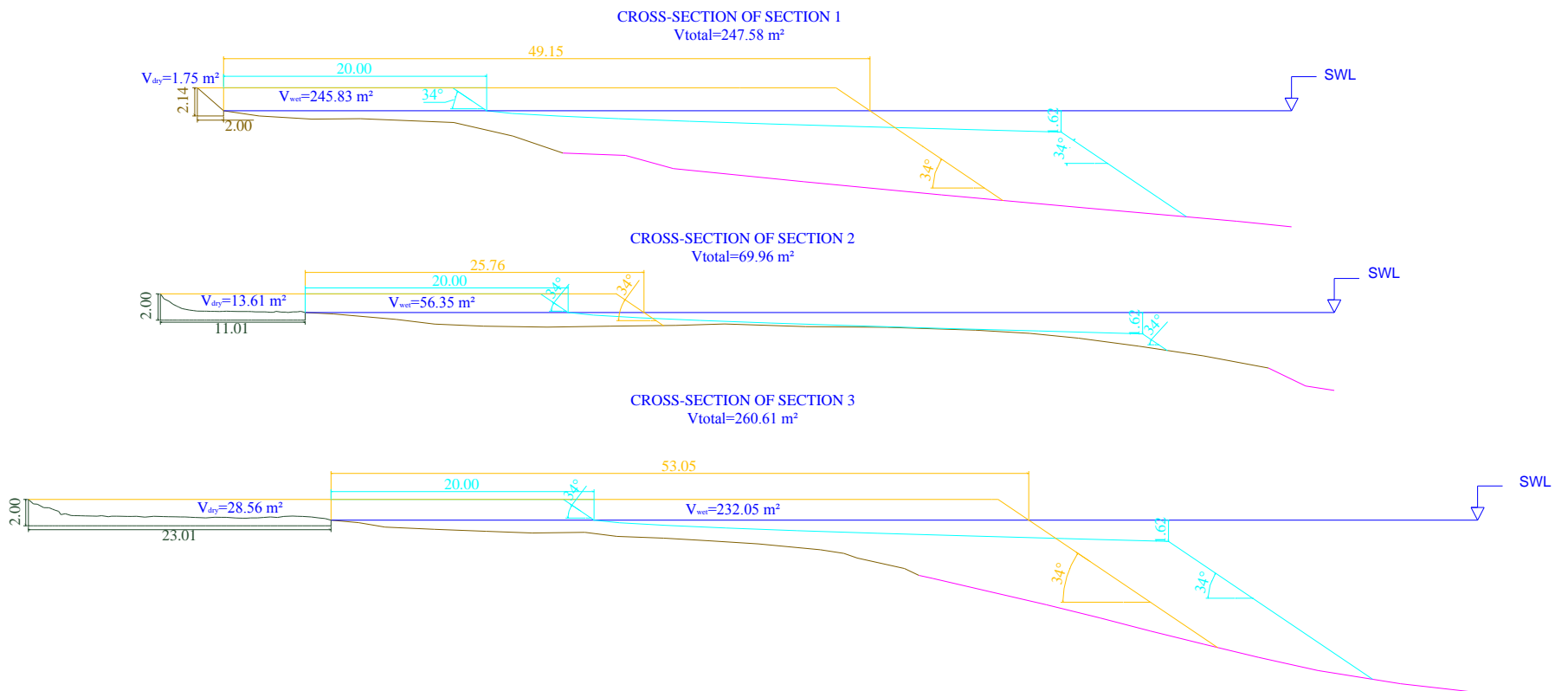


Figure B.7. Design profiles of Section 1,2 and 3 for 20 m new dry beach width ($D_{fill}=0.32$ mm).

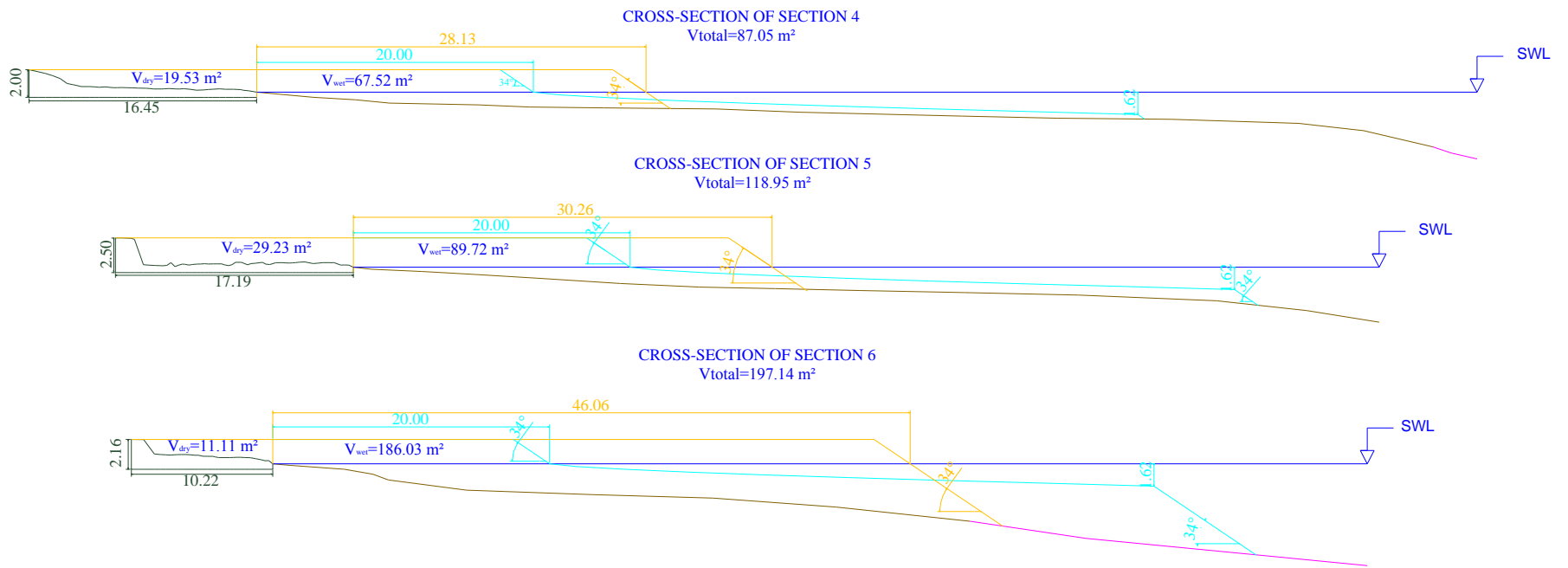


Figure B.8. Design profiles of Section 4,5 and 6 for 20 m new dry beach width ($D_{fill}=0.32$ mm).

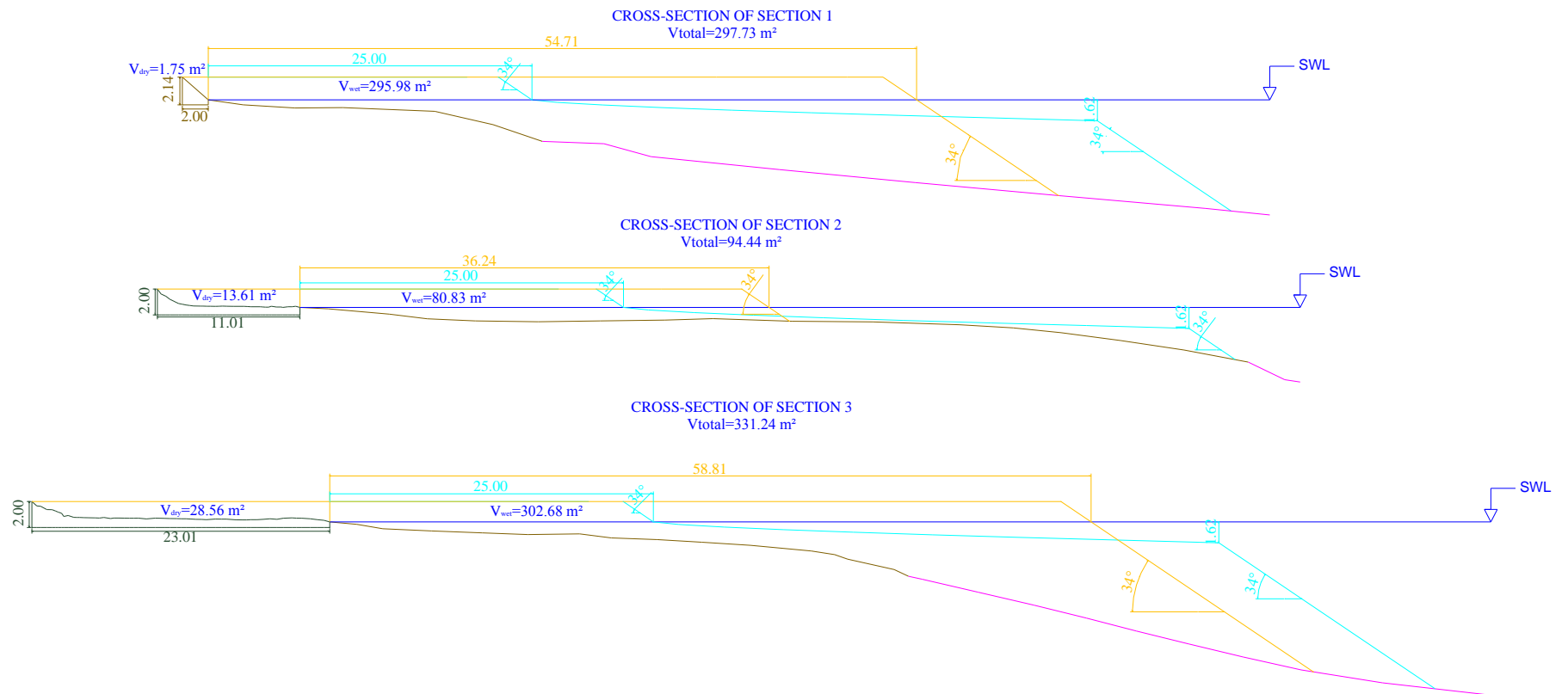


Figure B.9. Design profiles of Section 1,2 and 3 for 25 m new dry beach width ($D_{fill}=0.32 \text{ mm}$).

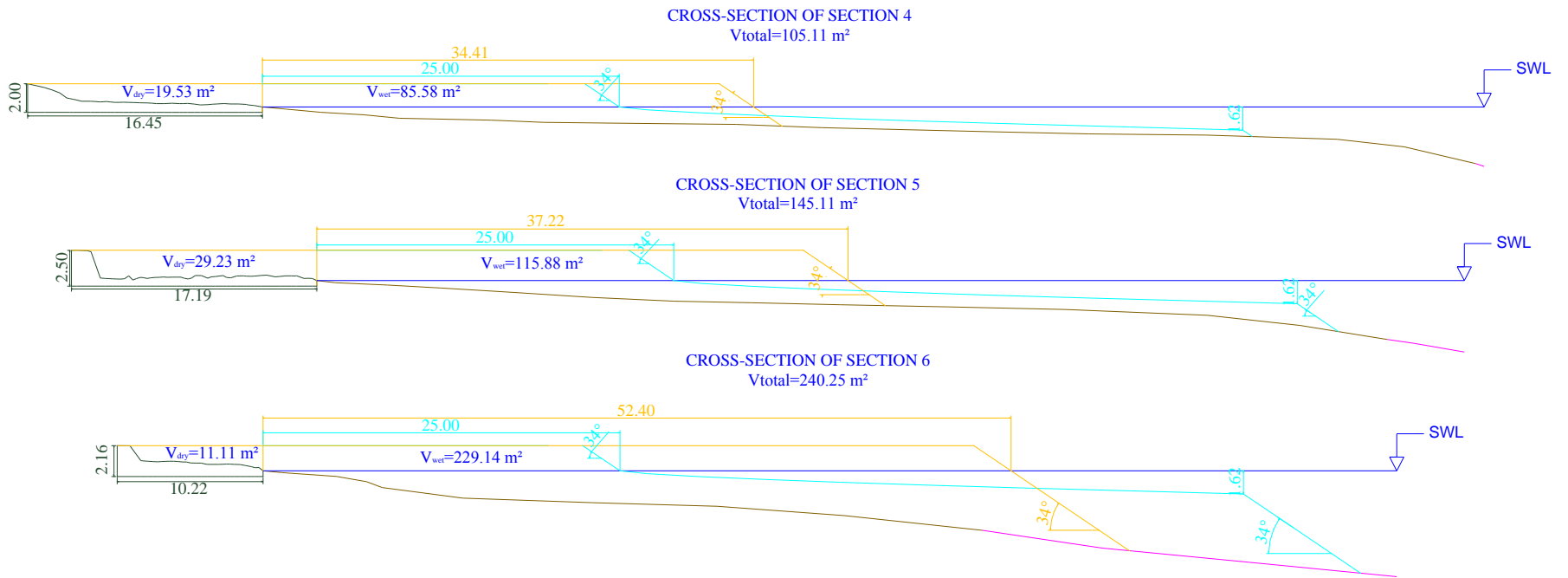


Figure B.10. Design profiles of Section 4,5 and 6 for 25 m new dry beach width ($D_{\text{fill}}=0.32 \text{ mm}$).

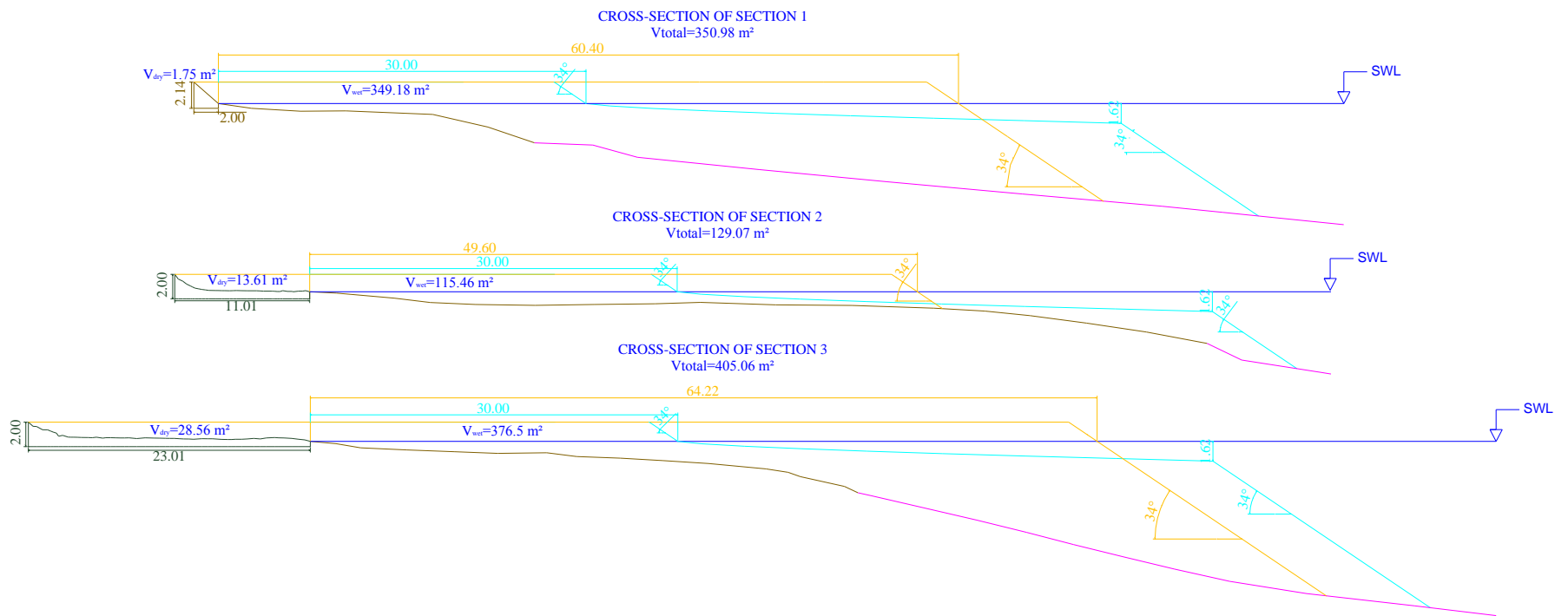


Figure B.11. Design profiles of Section 1,2 and 3 for 30 m new dry beach width ($D_{fill}=0.32$ mm).

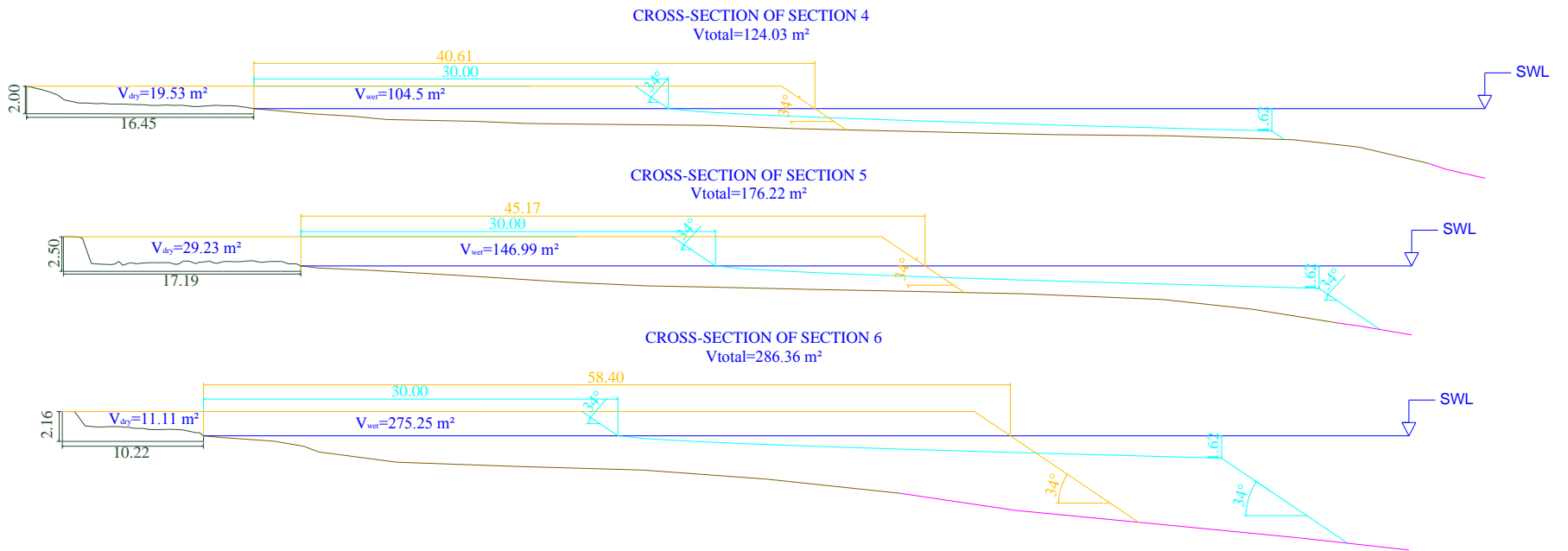


Figure B.12. Design profiles of Section 4,5 and 6 for 30 m new dry beach width ($D_{\text{fill}}=0.32 \text{ mm}$).

B.2. Design Profiles for Grain Diameter 0.45 mm

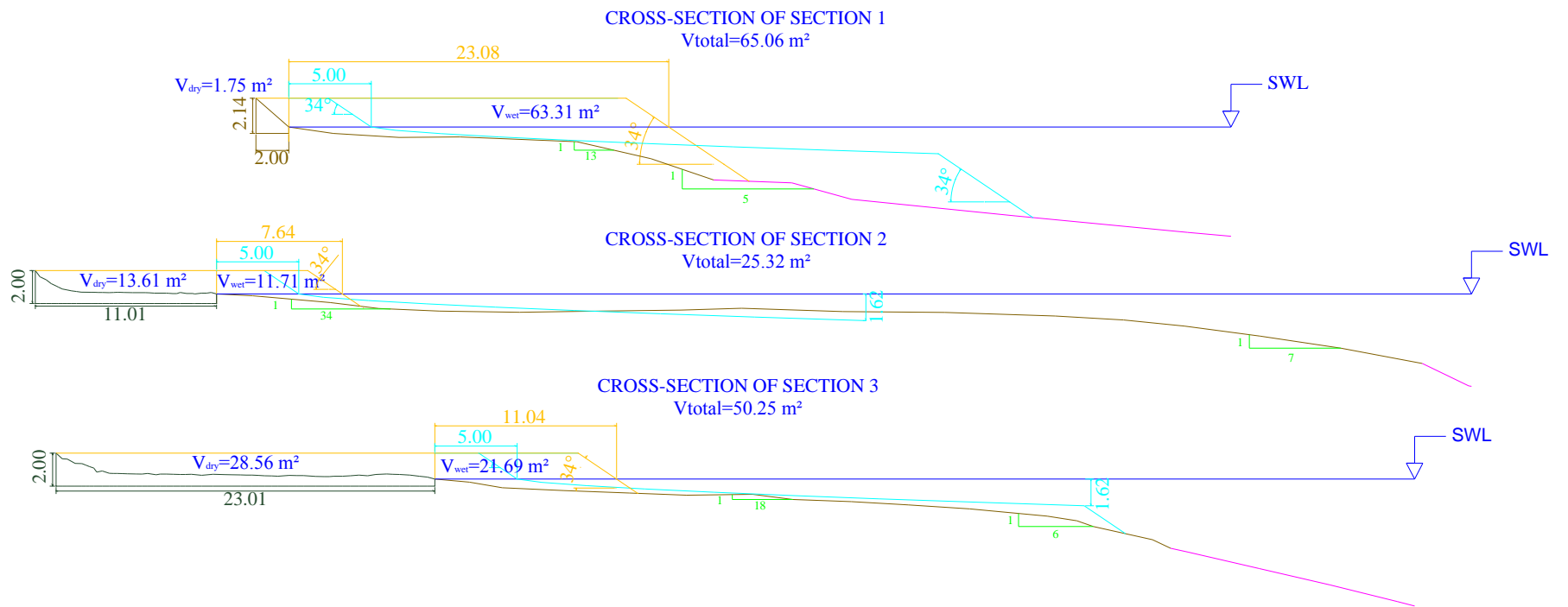


Figure B.13. Design profiles of Section 1,2 and 3 for 5 m new dry beach width ($D_{\text{fill}}=0.45 \text{ mm}$).

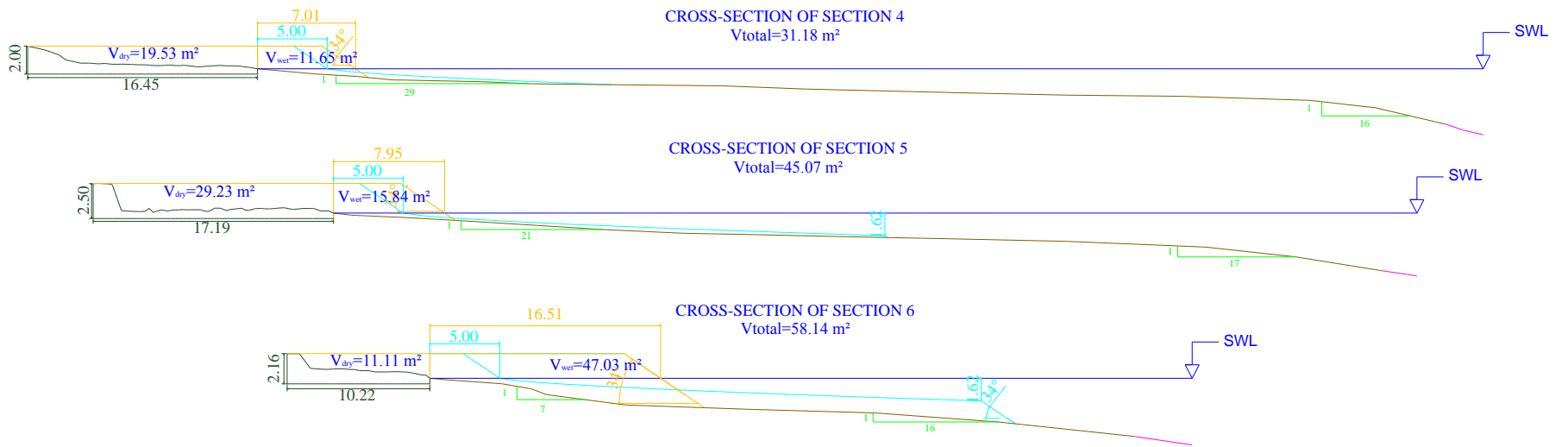


Figure B.14. Design profiles of Section 4,5 and 6 for 5 m new dry beach width ($D_{fill}=0.45$ mm).

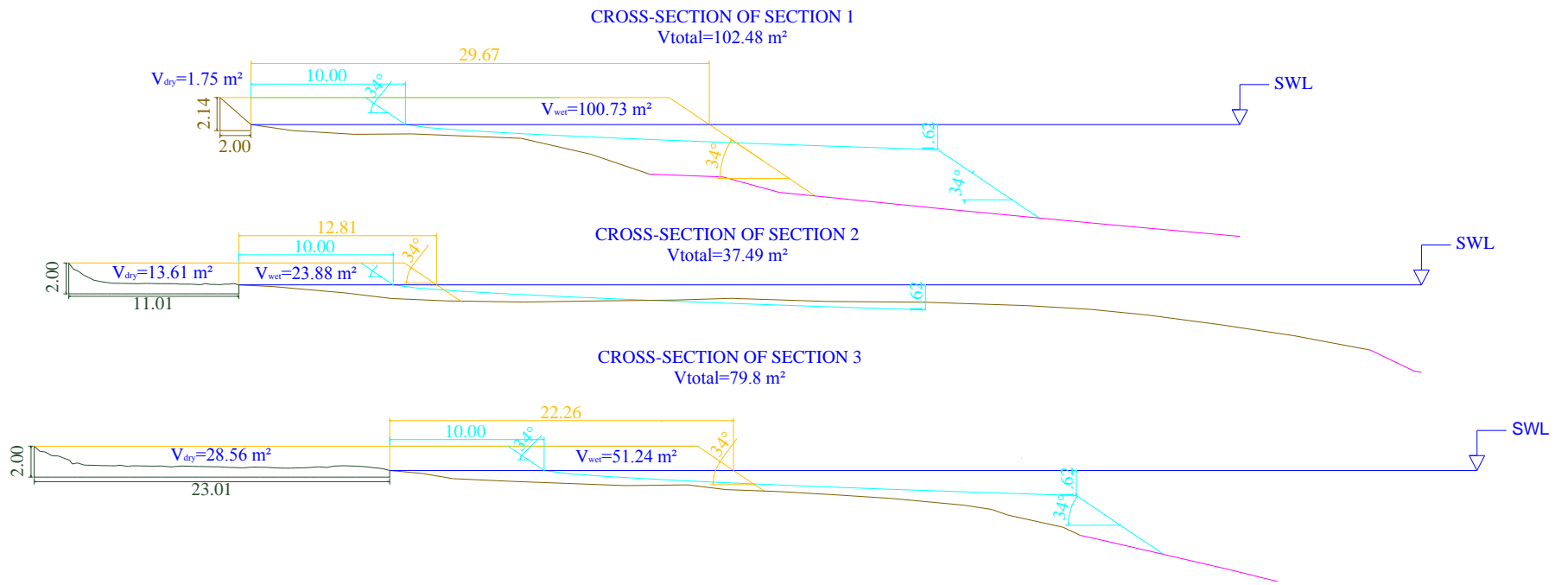


Figure B.15. Design profiles of Section 1,2 and 3 for 10 m new dry beach width ($D_{\text{fill}}=0.45 \text{ mm}$).

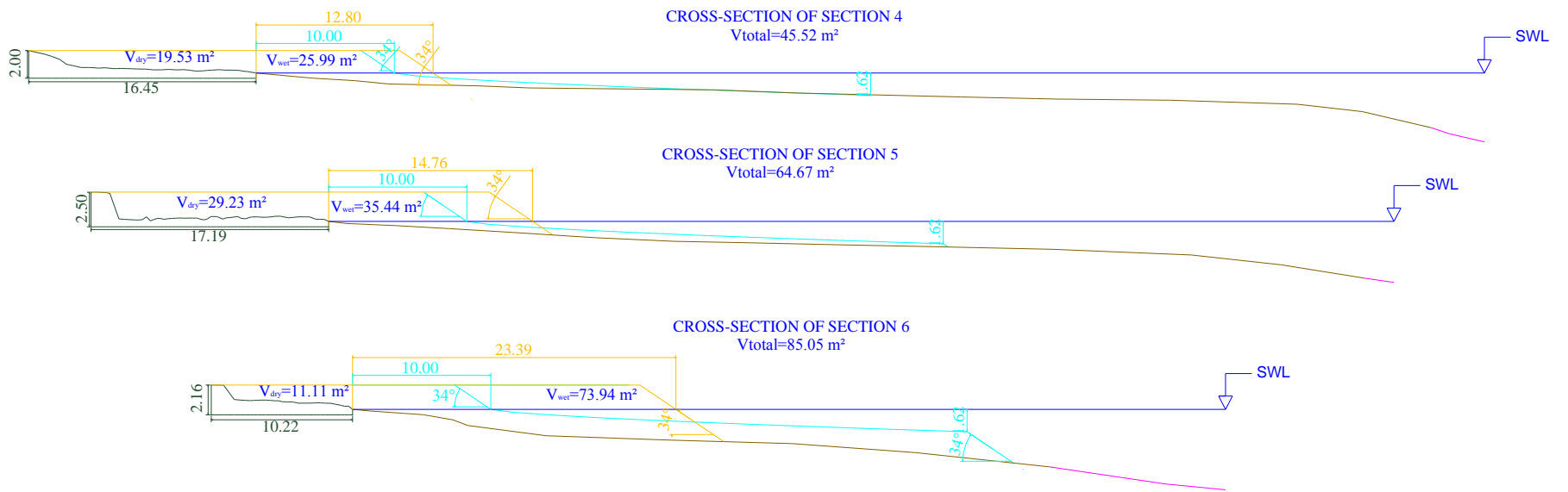


Figure B.16. Design profiles of Section 4,5 and 6 for 10 m new dry beach width ($D_{fill}=0.45 \text{ mm}$).

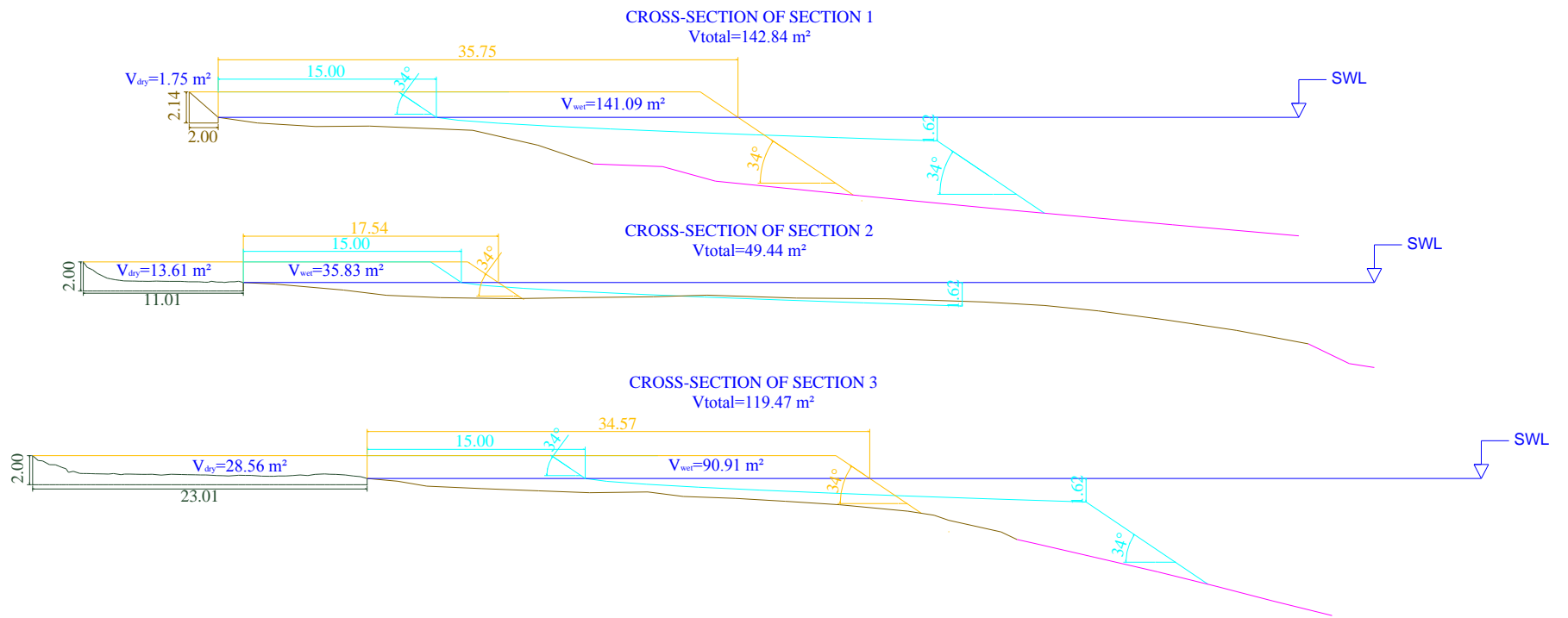


Figure B.17. Design profiles of Section 1,2 and 3 for 15 m new dry beach width ($D_{\text{fill}}=0.45 \text{ mm}$).

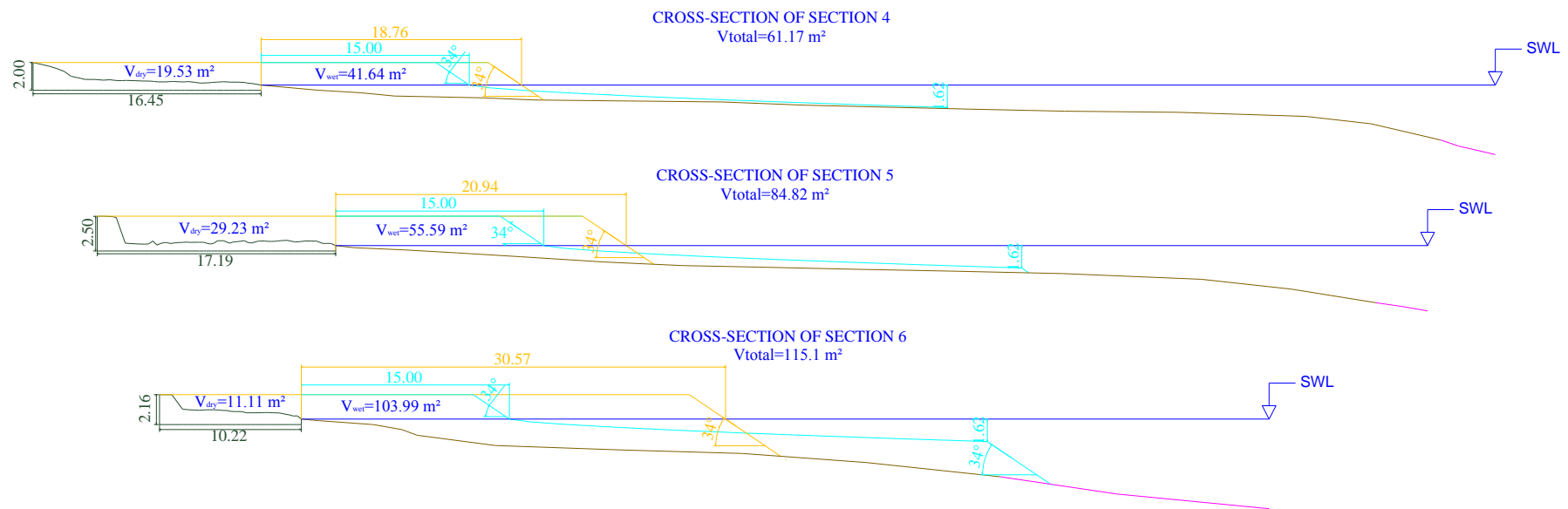


Figure B.18. Design profiles of Section 4,5 and 6 for 15 m new dry beach width ($D_{\text{fill}}=0.45 \text{ mm}$).

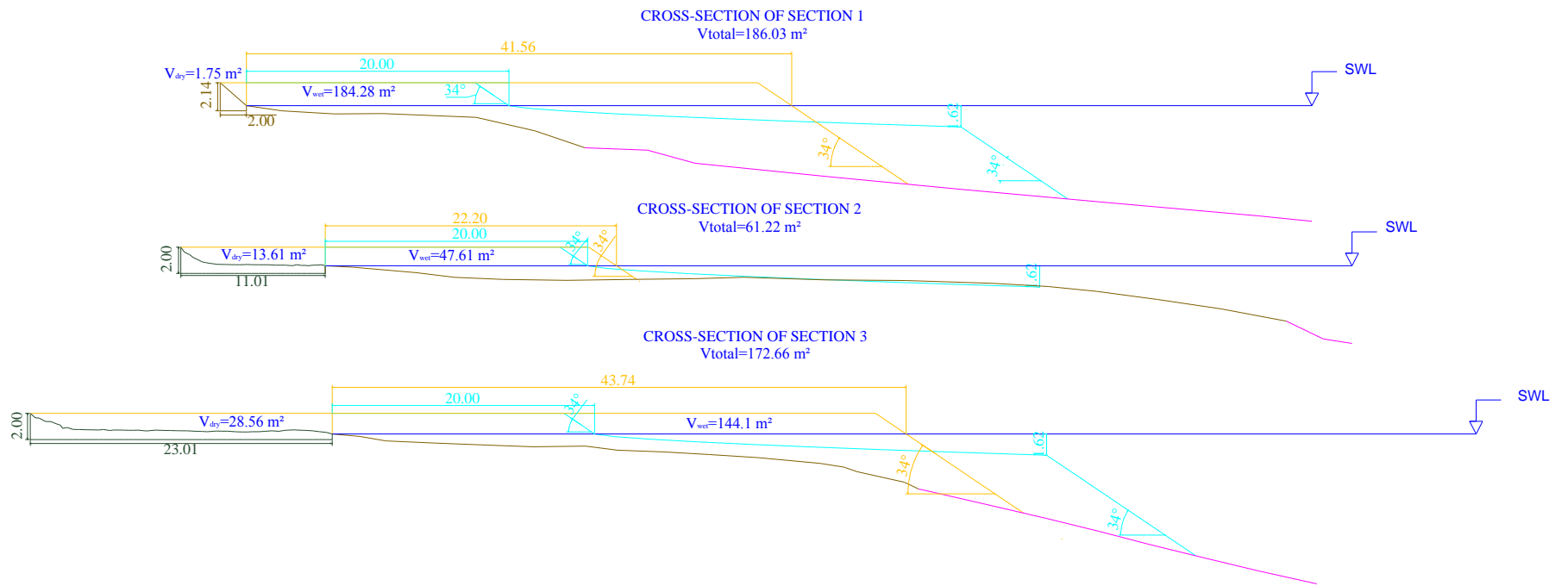


Figure B.19. Design profiles of Section 1,2 and 3 for 20 m new dry beach width ($D_{fill}=0.45 \text{ mm}$).

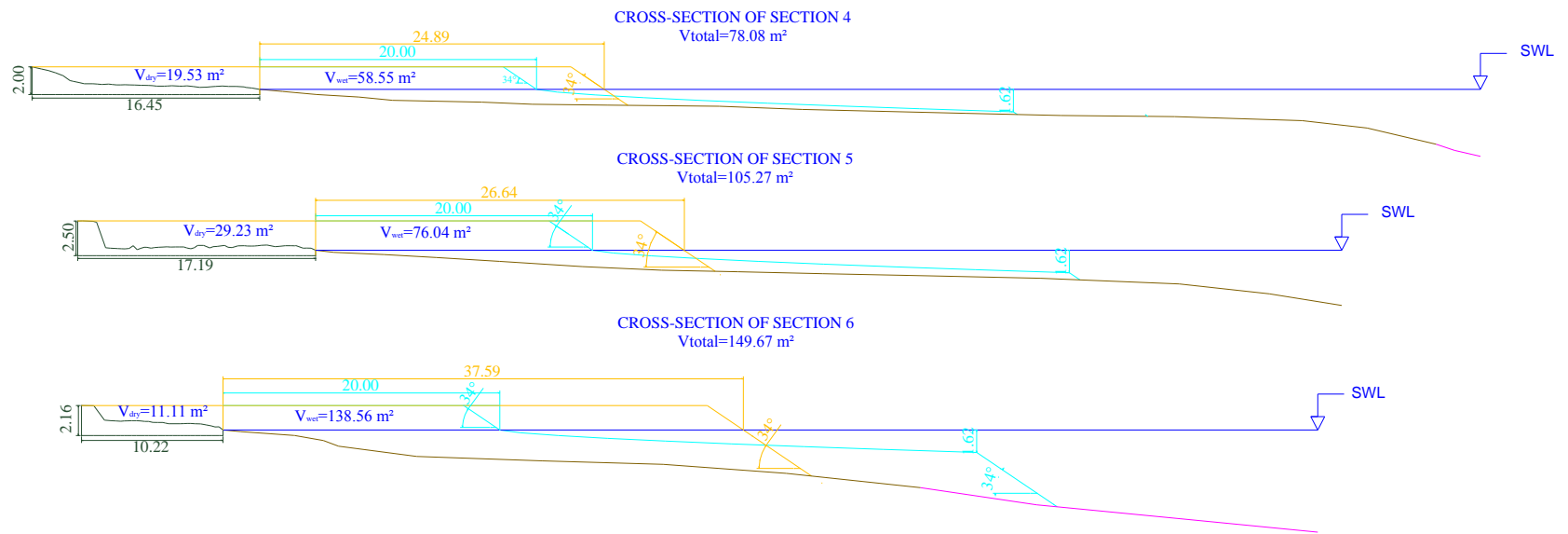


Figure B.20. Design profiles of Section 4,5 and 6 for 20 m new dry beach width ($D_{fill}=0.45$ mm).

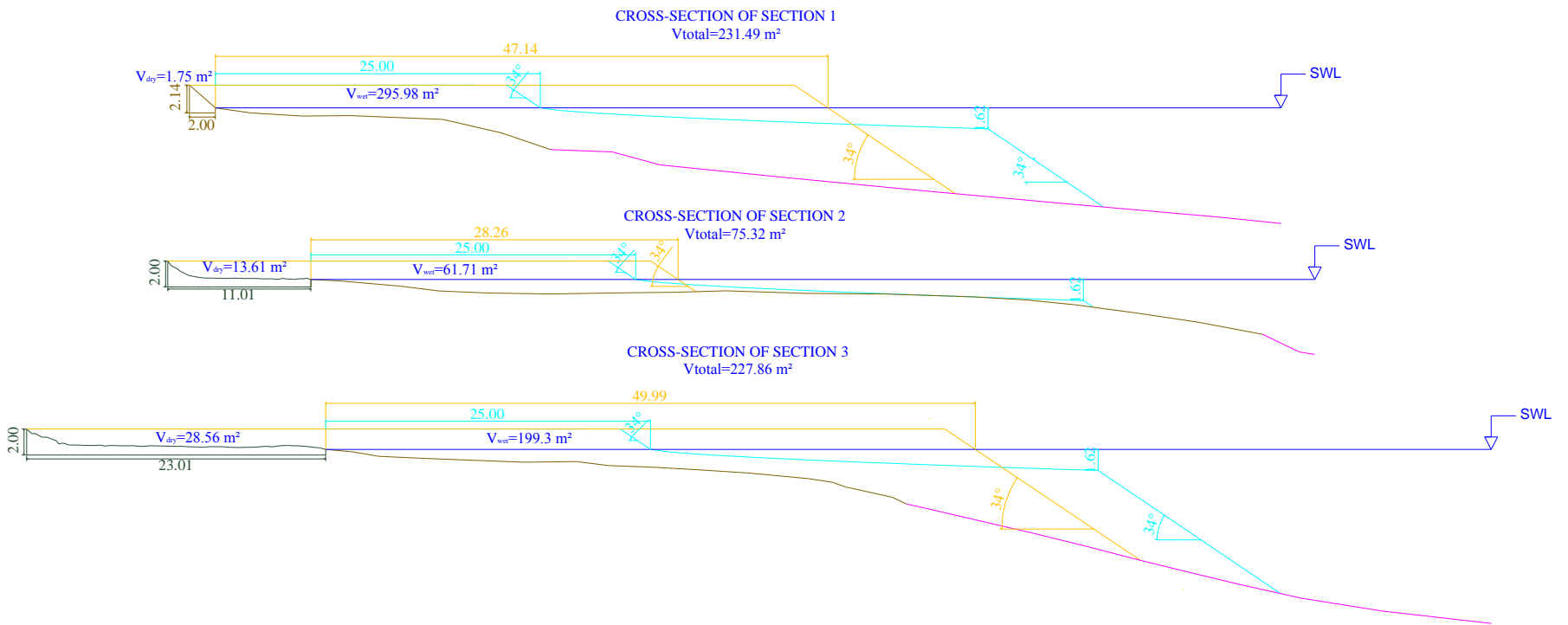


Figure B.21. Design profiles of Section 1,2 and 3 for 25 m new dry beach width ($D_{fill}=0.45 \text{ mm}$).

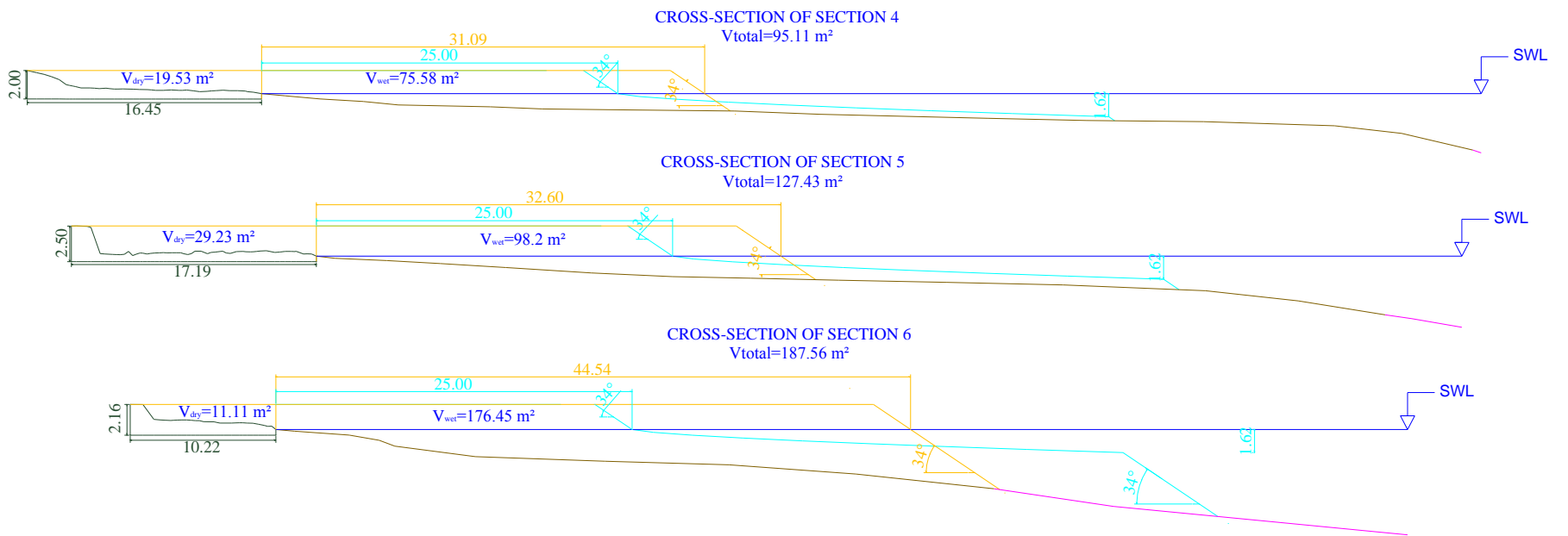


Figure B.22. Design profiles of Section 4,5 and 6 for 25 m new dry beach width ($D_{\text{fill}}=0.45 \text{ mm}$).

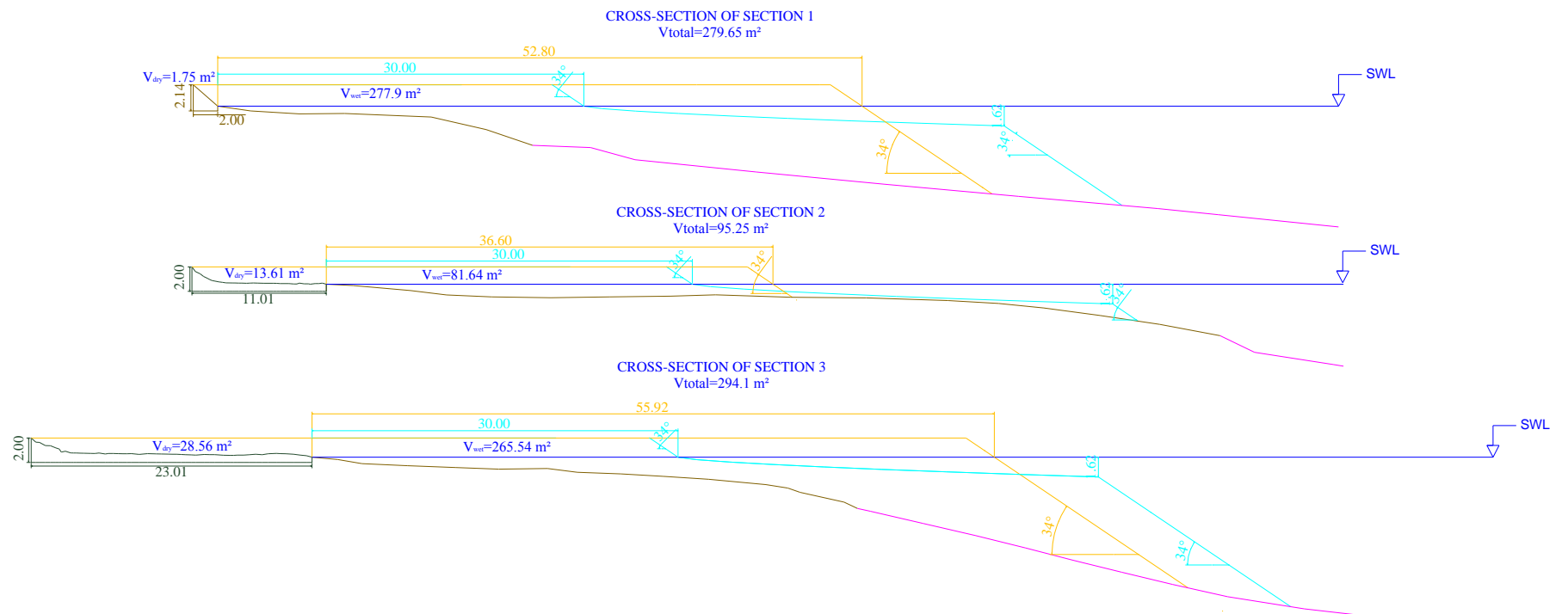


Figure B.23. Design profiles of Section 1,2 and 3 for 30 m new dry beach width ($D_{fill} = 0.45 \text{ mm}$).

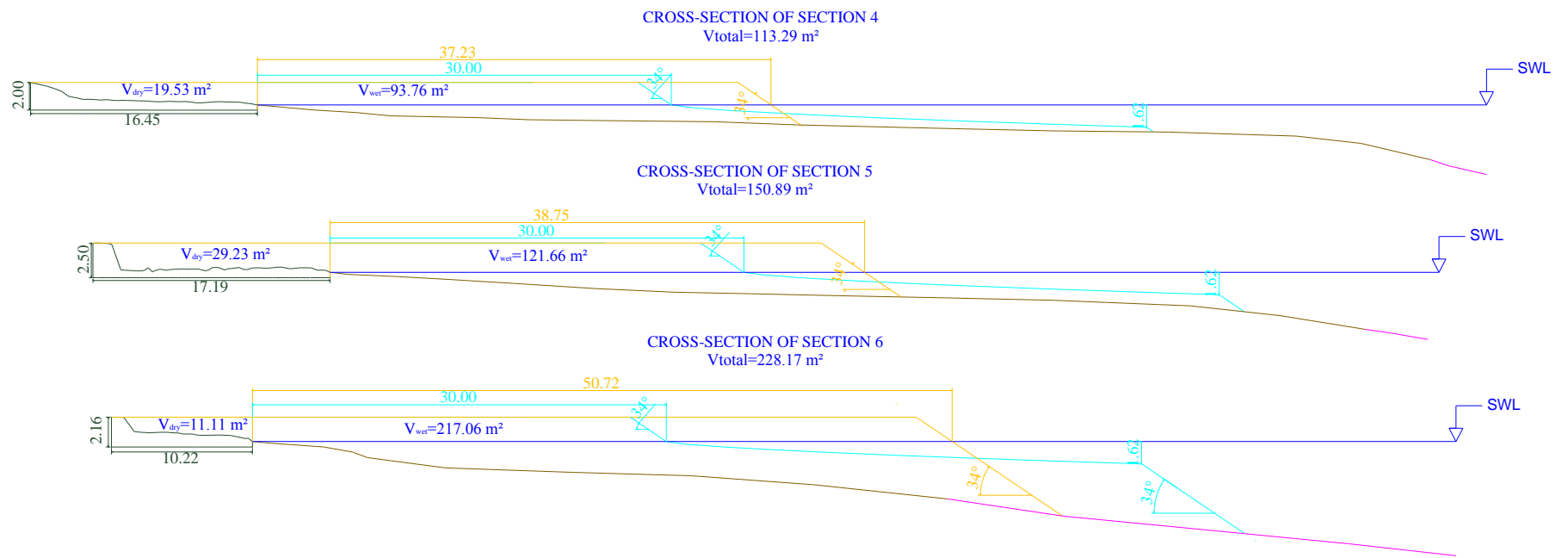


Figure B.24. Design profiles of Section 4,5 and 6 for 30 m new dry beach width ($D_{\text{fill}}=0.45 \text{ mm}$).

B.3. Plan View of 20 m Beach Width for Grain Diameter 0.45 mm

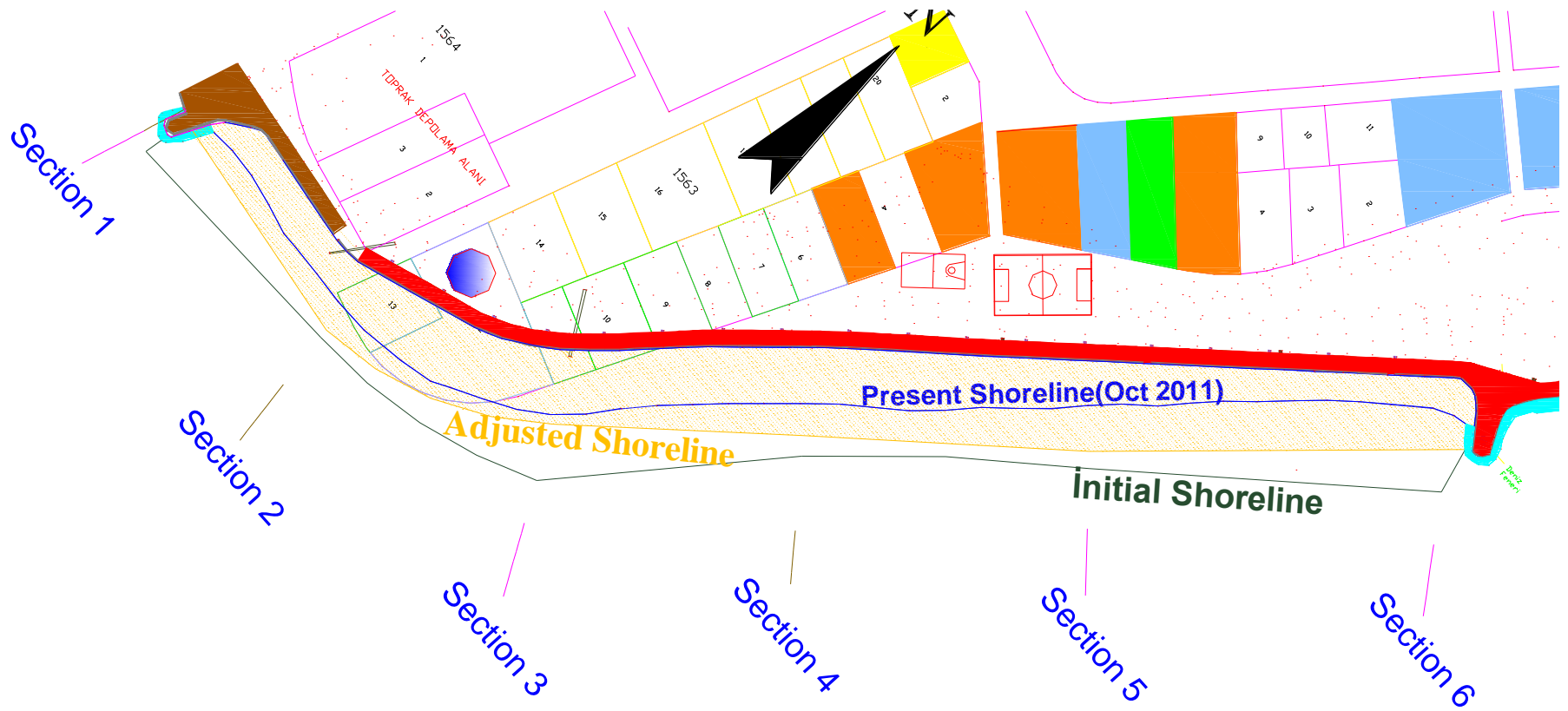


Figure B.25. Design plan view for 20 m new dry beach width ($D_{fill}=0.45$ mm).

REFERENCES

- Aubry, A., S. Lesourd, A. Gardel, P. Dubuisson and M. Jeanson, 2009, "Sediment Textural Variability and Mud Storage on a Large Accreting Sand Flat in a Macrotidal, Storm-wave Setting: the North Sea Coast of France", *Journal of Coastal Research*, ICS2009 (Proceedings), Special Issue 56, pp. 163-167.
- Bruun, P., 1954, "Coast Erosion and the Development of Beach Profiles", *Technical Memorandum*, No. 44, Beach Erosion Board.
- Da Silva, C. P., 2002, "Beach Carrying Capacity Assessment: How imported is it?", *Journal of Coastal Research*, ICS2002 (Proceedings), Special Issue 36, pp. 190-197.
- Dalrymple, R. A. and R. G. Dean, 1984, *Water Wave Mechanics for Engineers and Scientist*, Prentice-Hall, New Jersey.
- Dean, R. G., 1974, "Compatibility of Borrow Material for Beach Fills", ASCE, *14th International Conference on Coastal Engineering*, Copenhagen, pp. 1319-1333.
- Dean, R. G., 1977, "Equilibrium Beach Profiles: U.S. Atlantic and Gulf Coasts", *Ocean Engineering Technical Report*, No.12, Department of Civil Engineering and Collage of Marine Studies, University of Delaware.
- Dean, R. G., 1991, "Equilibrium Beach Profiles: Characteristics and Applications", *Journal of Coastal Research*, Vol. 7, No. 1, pp. 53-84.
- Dean, R. G., 2002, *Beach Nourishment Theory and Practice*, Advanced Series on Ocean Engineering, Vol. 18, World Scientific, Singapore.

- Environmental Protection and Control Department of Kocaeli Metropolitan Municipality, 2005, *Aerial Photos of İzmit Bay*, ANA-KENT, Kocaeli.
- Environmental Protection and Control Department of Kocaeli Metropolitan Municipality, 2011, *Hydrographic Survey of Project Site*, MCH-TECH Marine Research.
- Hallermeier, R. J., 1978, “Uses for a Calculated Limit Depth to Beach Erosion”, ASCE, *16th International Conference on Coastal Engineering*, Hamburg, pp. 1493-1512.
- Hallermeier, R. J., 1985, “Unified Modeling Guidance Based on a Sedimentation Parameter for Beach Changes”, *Coastal Engineering*, Vol. 9, No. 1, pp 37-70.
- Housing and Urban Development Department of Kocaeli Metropolitan Municipality, 2008, *Geological-Geotechnical Research Report of Derince*, KES-KA Soil Mechanics Laboratory, Kocaeli.
- Housing and Urban Development Department of Kocaeli Metropolitan Municipality, 2006, *Photogrammetric map of Kocaeli*, ANA-KENT, Kocaeli.
- Housing and Urban Development Department of Kocaeli Metropolitan Municipality, 2011, *Shoreline Measurement of the Coast of Derince*, Kocaeli.
- Housing and Urban Development Department of Kocaeli Metropolitan Municipality, 2006, *Shoreline of the Site Drawn from Aerial Photos*, Kocaeli.
- Housing and Urban Development Department of Kocaeli Metropolitan Municipality, 2011, *Topography Measurements of the Site*, Kocaeli.

- Hughes, S. A., 1993, *Physical Models and Laboratory Techniques in Coastal Engineering: Sediment Transport Models*, Advanced Series on Ocean Engineering, Vol. 7, World Scientific, Singapore.
- Infrastructural Operations Department of Kocaeli Metropolitan Municipality, 2011, *Shoreline Measurement of the Coast of Derince*, Kocaeli.
- Ito, M. and Y. Tsuchiya, 1984, "Scale-Model Relationship of Beach Profile", ASCE, *19th International Conference on Coastal Engineering*, pp. 1386-1402.
- Jepsen, R., J. Roberts and J. Gailani, 2010, "Effects of Bed Load and Suspended Load on Separation of Sands and Fines in Mixed Sediment", *Journal of Waterway, Port, Coastal, and Ocean Engineering*, ASCE, Vol. 136, Issue 6, pp. 319-326.
- Krumbein, W. G. and W. R. James, 1965, "A Lognormal Size Distribution Model for Estimating Stability of Beach Fill Material", *Technical Memorandum*, No. 16, U.S. Army Coastal Engineering Research Center.
- Moore, B., 1982, *Beach Profile Evolution in Response to Changes in Water Level and Wave Heights*, M.S. Thesis, University of Delaware, Newark.
- Noda, E. K., 1971, "Coastal Movable-Bed Scale-Model Relationship", TETRAT-P-71-191-1, Tetra Tech, Inc., Pasadena, California.
- Noda, E. K., 1972, "Equilibrium Beach Profile Scale-Model Relationship", *Journal of Water Ways, Harbors and Coastal Division*, ASCE, Vol. WW4, pp. 511-528.
- Ochi, M. K., 1998, *Ocean Wave: The Stochastic Approach*, Cambridge University Press, Cambridge.
- Office of Navigation Hydrography and Oceanography, 1992, *Oceanography Map of İzmit Bay (SH-291)*, İstanbul.

Office of Navigation Hydrography and Oceanography, 1997, *Oceanography Map of Port of Izmit (SH-2911)*, İstanbul.

Shore Protection Manual, 1984, U.S. Army Corps and Engineers, Coastal Engineering Research Center, Vicksburg, MS.

Srisuwan, C., M. İ. Kömürcü, P. A. Work, S. Karasu and İ. H. Özölçer, 2011, “Kıyıya Dik Profil Gelişiminin Fiziksel Modellenmesi ve Tane Sınıflanması”, 7. *Kıyı Mühendisliği Sempozyumu Bildiriler Kitabı*, İMO2011, Kıyı Hidrodinamiği, pp. 137-143.

TUBITAK-Marmara Research Center, 2006, *Geology map of the East Marmara*, Environmental Protection and Control Department of Kocaeli Metropolitan Municipality.

Turkish State Meteorological Service (TSMS), 2010, 29-year Wind Data of İzmit Meteorology Station, Ankara.

Yamashita, T., P. Jungwook, and M. Ito, 2004, “Profile Change of Coarse and Fine Material Composite Beach”, *Coastal Engineering 2004*, pp. 2353-2363.